ROLE OF ANGIOSTATIN IN NEUTROPHIL BIOLOGY AND ACUTE LUNG INJURY

A Thesis Submitted to the College of

Graduate Studies and Research

In Partial Fulfillment of the Requirements

For the Degree of Doctor of Philosophy

In the Department of Veterinary Biomedical Sciences

University of Saskatchewan

Saskatoon

By

GURPREET KAUR AULAKH

Keywords: angiostatin, acute lung injury, intravital microscopy, neutrophils, confocal microscopy, diffraction enhanced imaging

PERMISSION TO USE

In presenting this thesis in partial fulfilment of the requirements for a Postgraduate degree from the University of Saskatchewan, I agree that the Libraries of this University may make it freely available for inspection. I further agree that permission for copying of this thesis in any manner, in whole or in part, for scholarly purposes may be granted by the professor or professors who supervised my thesis work or, in their absence, by the Head of the Department or the Dean of the College in which my thesis work was done. It is understood that any copying or publication or use of this thesis or parts thereof for financial gain shall not be allowed without my written permission. It is also understood that due recognition shall be given to me and to the University of Saskatchewan in any scholarly use which may be made of any material in my thesis.

Requests for permission to copy or to make other use of material in this thesis in whole or part should be addressed to:

Head of the Department of Veterinary Biomedical Sciences

University of Saskatchewan

Saskatoon, Saskatchewan (S7N 5B4)

ABSTRACT

Acute lung injury is marked by profound neutrophil influx along with fluid accumulation that impairs lung function at the cost of high mortality (up to 40%). Neutrophils are activated and their constitutive apoptosis is inhibited during this phase in order to be competent phagocytes over the next few hours. Activated neutrophils release copious amounts of toxic mediators that cause tissue damage leading to impaired barrier function and finally, impaired lung function. Therefore, one of the critical needs is to identify molecules that regulate neutrophil migration and silence activated neutrophils to prevent exuberant tissue damage. Angiostatin is an anti-angiogenic molecule highly expressed in lavage fluid of patients with acute respiratory distress syndrome. Angiostatin has recently been shown to inhibit neutrophil infiltration in mice peritonitis. However, the role of angiostatin in modulating neutrophil physiology and lung inflammation remains unknown.

I studied the role of angiostatin, an anti-angiogenic molecule, in neutrophil activation and recruitment *in vivo* and *in vitro*. Angiostatin was endocytosed only by activated neutrophils, inhibited neutrophil polarity in fMLP-activated neutrophils probably through integrin $\alpha_V\beta_3$, and inhibited MAPK signalling in LPS-activated neutrophils. Angiostatin suppressed formation of reactive oxygen species and activated caspase-3 in neutrophils in both pre-and post-LPS treatments. Finally, angiostatin reduced adhesion and emigration of neutrophils in post-capillary venules of TNFα-treated cremaster muscle.

The next study was designed to investigate the role of angiostatin in acute lung injury. I used *E. coli* lipopolysaccharide induced acute lung injury mouse model to test the effects of angiostatin through analyses of bronchoalveolar lavage and lung tissues. In addition, I made novel use of synchrotron diffraction enhanced imaging of mouse lungs to assess lung area and

contrast ratios over 9 hours as surrogates for lung inflammation. Subcutaneous treatment with angiostatin reduced neutrophil influx, protein accumulation, lung Gr1+ neutrophils and myeloperoxidase activity, phosphorylated p38 MAPK without affecting the levels of MIP-1α, IL-1β, KC and MCP-1 in lavage and lung homogenates. Diffraction enhanced imaging showed that angiostatin causes a time-dependent improvement in lung area and lung contrast ratios that reflect improvement in lung edema. Overall, the study shows that angiostatin is a novel inhibitor of acute lung injury in mice. Moreover, DEI offers a highly useful technique in evaluating dynamics of lung inflammation and to investigate the therapeutic impact of new drugs on lung inflammation.

I conclude that angiostatin is a novel inhibitor of neutrophil migration, activation and acute lung injury.

ACKNOWLEDGMENTS

Any piece of work carried out cannot be acknowledged without thanking Almighty GOD.

Having said this, I am lucky to have been supervised by the elite “Master Teacher”, Dr. Baljit Singh, whose dynamic guidance let me conduct my doctorate research in a radical way. He has been exemplary in setting the benchmark of research standards, research without bars. I can, but only, thank him for every support, right from adapting to Canadian work culture to honing my research skills. In all, he has been a very fine mentor.

My due thanks to all honorable advisory members of my graduate committee, Dr. Lixin Liu, Dr. George Mutwiri, Dr. Matthew Loewen, Dr. Jaswant Singh, Dr. Gillian Muir and Dr. Linda Hiebert, for their critical, yet encouraging mentoring. I would fail in my acknowledgement had I not mentioned the ever-willing support by Dr. Lixin Liu and his graduate students, Jennifer and Xei Le, in tirelessly training me towards cremaster muscle intravital microscopy. Although Dr. Dean Chapman was not on my committee, he has been instrumental in shaping my understanding of synchrotron imaging for what an effortless physicist and mentor he is!

Although there would a lengthy list of people to thank from the department, I would like to mention that the very research milieu of Western College of Veterinary Medicine including Dr. John Gordon’s lab, the Westgen facility, WCVM’s Animal Care facility, enabled smooth management of my research project. I would start from the faculty and staff members, Dr. Barry Blakley, Dr. Colette Wheler, Jim Gibbons, Cathy Coghlin, Darlene Hall, Kim Tran, Xiaobei Zhang, Jennifer Town, Vivian Pulga, Paula Mason, Monique Burmester, Susan Cook, Sandra Rose, Diane Matovich, Cheryl Hack and Susan Fjeldstrom for their unique ways of lending a helping hand and comforting words. Without the technical expertise of Dr. Dean Chapman, Dr. Geroge Belev and Steve Hanson, execution of synchrotron experiments

would not be possible. A special mention for Daryoush Hajinezhad who bore the brunt of staying back for all the technical support during confocal microscopy. I would end my thanking my colleagues and peers for their kind support. Various colleagues from the lung pathobiology lab, like Dr. Chandrashekhar Charavaryamayath, Dr. Sarabjeet Suri, Yadu Balachandran, Vanessa Vrolijk, Steve Mills, Lorilee Sereda and the entire lab crew has been supportive in many ways.

I would like to mention Dr. Wolfgang Kuebler's valuable comments in neutrophil migration and activation studies. I acknowledge the kind support by Dr. Baljit Singh's Natural Sciences and Engineering Council of Canada's Discovery Grant, Canadian Institute of Health Research, Canadian Light Source at University of Saskatchewan.

I want to pay sincere thanks to my previous supervisor, Late Dr. Manjeet Singh, whose motivated teaching style and vision for all his students, instilled a very earnest and rational approach towards studying and doing science.

I would thank my friends elsewhere for their untold ways. My husband, daughter, in-laws and parents have been the biggest source of strength and inspiration through my journey to this moment. I am blessed to have such a wonderful family. I hope to do them proud!

TO
MY LOVING FAMILY
WITH THE GRACE OF GOD

TABLE OF CONTENTS

page

LIST OF TABLES

Table page

LIST OF FIGURES

LIST OF ABBREVIATIONS

Abbreviation	
ALI	Acute lung injury
ANG	Angiostatin
AMOT	Angiomotin
ARDS	Acute respiratory distress syndrome
ATP	Adenosine triphosphate
Bad	Bcl-2 associated death promotor
Bax	Bcl-2 associated X protein
Bcl-2	B-cell lymphoma 2
BAL	Bronchoalveolar lavage
Bid	BH3 interacting domain death agonist
BSA	Bovine serum albumin
CD	Cluster of differentiation
cdc-42	cell division control protein-42
cdk	cyclin-dependent kinase
c-FLIP	FLICE-like inhibitory protein
CHO	Chinese hamster ovary cells
DAPI	4',6-diamidino-2-phenylindole
DEI	Diffraction enhanced imaging
DOCK 2	Dedicator of cytokinesis 2
EC	Endothlial cell
E. coli	*Escherichia coli*

ERK	Extracellular signal regulated kinase
ESAM	Endothelial cell-selective adhesion molecule
E-selectin	Endothelial selectin
F-actin	Filamentous actin
FITC	Fluorescein isothiocyanate
FKHRL1 (rhabdomyosarcoma) like 1	Forkhead (Drosophila) homolog
fMLP	Formyl-methionyl-leucyl-phenylalanine
GAP	GTPase activating protein
GDP	Guanosine diphosphate
GEF	Guanine nucleotide exchange factor
GFP	Green fluorescent protein
GTP	Guanosine triphosphate
HGF	Hypoxia induced growth factor
hsp	Heat shock protein
HUVEC	Human umbilical vein endothelial cells
ICAM	Intercellular adhesion molecule
IL	Interleukin
JAM	Junctional adhesion molecule
K	Kringle
KC	Keratinocyte chemoattractant
LFA-1	Lymphocyte-function associated antigen 1
LPS	Lipopolysaccharide

L-selectin	Leukocyte selectin
Mac-1	Macrophage-1 antigen
MAPK	Mitogen-activated protein kinase
MCD	Methyl-β-cyclodextrin
MCP	Monocyte chemoattractant protein
MDCK	Madin-Darby canine kidney
MEK	Mitogen-activated protein kinase kinase
MIP	Macrophage inflammatory protein
MMP	Matrix metalloproteinase
MPO	Myeloperoxidase
MUPP1	Mutliple PDZ domain protein 1
NE	Neutrophil elastase
NF-κB	Nuclear factor kappa-light-chain-enhancer of activated B cells
PAGE	Polyacrylamide gel electrophoresis
Pals	Proteins associated with Lin-7
Par-3	Partitioning defective 3 homolog
Patj	Pals1-associated tight junction protein
PBS-T	Phosphate buffered saline+tween-20
PECAM	Platelet endothelial cell adhesion molecule
PDZ	**P**ost synaptic density protein (PSD95), **D**rosophila disc large tumor suppressor (DlgA), and **Z**onula occludens-1 protein (zo-1)
PGK	Phospho glycerate kinase

PI3K	Phosphatidyl inositol 3-kinase
PIP2	Phosphatidyl inositol 4,5-biphosphate
PIP3	Phosphatidyl inositol 3,4,5-triphosphate
PKC	Protein kinase C
PMNs	Polymorphonuclear cells
P-selectin	Platelet selectin
PSGL	Platelet selectin glycoprotein ligand
PTEN	PI3K-phosphatase and tensin homolog pathway
PTK	Protein tyrosine kinase
Ras	RAt sarcoma
RBC	Red blood cells
RGD	Arg-Gly-Asp
Rho	RAS homologue
RICH	Regeneration-induced CNPase homolog
ROS	Reactive oxygen species
SDS	Sodium dodecyl sulphate
SILAC culture	Stable-isotope labelling with amino-acids in cell
S. pneumoniae	*Streptococcus pneumoniae*
src	Sarcoma
TJ	Tight junctions
TLR	Toll-like receptor
TNF	Tumor necrosis factor

tPA	Tissue-type plasmonogen activator
TRALI	Transfusion related acute lung injury
uPAR	Urokinase-type plasminogen activator receptor
VCAM	Vascular cell adhesion molecule

CHAPTER 1
REVIEW OF LITERATURE

1.1. Acute Lung Injury

Localized pathologic changes in acute inflammation have been reported since more than 2000 years ago by Cornelius Celsus as "*rubor et tumor cum calore et dalore*" meaning "redness and swelling with heat and pain". Rudolph Virchow extended this definition by "loss of function" ("*functio laesa*") observed in more severe inflammation. Julius Cohnheim explained these observations in frog tongue under a microscope for the first time. The redness and heat reflect an increased blood flow; the swelling is due to exudation of fluid and cell accumulation and pain follows. Elie Metchnikoff concluded that inflammation is a local reaction produced by phagocytic activity of leukocytes and a chemical reaction, now recognized as production of various mediators, of blood plasma and tissue fluids (Plytycz, Seljelid 2003). Most of the times, acute inflammation is beneficial and resolves after some time. In an event of severe infection or insult, it can progress to chronic inflammation.

Acute lung injury (ALI) and acute respiratory distress syndrome (ARDS) are medical emergency conditions with reported mortality of up to 40% resulting from a wide array of diseases, both infectious and non-infectious, like pneumonia, influenza, acid aspiration, sepsis, pancreatitis and transfusion-related ALI (Grommes, Soehnlein 2011, Jain, Bellingan 2007). While most of the above mentioned diseases cause direct lung damage, the last two are indirect causes, which lead to systemic inflammatory response syndrome that further causes ALI/ARDS. ALI is a less severe form of sepsis whereas ARDS manifests as multiple organ dysfunction in all instances. ALI is characterized by increased permeability of alveolar-capillary barrier resulting in lung edema and protein exudation leading to impaired blood oxygenation. Neutrophil activation and accumulation in the interstitium and bronchoalveolar space is a hallmark of ALI/ARDS. Although neutrophils are components of the host innate immune mechanism, activated

neutrophils live longer and they cause tissue damage through their inflammatory products such as proteinases, cationic polypeptides, cytokines and reactive oxygen species (ROS) (Witko-Sarsat, Rieu et al. 2000, Dallegri, Ottonello 1997, Haslett 1999, Haslett, Savill et al. 1989). In ARDS patients, neutrophil numbers in bronchoalveolar lavage fluid (BAL) correlate with ARDS severity and outcome (Parsons, Fowler et al. 1985, Matthay, Eschenbacher et al. 1984). Moreover, mice models of ALI show improvement upon neutrophil depletion (Abraham, Carmody et al. 2000) or by inhibiting neutrophil chemokine, IL-8 in rabbits (Folkesson, Matthay et al. 1995). However, it must also be noted that neutrophil transmigration can occur without endothelial damage (Martin, Pistorese et al. 1989). Neutropenic children can develop ALI/ARDS indicating the presence of neutrophil-independent mechanisms (Laufe, Simon et al. 1986, Ognibene, Martin et al. 1986, Sivan, Mor et al. 1990). A majority of literature, however, highlights key role of neutrophils in the progression of ALI/ARDS. Therefore, it is important to modulate neutrophil activation and transmigration to attenuate the deleterious tissue effects while preserving their anti-bacterial function. Below is a detailed account of sub-cellular events controlling the directional movement of neutrophils towards site of injury called chemotaxis.

1.1.1. Neutrophil Chemotaxis

Cells are programmed and equipped to migrate. There are two major kinds of cell movements, single cell (amaeboid and mesenchymal or haptokinetic) and collective (cell sheets, strands, tubes, clusters) migration modes. Collective migration involves maintenance of cell-cell junctions and communication as observed in vascular sprouts, invading epithelial strands or tubes and tumor clusters. Based on the focus of this research project, a detailed discussion of collective cell migrations is beyond the scope of this review. Mesenchymal or the haptokinetic cells such as fibroblasts, endothelial cells, myoblasts or sarcoma cells, form spindle shaped morphology and establish firm integrin-mediated contacts with substrate as well as high traction

at both cell poles resulting in very low migration velocities of 0.1-2 μm/min (Friedl, Borgmann et al. 2001). Among single cell movements, amoeboid are the most primitive form of highly mobile single cell movements. Leukocytes fall under this category as they undergo rapid morphological changes while establishing minimal or nascent contacts with substrate. This property of deformability enables rapid migration velocities of 2-30 μm/min (Friedl, Borgmann et al. 2001). Cortical filamentous actin mediates cell dynamics but mature focal contacts and stress fibers are lacking. Chemotaxis is the directional movement of such specialized immune cells towards specific chemoattractant molecules enabling these cells to efficiently reach the site of inflammation, howsever small it may be, in the shortest possible time. Neutrophils (PMNs) are a seminal cell population found at acute inflammation sites. This is afforded by property of chemotaxis. In fact, PMNs can respond to as low as $1/100^{th}$ of chemoattractant gradients and yet prioritize their migration towards bacterial peptides over a multitude of other chemoattractants to finally reach the site of inflammation (Insall 2010). Neutrophils adopt the eukaryotic chemotaxis model, known as the pseudopod-centered model, in which random pseudopods are generated in the presence of very shallow chemoattractant gradients that enable swift directional changes while moving randomly (Insall 2010, Insall, Machesky 2009). A comprehensive review of biology of these events is provided in the next couple of paragraphs.

1.1.1.1. Actin Dynamics

Neutrophils respond to chemoattractants by formation of ruffles all over the cell body, accompanied by a two to three fold transient rise in polymerized cortical F-actin in the ruffles. A minute later their shape changes with contracted tail in the rear and F-actin rich ruffles in the front (Campellone, Welch 2010, Niggli 2003) (Figure 1). The process of actin polymerization is dynamic due to requirement of continual tail de-adhesion and leading edge formation in order for

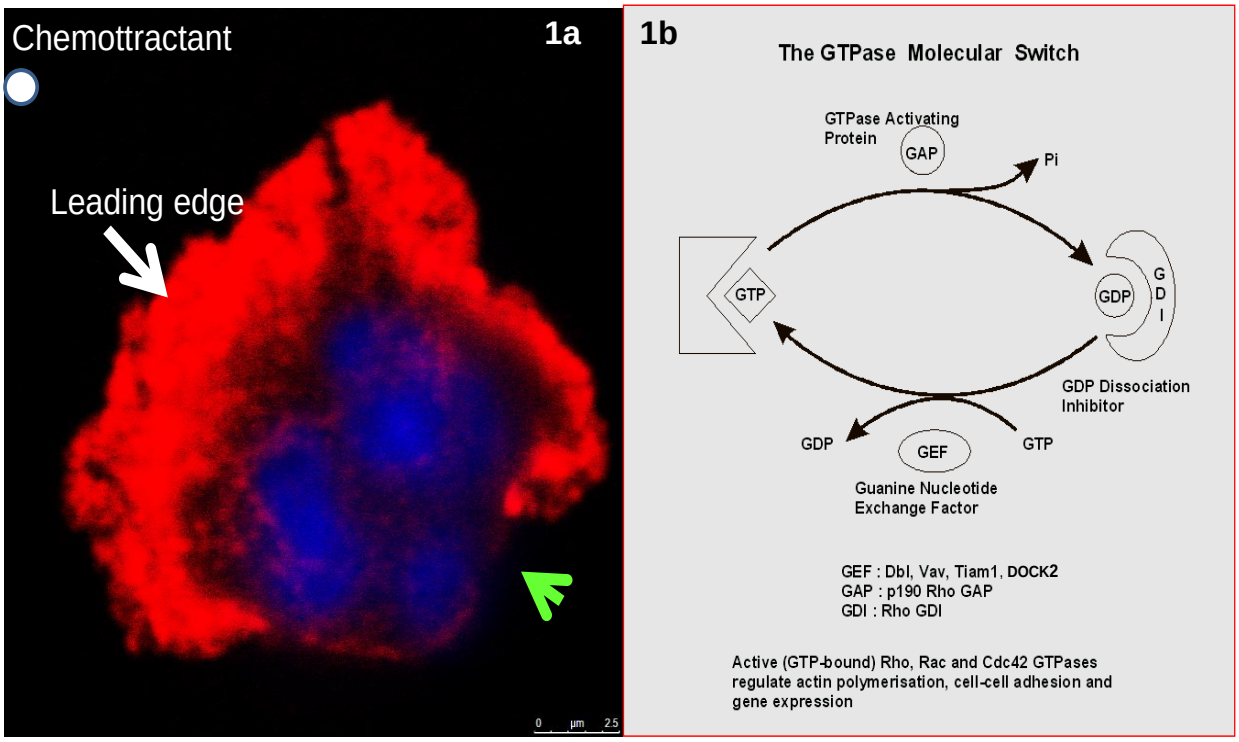

Figure 1a: Neutrophil actin stained with rhodamine phalloidin (in red), nucleus stained with DAPI (in blue) in response to 100nM formyl-methionyl-leucyl-phenylalanine, fMLP. Neutrophil leading edge shows membrane ruffles rich in polymerized F-actin (depicted by white arrow) and rear tail (depicted by green arrow head).

Figure 1b: A schematic representation of GTPase molecular switch showing GTP recycling by two enzymes GTPase activating protein (GAP) and Gunanine nucleotide exchange factor (GEF). At the time these events are occurring at the leading edge, the rear tail of the cell also undergoes cytoskeletal microtubule destabilization (Eddy, Pierini et al. 2002, Ehrengruber, Deranleau et al. 1996). This occurs by small heat shock protein-27 (hsp-27) phosphorylation (Jog, Jala et al. 2007).

neutrophils to roll on endothelial cells or in the interstitium. Chemoattractants such as IL-8, formyl-methionyl-leucyl-phenylalanine (fMLP) couple to βγ subunits of G proteins that signal through GTP bound small GTPases like Rho, Rac and cdc-42 (Szczur, Zheng et al. 2009, Szczur, Zheng et al. 2009, Hall 1992, Hall 1992, Geiszt, Dagher et al. 1998, Lad, Olson et al. 1985). Small G-proteins require continual recycling of guanine nucleotide triphosphate (GTP) to guanine nucleotide diphosphate (GDP) and inorganic phosphate. GDP pools are bound to a protein called GDP Dissociation Inhibitor which is facilitated by enzymes such as GTPase activating proteins (GAPs) like p190 Rho GAP and guanine nucleotide exchange factors (GEFs) like DOCK2, VAV1, VAV3 (Niggli 2003, Matsumoto, Molski et al. 1987). Figure 1b describes a schematic of the GTPase molecular switch.

1.1.2. *In vivo* Neutrophil Recruitment

Intravascular immunity had long been ignored due to lack of technical advances in *in vivo* imaging. Intravital microscopy provides the required high spatio-temporal resolution for tracking directed leukocyte migration. In the past decade, fluorescent spinning disk intravital imaging has enabled new insight into immune cell recruitment. But tracking of all leukocyte subsets has not been possible due to lack of lineage-specific markers. Genetic engineering of green fluorescent protein (GFP) tagged leukocyte subsets has, however, enabled visualization of patrolling monocytes and neutrophil migration behaviors in CX3CR1$^{gfp/gfp}$ mice (Auffray, Fogg et al. 2007). Recently, a group has shown monocyte dependent neutrophil extravasation in mice lungs by utilizing two-photon microscopy (Kreisel, Nava et al. 2010).

1.1.2.1. Intravital Microscopy of Cremaster Tissue. Simple vascular beds of tissues such as mesentery and cremaster muscle are easily visualized upon transillumination and with minimal preparation-induced inflammation. In contrast, it is a major technical

challenge to image complex vascular system of organs such as the lung and liver. Therefore, cremaster muscle has been extensively used to elucidate the basic mechanisms of leukocyte recruitment. Although it is extremely difficult to eliminate basal rolling due to surgical trauma, the basal adhesion and emigration should be near zero values. The anesthetized mouse is placed on a board that has circulating warm water running through a milled internal cavity (Figure 2). An incision is made in the scrotal skin to expose the left cremaster muscle, which is carefully removed from the associated fascia. A lengthwise incision is made on the ventral surface of the cremaster muscle using a cautery. The testicle and the epididymis is separated from the underlying muscle and moved into the abdominal cavity. The muscle is then spread out over an optically clear viewing pedestal and secured along the edges with threads. The exposed tissue is superfused with warm bicarbonate-buffered saline.

1.1.2.2. Evaluation of leukocyte recruitment. The number of rolling, adherent, and emigrated leukocytes is determined off-line during video playback analysis. Rolling leukocytes are defined as those cells moving at a velocity less than that of erythrocytes within a given vessel. The flux of rolling cells is measured as the number of rolling cells passing by a given point in the venule per minute. A leukocyte is considered to be adherent if it remained stationary for at least 30 s, and total leukocyte adhesion is quantified as the number of adherent cells within a 100 μm length of a venule. Leukocyte emigration is defined as the number of cells in the extravascular space within a 200 × 300 μm area. Only cells adjacent to and clearly outside the vessel under study are counted as emigrated. The experiment is videotaped in real-time. Numerous parameters are generally recorded as indicated in (Table 1).

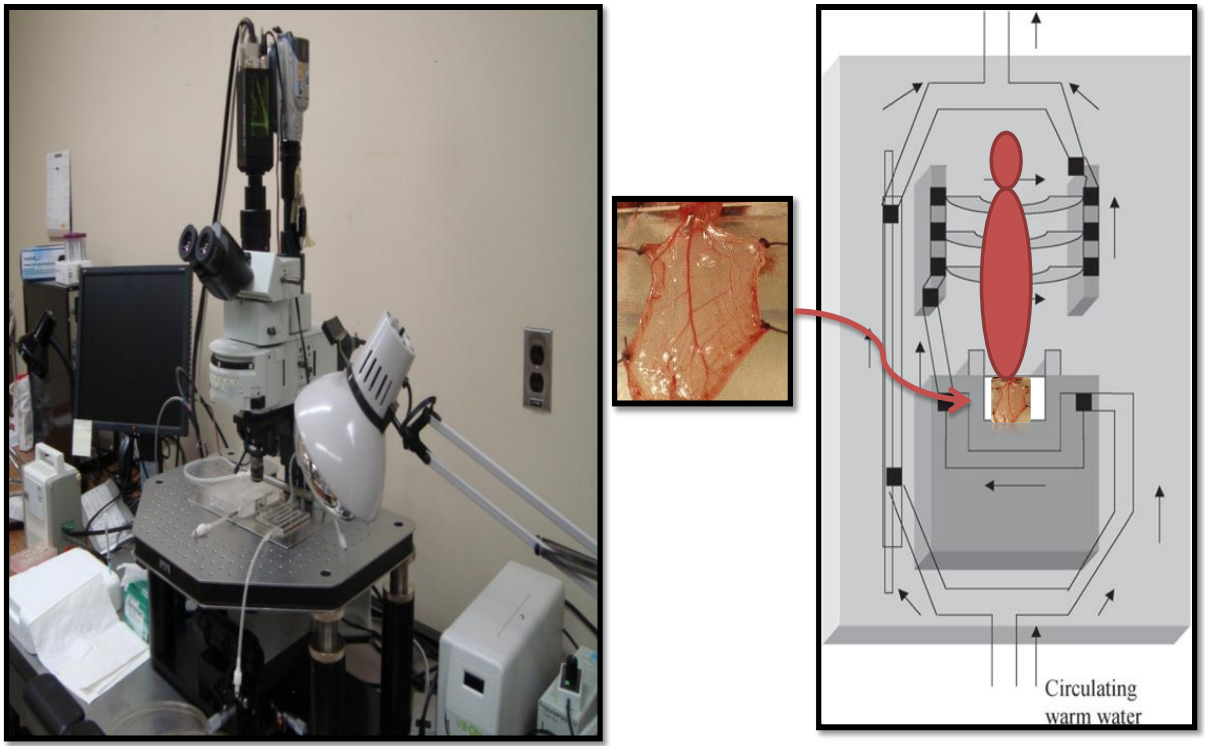

Figure 2: Intravital set-up and design of cremaster board with warm circulating water (Modified from Cara and Kubes, 2003)

Time Point	Video (Start)	Rec.(Day) Start	Rec.(Day) Stop	Diameter (µm)	Velocity RBC	FLUX (cells/min)	ADHESION (cells/5min)	Emigration (cells)	WBC sec/100 µm (first 20 cells)	Velocity WBC (µM/sec)

Table 1: Parameters recorded off-line from intravital microscopy recording.

Immune cells undergo a series of sequential steps during extravasation from blood vessels to tissues. These include tethering, rolling, crawling, and transmigration (Ley, Laudanna et al. 2007, Liu, Kubes 2003) (Figure 3a).

1.1.2.3. **Rolling.** The family of selectin adhesion molecules, especially P-selectin and E-selectin, expressed by endothelial cells facilitate initial tethering and rolling of neutrophils in post-capillary venules of peripheral vasculature. In lungs, selectin blockade is unable to reduce leukocyte recruitment in some but not all forms of inflammation (Doerschuk, Quinlan et al. 1996, Mizgerd, Meek et al. 1996). In lungs, leukocyte adhesion occurs in capillaries without requirement of rolling, also termed as "sequestration" (Selby, MacNee 1993). Although physical trapping of leukocytes could afford one reason, there is no conclusive evidence and there could be other adhesion molecules involved in lung (Figure 3b). Constitutive rolling in non-inflamed tissues such as skin is due to constitutive expression of E- and P-selectin (Weninger, Ulfman et al. 2000). As skin is constantly exposed to external environment, constitutive rolling is a sentinel mechanism by which leukocytes patrol the vascular endothelium to detect any infection. Studies in which tissues are surgically exteriorized show P-selectin dependent rolling in non-inflamed tissues but this has been attributed as a response to surgery (Kubes, Kanwar 1994). Therefore, it is not known whether constitutive rolling is seen in non-inflamed tissues in peripheral vascular beds, lungs and intestine. Neutrophil transit time is extended in lungs suggesting retention in pulmonary vasculature (Selby, MacNee 1993, Hogg, Doerschuk et al. 1992, Doerschuk, Downey et al. 1990, Doerschuk, Allard et al. 1987).

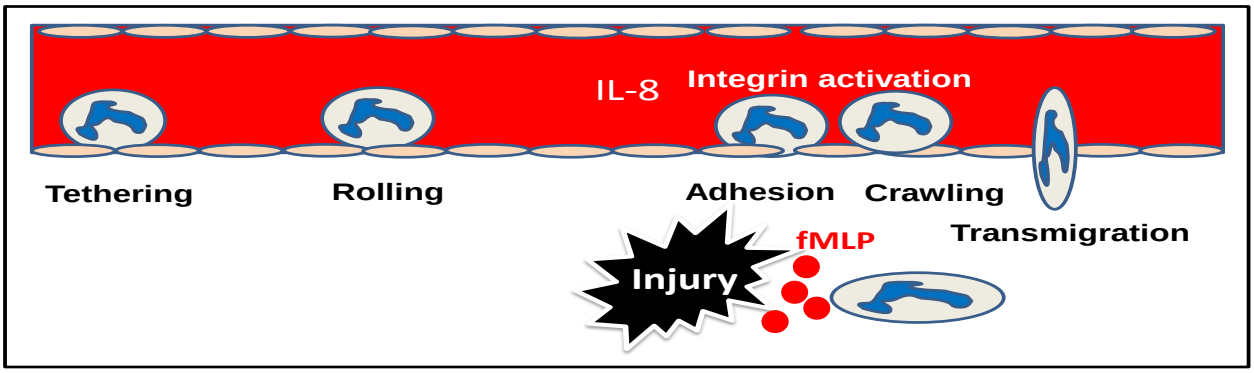

Figure 3a: A schematic showing the major steps of neutrophil migration in a peripheral post-capillary venule in response to injury namely tethering, rolling, crawling, and transmigration. Neutrophils typically migrate from venules in response to injury. Neutrophil migration begins through the formation of selectin-mediated nascent contacts with the endothelium followed by firm adhesion induced by integrins and finally transmigration across the endothelium towards injury site.

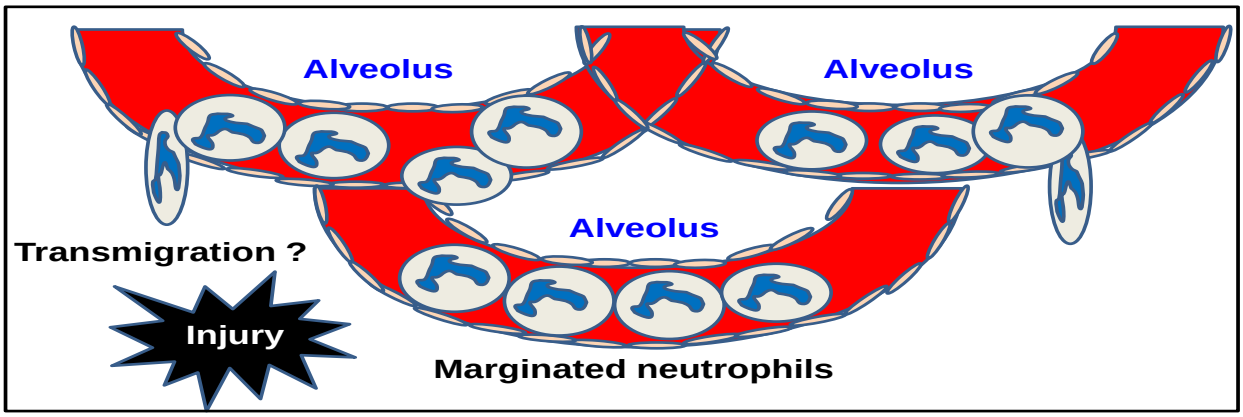

Figure 3b: A schematic showing neutrophil migration in a lung capillaries in response to injury. Neutrophil migration in the lungs defies this paradigm for many reasons. First, narrow diameter and tortuous nature of the lung capillaries results in retention of large number of neutrophils. Second, pulmonary vasculature is a low blood pressure zone compared to the peripheral vasculature. Finally, the recruitment appears to be independent of selectins and β_2 integrins.

1.1.2.4. Crawling. Adhesion to the endothelium occurs through α_4 and β_2 integrins after chemokine presentation on the surface of endothelium following extravascular damage and/or infection. Ligand-induced integrin clustering and allosteric conformational changes probably initiate outside-in signalling and the formation of signalosomes, which are required for recruitment of protein tyrosine kinases (PTKs) (Liu, Kiosses et al. 2002). FGR and HCK (haemopoeitic cell kinase), two *src*-like PTKs that are crucial transducers of outside-in signalling by LFA1 and MAC1, are not required for chemoattractant-triggered upregulation of LFA1 affinity (inside-out signalling) and rapid neutrophil adhesion under flow (Giagulli, Ottoboni et al. 2006). However, the lack of β_2-integrin outside-in signalling accelerates the detachment of adherent neutrophils under flow. Neutrophils lacking the GEFs VAV1 and VAV3 (Martinez Gakidis, Cullere et al. 2004) or PI3Kγ (Smith, Deem et al. 2006) also detach easily. These "hot spots" for adhesion mediated via lymphocyte function-associated antigen 1 (LFA1 also known as $\alpha_L\beta_2$ integrin) on neutrophils are often not the final sites of extravasation. The adherent neutrophils often crawl, not necessarily in the direction of flow, to junctions and finally emigrate out of the vasculature (Phillipson, Heit et al. 2006). Inhibition of crawling delays but does not inhibit emigration *in-vivo*. However, *in-vitro* monocytes' crawling has been shown to be an essential step for diapedesis (Schenkel, Mamdouh et al. 2004).

1.1.2.5. Transmigration. The site of neutrophil emigration is not well defined. Most of the studies indicate that neutrophils migrate at inter-endothelial junctions (paracellular route) (Phillipson, Heit et al. 2006, Schenkel, Mamdouh et al. 2004). There is some evidence of migration of neutrophils through endothelial cells too (transcellular route) (Ley, Laudanna et al. 2007, Kamei, Carman 2010, Carman, Springer 2004, Feng, Nagy et

al. 1998). Molecular mechanisms of transmigration are even less understood than the site of emigration. There are reports of involvement of platelet/endothelial cell adhesion molecule (PECAM; also known as CD31), junctional adhesion molecules (JAMs), CD99, endothelial cell adhesion molecule 1 (ECAM1) and possibly intercellular adhesion molecules (ICAMs) and integrins (Ley, Laudanna et al. 2007, Muller 2009). Extension of leukocyte membrane protrusions into the endothelial-cell body and endothelial-cell junctions is triggered by ligation of intercellular adhesion molecule 1 (ICAM1) by MAC1 (macrophage antigen 1) (Phillipson, Heit et al. 2006, Schenkel, Mamdouh et al. 2004). Ligation of ICAM1 is associated with increased intracellular Ca^{2+} and activation of p38 mitogen-activated protein kinase (MAPK) and RAS homologue (Rho) GTPase, which may collectively activate myosin light-chain kinase leading to enhanced endothelial-cell contraction and hence opening of interendothelial contacts. Leukocyte migraton through endothelial cell barrier is rapid (<2-5 minutes) but penetration of endothelial cell basement membrane is slower (>5-15 minutes) (Ley, Laudanna et al. 2007). Transmigration can by triggered by luminal chemoattractants along with shear flow (Cinamon, Shinder et al. 2004). As indicated earlier, adherent leukocytes can induce formation of "docking structures" or "transmigratory cups" or "endothelial domes" which are endothelial cell projections rich in leukocyte-specific protein 1 (LSP-1), ICAM1 and VCAM1 and cytoplasmic molecules such as ezrin, radixin and moesin proteins and cytoskeletal components (such as vinculin, α-actinin and talin-1) (Kamei, Carman 2010, Carman, Springer 2004, Petri, Kaur et al. 2011, Riethmuller, Nasdala et al. 2008). Such endothelial domes are an efficient way of providing a protective barrier against excessive plasma and protein loss as evidenced in $LSP1^{-/-}$ mice (Petri, Kaur et al. 2011).

1.1.2.6. Paracellular migration involves the release of endothelial-expressed vascular endothelial cadherin (VE-cadherin) and is facilitated by intracellular membrane compartments containing a pool of platelet/endothelial-cell adhesion molecule 1 (PECAM1) and possibly other endothelial-cell junctional molecules, such as junctional adhesion molecule A (JAM−A). Other molecules involved in paracellular transmigration are endothelial cell-selective adhesion molecule (ESAM), ICAM2 and CD99.

1.1.2.7. Transcellular migration occurs in 'thin' parts of endothelial cells, which create a shorter distance for a leukocyte to migrate (Feng, Nagy et al. 1998). ICAM1 ligation leads to translocation of ICAM1 to actin- and caveolae-rich regions. ICAM1-containing caveolae link together forming vesiculo-vacuolar organelles (VVOs) creating an intracellular passage for the leukocyte migration. Ezrin, radixin and moesin proteins could act as linkers between ICAM1 and cytoskeletal proteins (such as actin and vimentin), causing their localization around the channel, thereby providing structural support for the cell under these conditions (Kamei, Carman 2010, Carman, Springer 2004, Barreiro, De La Fuente et al. 2007, Barreiro, Yáñez-Mó et al. 2002).

1.1.2.8. Migration through the endothelial basement membrane and pericyte sheath. This can occur through gaps between adjacent pericytes and regions of low protein deposition within the extracellular matrix. This response can be facilitated by $\alpha_6\beta_1$-integrin and possibly proteases, such as matrix metalloproteinases (MMPs) and neutrophil elastase (NE) (Ley, Laudanna et al. 2007, Vestweber 2007).

To sum up, the prevailing mode of migration is considered to be "haptokinetic" (Friedl, Borgmann et al. 2001), that is, a migrating cell follows adhesion predetermined paths. Specificity and diversity is attributed firstly to eight subunits assorting to 18 subunits forming 24 distinct

integrins, and secondly to various matrix metalloproteinases (MMPs) degrading the extracellular matrix (ECM). How all cell types fit into this model and still be adequately regulated in response to an acute immune attack or for maintaining overall homeostasis is not well understood. A recent study has elegantly shown that in pan-integrin deficient mice, rapidly migrating cells such as neutrophils and dendritic cells do not follow this haptokinetic mode. In contrast to two-dimensional intravascular migration, the migration through three dimensional ECM was shown to be integrin but not protrusion independent (Lammermann, Bader et al. 2008). The authors proposed a "flowing and squeezing" model whereby protrusion drives basal locomotion and actin-myosin mediated trailing edge contraction propels the nucleus of migrating cell that is functionally dissociated into a front and back. There is no digestion and remodelling, hence avoiding collateral tissue damage.

1.1.3. Chemotaxis Signaling Pathways

Numerous downstream signaling pathways are activated after chemoattractant ligation to heterotrimeric G proteins (Campellone, Welch 2010, Niggli 2003). The lipid phosphatidyl inositol 4,5-biphosphate [PtIns(4,5)P_2] can be hydrolyzed by phospholipase C to diacylglycerol that activates protein kinase C (PKC) isoforms and inositol 1,4,5-triphosphate that activates intracellular calcium release. [PtIns(4,5)P_2] can also be hydrolyzed by phosphoinositide 3-kinase (PI 3K) into phosphatidyl inositol 3,4,5-triphosphate [PtIns(3,4,5)P_3] (also commonly called PIP3) and phosphatidyl inositol 3,4-biphosphate [PtIns(3,4)P_2] (Stephens, Ellson et al. 2002). Mitogen activated protein kinases (MAPK) and phosphatases are activated downstream of Rho family of GTP binding small G proteins. Tyrosine kinases are activated via seven-transmembrane-domain receptors, tyrosine kinase linked-receptors and integrin engagement.

Signaling via PI3-kinase enzyme is of recent interest because of strong evidence of a very fast internal compass comprised of polarized phospholipids as discussed in detail below (Wong, Heit et al. 2010, Knall, Worthen et al. 1997). Neutrophils express PI3-kinase α, β, γ and δ isoforms. PI3-kinase γ is activated by heterotrimeric G-proteins whereas others are regulated by tyrosine kinases. Neutrophils produce highest amounts of these lipids (Stephens, Ellson et al. 2002). PI3K is also involved in MAPK activation (Niggli 2003). PI3Kγ, in neutrophils and not endothelium, is important for neutrophil emigration from circulation in response to brief stimulation and PI3Kδ is responsible for emigration after longer chemokine stimulation (Liu, Puri et al. 2007, Puri, Doggett et al. 2005, Puri, Doggett et al. 2004). Having said this, PI3Kγ is responsible for neutrophil chemokinesis i.e. cell motility in response to fMLP, can regulate integrins and some aspects of polarization but is not unique to neutrophil's "chemotactic compass" (Andrew, Insall 2007, Ferguson, Milne et al. 2007). LPS primed neutrophils, when exposed to fMLP, are completely insensitive to PI3K inibitors (Ferguson, Milne et al. 2007). These studies show an important context-dependent role of PI3Kγ in neutrophil motility. Shallow chemoattractant gradients induce random pseudopods that are split from a leading edge and finally a dominant pseudopod is sustained. PI3K inhibitors lead to lower frequency of pseudopod generation but do not affect directionality (Insall 2010, Andrew, Insall 2007). Therefore, where early PIP3 redistribution localizes DOCK2 at the pseudopod for neutrophil chemotaxis early-on, a later activation of phosphatidic acid (PA) localizes DOCK2 to the pseudopod slowly to maintain neutrophil chemotactic response that is independent of PIP3 (Nishioka, Frohman et al. 2010, Nishikimi, Fukuhara et al. 2009, Kunisaki, Nishikimi et al. 2006). It seems neutrophils have adapted various inter-related signaling pathways for neutrophil pseudopod persistence and directionality. And many questions still remain to clarify the basic function of each pathway.

Neutrophils encounter and 'prioritize' many chemoattractant gradients to pursue bacteria. For example, neutrophils adhere to the endothelium of blood vessels in response to chemokines including CXCL8 (also known as IL-8). However, while still in the presence of this initial stimulus, they must eventually be able to respond to bacterial chemoattractants such as fMLP. IL-8 stimulates PI3K-phosphatase and tensin homolog (PTEN) pathway whereas fMLP stimulates p38 MAPK pathway with latter dominating over the PI3K pathway (Heit, Tavener et al. 2002, Foxman, Campbell et al. 1997). In response to IL-8, [PtIns(3,4,5)P_3] is localized at the leading edge of migrating neutrophil and PTEN (which converts [PtIns(3,4,5)P_3] to [PtIns(4,5)P_2]) accumulates along sides and uropod of the cell (Li, Dong et al. 2005). fMLP also causes PTEN localization along sides and at the uropod but does not depend on [PtIns(3,4,5)P_3] (Heit, Robbins et al. 2008). In opposing gradients, PTEN distributes all around the cell circumference thus inhibiting [PtIns(3,4,5)P_3] and consequently allowing preferential migration towards bacterial products in a p38-dependent manner. Such prioritization is absent in PTEN-/- neutrophils resulting in compromised bacterial clearance *in vivo* (Heit, Robbins et al. 2008). Lipopolysaccharide, commonly called as LPS, is a cell wall component of Gram negative bacteria that blocks neutrophil migration towards chemokines such as IL-8 via Toll-like receptor 4 (TLR4) activation leading to induction of p38-dependent inhibition of [PtIns(3,4,5)P_3]. LPS also blocks chemotaxis in response to fMLP by an unknown mechanism (Heit, Tavener et al. 2002). LPS itself does not have chemoattractant properties so neutrophils stop and do not migrate towards LPS. Although systemic administration of LPS in mice causes neutrophil adhesion in the microcirculation, there is no transmigration into extravascular space despite administration of chemoattractant (Khan, Heit et al. 2005, Yipp, Andonegui et al. 2002). Neutrophils are rapidly diverted towards lung and liver avoiding peripheral sites, a well observed

fact, under systemic LPS challenge as in sepsis (Yipp, Andonegui et al. 2002, Andonegui, Bonder et al. 2003). There could be four possible explanations. First, LPS activates platelet TLR4 that can induce neutrophil activation and neutrophil extracellular trap (NET) formation under flow conditions *in-vivo* (Clark, Ma et al. 2007). There are many reports showing presence of platelets, similar to neutrophils, in lungs and liver of sepsis patients and mice models of sepsis (Andonegui, Kerfoot et al. 2005, Stohlawetz, Folman et al. 1999, Andonegui, Trevani et al. 1997). Mortality in sepsis patients shows direct correlation with degree of thrombocytopenia (Mavrommatis, Theodoridis et al. 2000). It is interesting that activated protein C, an effective therapeutic in severe sepsis, has both anti-thrombotic and anti-inflammatory effects. Second, increased expression of α_4 integrin on neutrophils will make them adhere to endothelial vascular cell adhesion molecule 1 (VCAM1) (Ibbotson, Doig et al. 2001). Third, C5a production formed via the classical complement activation of C3 as well as through thrombin-dependent pathway activates multiple receptors (Rittirsch, Flierl et al. 2008, Huber-Lang, Sarma et al. 2006, Czermak, Sarma et al. 1999) and induces neutrophil recruitment in lungs. Lastly, LPS induces p38 MAPK activation to set up a PTEN 'barrier' around the entire cell thus preventing neutrophil response to chemotactic stimulus. This point is observed following administration of tumor necrosis factor alpha (TNFα), which induces p38 MAPK (Lokuta, Huttenlocher 2005). This suggests that LPS or TNFα facilitate recruitment of neutrophils from vasculature by activating endothelial cells and macrophages and preventing neutrophil migration away from these sites. However, these mediators may serve to distract neutrophils from being recruited to appropriate tissues. The impact of PI3Kγ in acute lung inflammation is exemplified by the lack of adequate *Pneumococcus* clearance in the PI3K$\gamma^{-/-}$ mice or PI3Kγ inhibitor pretreated mice (Maus, Von Grote et al. 2002). This might affect immune surveillance in remote organs. This

situation is further compounded by the fact that LPS from certain organisms activates complement resulting in the generation of chemoattractant such as C5a (Czermak, Breckwoldt et al. 1999).

There are some specific examples of neutrophil recruitment distractors (Hickey, Kubes 2009). Bacterial products such as clostridia toxin damage the vasculature and inhibit microvascular blood flow, thereby limiting neutrophil recruitment and oxygen delivery to the affected site (Hickey, Kwan et al. 2008). *Staphylococcus aureus* expresses numerous such molecules such as complement inhibitor stabilizing C3 convertases which inhibit C3b deposition to affect neutrophil uptake of bacteria and neutrophil chemotaxis (Rooijakkers, Ruyken et al. 2006, Rooijakkers, Ruyken et al. 2005). Some methicillin-resistant *S. aureus* strains express α-type phenol soluble modulin peptides, which induce neutrophil recruitment and activation and subsequently promote neutrophil lysis (Kretschmer, Gleske et al. 2010, Wang, Braughton et al. 2007). Staphylococcal superantigen-like 5 binds to P-selectin glycoprotein ligand 1 (PSGL1), the main ligand of P-selectin, and inhibits rolling of neutrophils on endothelial cells (Bestebroer, Poppelier et al. 2007). *S. aureus* protein CHIPS (chemotaxis inhibitory protein of *S. aureus*) binds to G-protein coupled chemoattractant receptor for C5a and formyl peptides on immune cells, thus inhibiting binding of natural chemotactic ligands (Prat, Haas et al. 2009, Postma, Poppelier et al. 2004). In addition *S. aureus* extracellular adherence protein (Eap) binds to ICAM1 and inhibits β_2 integrin mediated neutrophil adhesion to endothelial cells (Chavakis, Hussain et al. 2002). Understanding of such molecular mechanisms of disruption of neutrophil recruitment in response to bacteria can help in design of better therapeutics.

1.2 . Angiostatin (ANG)

1.2.1. Synthesis of Angiostatin

ANG is the cleavage product of plasminogen and is composed of first four or three *kringle* domains (Wahl, Kenan et al. 2005, O'Reilly, Holmgren et al. 1994). K-5 of plasminogen also shows similar activity (Lu, Dhanabal et al. 1999). The following scheme (Figure 4) depicts conversion of plasminogen to plasmin, reduction of plasmin by phopshoglycerate kinase (PGK) followed by serine proteinase dependent release of *kringle* (K) 1-4½ and finally matrix metalloproteinase (MMP)-dependent trimming of K 1-4½ to K 1-4 or K1-3 (Lay, Jiang et al. 2000).

Generation of angiostatic molecules in non-neoplastic settings has been previously described in *in vitro* as well as *in vivo* settings by proteolysis of membrane-bound plasmin (Falcone et al., 1998). Western blots from cutaneous wound model detect ANG forms and plasminogen as early as day 1 and day 3 after generation of the wounds (i.e., at the initial phase of wound healing). In this model, wound healing is complete after 8 to 9 days. The expression of angiostatin forms peaked at the last phase of wound healing (day 7 after generation of the wounds), and almost disappeared after wound healing was complete at day 10 (Chavakis, Athanasopoulos et al. 2005). PMNs have been shown to mediate the initial angiogenic switch in mouse model of multi-stage carcinoma (Nozawa et al., 2006), release ANG with the help of MMP-9, urokinase (BENELLI, MORINI et al. 2002, Scapini, Nesi et al. 2002). Platelets are well known to produce ANG because of presence of uPA (JURASZ, SANTOS-MARTINEZ et al. 2006). Interaction of uPA with its cellular receptor, urokinase-type plasminogen activator receptor (uPAR) also promotes cellular signaling, which can influence the course of lung inflammation or cancer. A recent finding indicates that PGK interacts with the uPAR mRNA coding region and regulates expression of uPAR at the cell surface (Shetty, Idell 2004).

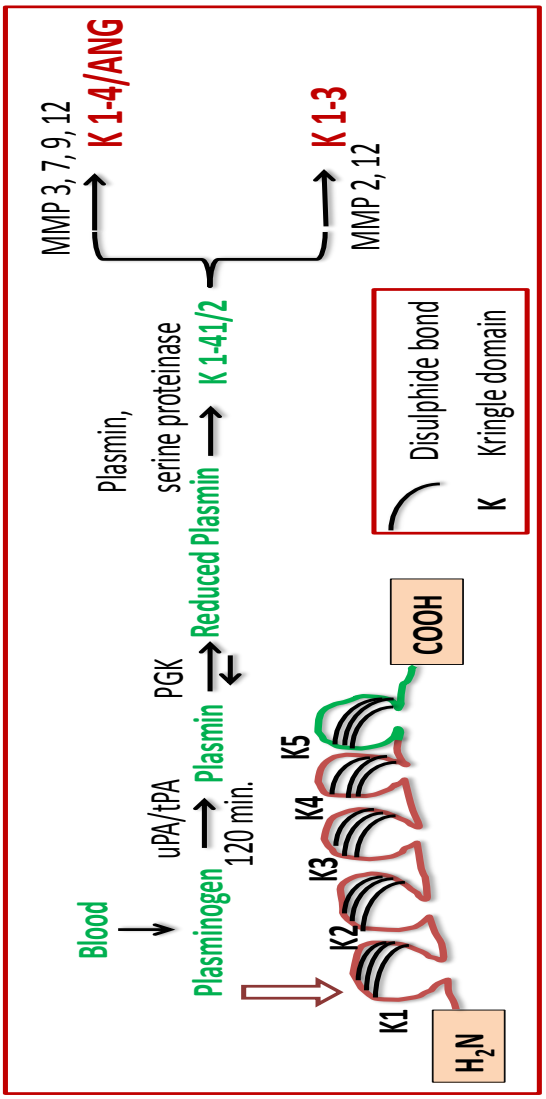

Figure 4: General Scheme of biosynthesis of two major angiostatin forms (K1-4 and K1-3). The rate limiting step for angiostatin biosynthesis is the activation of Plasminogen to plasmin in presence of urokinase (uPA) or tissue type plasminogen activator (tPA). Phosphoglycerate kinase (PGK) acts as a reducing agent. Each kringle (K) is a highly folded domain. K1-4 is termed as angiostatin. K1-41/2 and K5 also show anti-angiogenic activities.

This mechanism represents a potential pathway by which uPAR-dependent responses of the lung epithelium may be controlled in the context of lung injury and repair, neoplastic transformation, or in the growth and spread of lung neoplasms. These extrapolations are yet to be clarified.

1.2.2. Angiostatin Binding Proteins

ANG binds to several endothelial cell surface proteins (Wahl, Kenan et al. 2005, Tabruyn, Griffioen 2007) such as ATP synthase F_1F_0, heat shock protein-27 (hsp-27), annexin II, $\alpha_V\beta_3$ integrin and angiomotin (amot).

1.2.2.1. F_1F_0 ATP Synthase. Binding to F_1F_0 ATP synthase inhibits ATP synthesis and hydrolysis and ultimately leads to a caspase-mediated apoptosis, and direct cell toxicity at low intracellular pH (Chi, Pizzo 2006, Kenan, Wahl 2005, Veitonmäki, Cao et al. 2004, Moser, Kenan et al. 2001), conditions that are fertile for shutting down the oxidative phosphorylation machinery in inflammation and tumorigenesis (Wahl, Kenan et al. 2005). Recently, a monoclonal antibody, MAb3D5AB1, directed against catalytic β-subunit of F_1F_0 ATP synthase displayed similar, but potent, *in vitro* and *in vivo* anti-angiogenic effects compared to angiostatin (Chi, Wahl et al. 2007). Besides, the extracellular nucleotides are emerging as potential inflammatory mediators as depicted by their *in vitro* as well as *in vivo* (Kukulski, Ben Yebdri et al. 2007) chemotactic or transmigratory roles and *in vivo* lung inflammation mediation through dendritic cells (Idzko, Hammad et al. 2007) possibly through variable purinergic receptor activation viz A3, $P2Y_2$, $P2Y_6$ (Chen, Wu et al. 2006). Human lung and blood cells have almost ubiquitously distributed purinergic receptors (Bours, Swennen et al. 2006). Also, the human astrocytoma $P2Y_2$ receptor RGD sequences interact with α_v integrins on these cells to mediate G_{12} chemotactic signaling (Liao, Seye et al. 2007). The functional consequence of angiostatin's binding and inhibition of ATP synthase might as well translate into an anti-inflammatory profile.

1.2.2.2. Heat Shock Proteins. Binding of ANG with heat shock proteins (hsp) 27 and 70 is also concentration and *kringle* dependent (Dudani, Mehic et al. 2007). Hsps are implicated in regulation of stress as their expression increases under heat shock, oxidant exposure and other environmental insults. Hsp 27 has been implicated in cell actin organization, cell growth and migration (Kostenko, Moens 2009).

1.2.2.3. Annexin II, a calcium binding protein that regulates the conversion of plasminogen to plasmin, is also a target of ANG (Syed, Martin et al. 2007, Sharma, Rothman et al. 2006). Annexin II is also a substrate for src tyrosine kinase and protein kinase C that mediate its downstream signaling. Both ANG and plasminogen compete for annexin II binding but ANG has a lower dissociation constant than plasminogen, therefore acting as a physiological antagonist of plasminogen in mediating endothelial apoptosis and inhibition of proliferation (Sharma, Sharma 2007, Tuszynski, Sharma et al. 2002).

1.2.2.4. $\alpha_V\beta_3$ Integrin. ANG also binds to $\alpha_V\beta_3$ integrin (Tarui, Miles et al. 2001) as evidenced by lack of stress fiber formation in Chinese hamster ovary (CHO) cells expressing β_3 integrin subunit and adhered to vitronectin. ANG with multiple *kringles*/integrin binding sites could effectively saturate $\alpha_v\beta_3$ on the cell surface without inducing signals and block the accumulation of plasmin on the cell surface (Tarui, Majumdar et al. 2002). ANG also induces apoptosis by anoikis, which is detachment of cells from the matrix leading to apopotosis. It is interesting that many endothelial and epithelial cells have integrin $\alpha_V\beta_3$ on their apical and basal surface (Singh, Fu et al. 2000). ANG could act through this integrin for aniokis.

1.2.2.5. Angiomotin/Amot belongs to a new protein family with only two additional members characterized by conserved coiled-coil domains and C-terminal PDZ binding motifs (Bratt, Birot et al. 2005, Moreau, Lord et al. 2005, Bratt, Wilson et al. 2002), namely

JEAP/Amot-like 1 and MASCOT/Amot-like 2. The Amot family forms protein-protein complexes with MUPP1 and Patj, with Patj having higher affinity for the Amot family (Sugihara-Mizuno, Adachi et al. 2007). Amot was identified via its interaction with angiostatin in yeast two-hybrid system where it induced focal adhesion kinase (FAK) activity and amot was shown to localize to lamellipodia of migrating endothelial cells (Troyanovsky, Levchenko et al. 2001a). Cell motility and cell-cell junctions are both closely regulated by the actin cytoskeleton and the Rho family of GTPases. It is possible that angiomotin regulates both permeability and motility by influencing the actin cytoskeleton (Gagne, Moreau et al. 2009). There is evidence that relates angiostatin and angiomotin to Rho signaling (Gupta, Nodzenski et al. 2001). Therefore, it would be tempting to further investigate if control of the actin cytoskeleton is at the heart of both properties of angiomotin (Bratt, Birot et al. 2005). Rich1 binds the scaffolding protein angiomotin (Amot) and is thereby targeted to a protein complex at tight junctions (TJs) containing the PDZ-domain proteins Pals1, Patj, and Par-3. Furthermore, the coiled-coil domain of Amot, with which it binds Rich1, is necessary for localization to apical membranes and is required for Amot to relocalize Pals1 and Par-3 to internal puncta. Rich1 and Amot, probably, maintain TJ integrity by the coordinate regulation of Cdc42 and by linking specific components of the TJ to intracellular protein trafficking as shown in MDCK epithelial cells (Wells et al., 2006). Cdc42 is a member of the Rho GTPase family, whose members interact with effectors when bound to GTP and terminate signaling upon GTP hydrolysis (Hall, Nobes 2000, Nobes, Hall 1994).

1.2.3. Anti-proliferative and Apoptotic Effects of Angiostatin

Angiostatin inhibits autophosphorylation of the hypoxia-induced growth factor (HGF) receptor (c-met), as well as downstream events including the phosphorylation of Akt and ERK1/2 in endothelial and smooth muscle cells. The inhibition appeared to be competitive, since

high concentrations of HGF could overcome the inhibition by angiostatin (Wajih, Sane 2003). Akt is a serine/threonine kinase that is rapidly activated as a downstream effector of phosphatidylinositol 3 (PI3) kinase in response to a variety of cytokines and growth factors, including HGF (Nakagami, Morishita et al. 2001). Akt plays multiple roles in cellular homeostasis including the regulation of glucose metabolism (Kohn, Summers et al. 1996), the activation of eNOS (Dimmeler, Fleming et al. 1999), and the suppression of apoptosis (Coffer, Jin et al. 1998). The antiapoptotic effect of Akt may occur through the phosphorylation of the apoptosis-inducing proteins BAD (Datta, Dudek et al. 1997, Del Peso, González-García et al. 1997), caspase-9 (Cardone, Roy et al. 1998), and FKHRL1 (Brunet, Bonni et al. 1999). The activation of Akt is also essential for the induction of a survival pathway involving ligation of $\alpha_v\beta_3$ (or $\alpha_v\beta_5$) and resulting in the up-regulation of bcl-2 expression (Matter, Ruoslahti 2001). The activation of the PI3K-Akt axis by both integrins and growth factor receptors emphasizes the importance of this signal pathway for cell survival. Finally, Akt promotes cell-cycle progression into the S-phase by repressing the expression of $p27^{kip1}$, an inhibitor of the cyclin E/cdk2 complex (Mirza, Kohn et al. 2000).

ANG inhibits the proliferation of EC by down-regulating the protein level of cyclin-dependent kinase (cdk) 5, a cdk absent in quiescent endothelial cells but induced after treatment with bFGF (Sharma, Tuszynski et al. 2004). cdk5 mediated phosphorylation results in inhibition of MAPkinase kinase 1(MEK1) catalytic activity and hence the phosphorylation of ERK1/2 (Sharma, Veeranna et al. 2002). The role of MAP kinase in cellular proliferation, survival and differentiation is well established (Pearson, Robinson et al. 2001). ANG also acts by upregulating the mRNA level of FasL and reducing the level of c-FLIP, which activates the extrinsic apoptotic pathway (death receptor pathway). Treatment of HUVEC with ANG results

in induction of the intrinsic pathway (mitochondrial) by inducing p53, Bax and tBid that lead to the release of cytochrome-c from the mitochondria and the activation of caspase-9 (Chen, Wu et al. 2006). In fact, a recent study also deduces inhibition of mitochondrial proteins such as malate dehydrogenase and ATP synthase as the target site for ANG's antiangiogenic and pro-apoptotic effects in tumor and tumor-endothelial cells (Lee, Muschal et al. 2009b). Nevertheless, ANG activates RhoA upon binding to EC followed by transient increase in ceramide level, which reorganises the actin stress fiber and finally causes cell detachment (Gupta, Nodzenski et al. 2001). ANG-induced apoptosis is restricted to proliferating EC, which also express integrin $\alpha_v\beta_3$ (Hari, Beckett et al. 2000). Interestingly, ANG induces the expression of adhesion molecules (ICAM-1, E-selectin) (Luo, Lin et al. 1998). Several recent findings suggest activation of nuclear factor- κB (NF-κB) to be a common mechanism of angiostatic agents to induce EC apoptosis and to improve immune response (Dirkx, oude Egbrink et al. 2006). Airway epithelium controls lung inflammation and injury through the NF-κB pathway (Cheng, Han et al. 2007). This may be another possible pathway for ANG to show an anti-inflammatory action in lung. ANG has recently been reported to upregulate the expression of antiangiogenic IL-12 (Albini, Brigati et al. 2009). Most of the mechanistic data in the field of ANG has been derived from secondary tumor inhibition studies. Ample evidence indicates the protective and therapeutic role of ANG in treatment of various cancers like breast, prostate, small-cell lung advanced colorectal and renal cancer (de Castro Junior, Puglisi et al. 2006). In an explicitly studied angiogenesis model, differentiating eight stages of angiogenic cascade *in vitro*, angiostatin invariably caused inverse angiogenesis irrespective of the stage at which angiostatin was added (Bahramsoltani, Plendl 2007). Overall, these data suggest a broad range of receptors for the ANG and many modes of action although specifics of actions are far from fully understood.

1.2.4. Inflammation and Angiostatin

ANG levels are reportedly increased in acute respiratory distress syndrome and septic patients (ARDS) (Hamacher, Lucas et al. 2002, Lucas, Lijnen et al. 2002, Singh, Janardhan et al. 2005). Interestingly, there are no data on the expression of ANG in endotoxin-induced acute lung injury or animal models of lung inflammation. Similarly, increasing amounts of ANG and related peptides coupled with degradation of plasminogen and lower levels of plasmin have been reported in wound fluid from chronic venous leg ulcers (Smith, Hoffman 2005, Hoffman, Starkey et al. 1998). ANG, through interaction with Mac-1 ($\alpha_M\beta_2$) integrin as well as reduced activation of NF-κB and related tissue factor expression, suppresses inflammation by inhibiting peripheral blood leukocyte recruitment and angiogenesis in a mouse model of acute peritonitis (Chavakis, Athanasopoulos et al. 2005). ANG inhibits HIV-Tat-induced inflammatory angiogenesis (Benelli, Morini et al. 2003), causes defective colonic healing (te Velde, Kusters et al. 2003) and has been also shown to inhibit macrophage migration by disrupting their actin cytoskeleton in mouse atheromas (Perri, Annabi et al. 2007, Moulton, Vakili et al. 2003). ANG reduces monocyte chemoattractant protein-1 levels, T-cell and macrophage infiltration in chronic kidney injury (Mu, Long et al. 2009).

1.3. Synchrotron Imaging

Synchrotron produces the light by using powerful electro-magnets and radio frequency waves to accelerate electrons to nearly the speed of light. Energy is added to the electrons as they accelerate so that, when the magnets alter their course, they naturally emit a very brilliant, highly focused light (http://www.lightsource.ca/education/pdf/materials/SSSRCBooklet_Final_B.pdf). The Canadian Light Source (CLS) has four major components (Figure 5):

i) **Electron gun and linear accelerator.** An electron gun that produces pulses of electrons via high voltage electricity through heated cathode. The electron gun supplies electrons to

the Linear Accelerator (LINAC). The electrons are accelerated by microwaves to 250 MeV.

ii) **Booster ring.** Microwaves further accelerate the electrons by increasing the energy from 250 MeV to 2900 MeV.

iii) **Storage ring.** Insertion devices like wigglers and undulators bend the beam many times over very short distances.

iv) **Beamlines and End-stations.** High-speed high-energy electrons accelerated or bent by powerful magnets produce an extremely brilliant, full spectrum beam of photons known as synchrotron light. There are fourteen beamlines and eight other under construction at CLS. Monochromators split the synchrotron light into portions of electromagnetic spectrum which is then focussed with specially curved mirror systems. The selected wavelength of synchrotron light is directed onto the sample and detected with specialized detectors depending upon the application.

Synchrotron sources of light pack more photons into a smaller beam of light as shown in Figure 5 left panel.

Dynamic imaging of small lung airways remains a challenge despite wide strides in imaging relatively static tissue beds. X-rays are still the only available diagnosis for lung pathologies that utilise absorption to highlight the hard tissue from soft tissue. However, this does not resolve soft tissues such as lungs. Positron emission tomography and magnetic resonance imaging offer 3D imaging of soft tissue excluding small airways of lungs. Synchrotron radiation computed tomography (SRCT) offers the highest level of spatio-temporal resolution for pre-clinical X-ray CT such as dynamic lung imaging through dual-energy SRCT and K-edge subtraction (KES) imaging using iodine or xenon as contrast agent allows simultaneous functional and

morphological studies, perfusion measurements of any organ like brain and all this can be achieved with comparably low radiation doses (Adam, Bayat et al. 2009).

1.3.1. Phase Contrast Imaging. Phase contrast x-ray imaging utilizes refractive index variations (phase information) in addition to conventional absorption information to produce x-ray images of tissues with greatly enhanced contrast, compared with conventional x-ray absorption techniques. It is able to achieve this because the parameter describing the phase shift of the x-rays is generally more than three orders of magnitude greater than the absorption term over the diagnostic x-ray energy range (20 keV–90 keV) (Lewis, Yagi et al. 2005). As a result, the phase shift of an x-ray beam propagating through tissue can be much larger than the absorption change and if phase effects are rendered visible they can enhance image contrast. An important consequence of this is that phase contrast images can be recorded with significantly lower dose than conventional images (Lewis 2004) which is particularly important for both longitudinal studies and dynamic studies especially those requiring repeated imaging.
Several techniques have been employed to realize phase contrast x-ray imaging, but in the experiments reported here, I utilized the simplest method which is known as propagation-based phase contrast imaging (Wilkins, Gureyev et al. 1996, Snigirev, Snigireva et al. 1995).This modality is a form of in-line holography, which has alternatively been named ‘refraction enhanced imaging (Suzuki, Yagi et al. 2002, Yagi, Suzuki et al. 1999). The method is straightforward and differs from conventional x-radiography only in that the object and detector are separated by a sufficient distance to allow the refracted rays to diverge from the undeviated ones. The amount of phase contrast depends upon the object–detector separation. If this is small, as in the conventional x-ray imaging, the deviated and the undeviated x-rays are not resolved by the detector and no phase contrast is observed. The technique works with both coherent

synchrotron radiation (Snigirev, Snigireva et al. 1995) and conventional micro-focus x-ray sources (Wilkins, Gureyev et al. 1996). However, the unique properties of synchrotron radiation, in particular its brightness, make it ideal for these experiments. The small source size and inherent collimation yields excellent phase contrast, whilst the large beam intensity allows monochromatic radiation and short exposure times. With this configuration and a high-speed detector, it is possible to acquire dynamic images with relative ease.

1.3.2. Diffraction Enhanced Imaging (DEI) derives contrast from an object's X-ray absorption, refraction gradient and ultra-small angle x-ray scatter properties (extinction) (USAXS) (Figure 6a) (Hasnah, Chapman 2008, Chapman, Pisano et al. 1998, Chapman, Nesch et al. 2006). Images are acquired with analyser crystal set on each side of the rocking curve. The analyser crystal serves to diffract the beam from the object that is dependent upon the refractive index differences within the object in addition to X-ray absorption and scattering (Chapman, Thomlinson et al. 1997).

Lungs are an excellent choice for DEI due to its soft tissue, air-filled alveoli that scatter light. This scattering is a metric of the projected number of air filled alveoli (Figure 6b). Thus, a larger amount of scatter implies a larger number of air filled alveoli. This scatter is reflected in the width of the scattering distribution measured with DEI. The DEI images can be obtained over both sides of the rocking curve that are indicative of the scatter produced by lungs. Synchrotron imaging may be highly useful in evaluating dynamics of lung inflammation and to investigate the therapeutic impact of new drugs on lung inflammation.

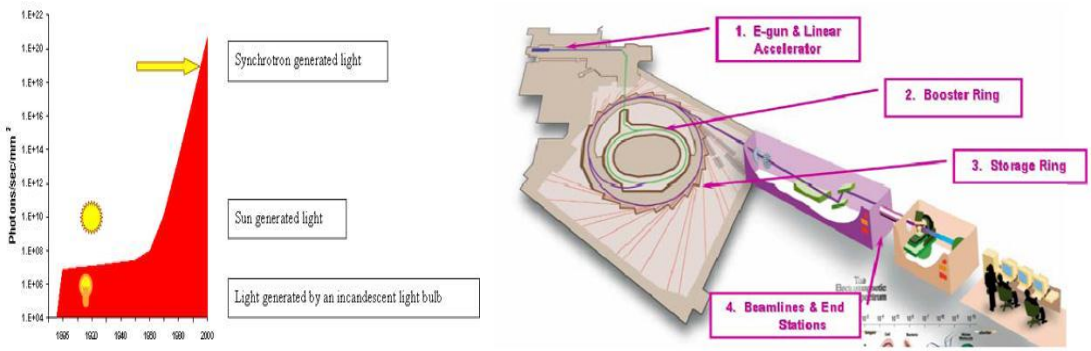

Figure 5: Left panel shows synchrotron light flux. Right figure shows the four components of CLS (Reproduced from http://www.lightsource.ca/education/pdf/materials/SSSRCBooklet_Final_B.pdf).

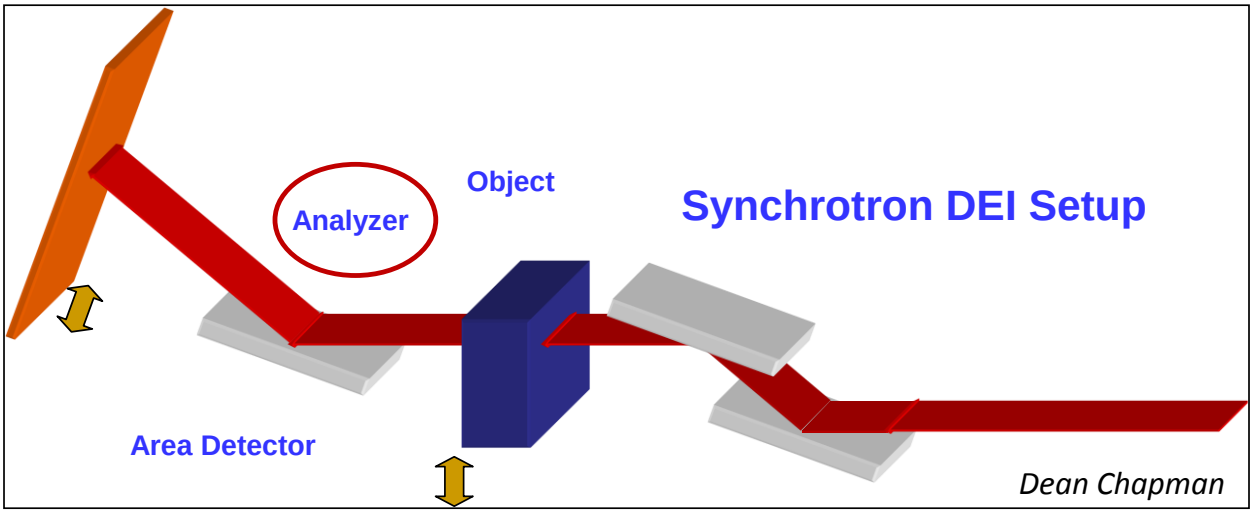

Figure 6a: Schematic arrangement of the diffraction-enhanced imaging or analyzer-based imaging system. The beam, monochromatized by a perfect crystal pair (monochromator), is passed through the object and then is analyzed by a matching crystal. (Reproduced from Chapman, 2011).

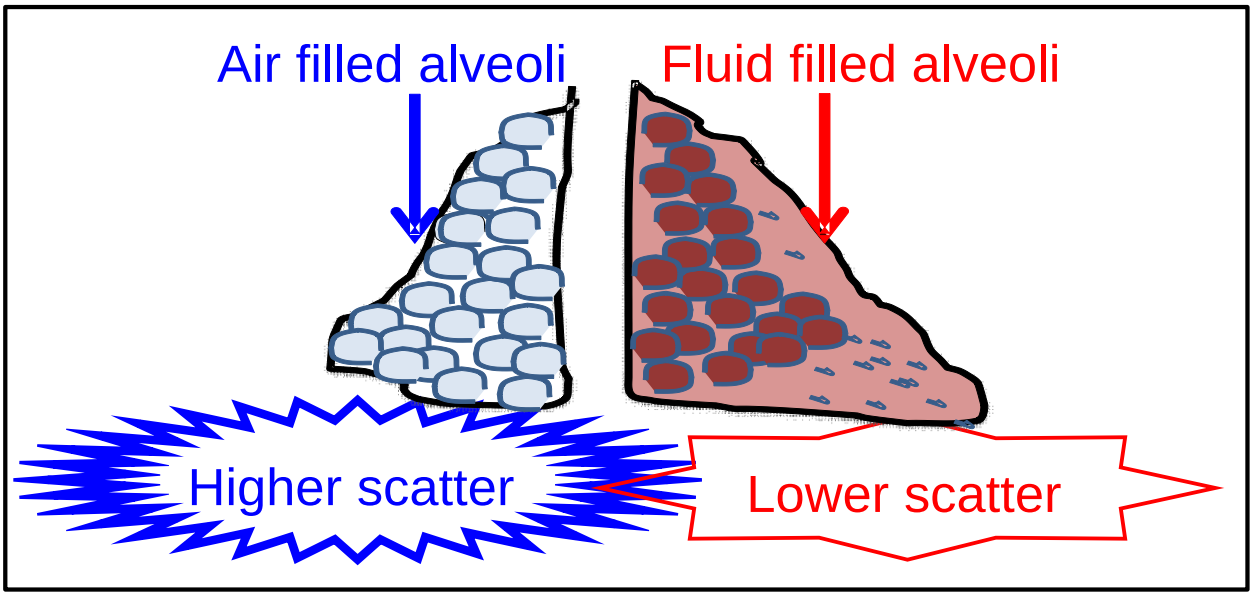

Figure 6b: A schematic illustrating scatter properties of lungs. Scattering is a metric of the projected number of air filled alveoli. For details refer text.

1.4. Summary and Conclusions

So far we have understood that neutrophils are the prime cells recruited and activated in response to an acute inflammatory stimulus. Acute lung injury involves a wide subset of diseases that result in high mortality principally due to lung and liver damage. The mechanisms of directed neutrophil recruitment are many with still a lot of unifying mediators left to be understood especially in lung. As ANG is an antiangiogenic molecule with potential anti-migratory activities as described *in-vitro* and in peripheral acute inflammation model in mice (BENELLI, MORINI et al. 2002), my study was designed to study the specific role of ANG in acute lung injury and on neutrophil biology.

CHAPTER 2

HYPOTHESES AND OBJECTIVES

2.1. Hypotheses:

1. ANG inhibits neutrophil chemotaxis and activation by binding to $\alpha_v\beta_3$ integrin.
2. ANG inhibits leukocyte migration under flow conditions.
3. ANG inhibits acute lung injury in mice.

2.2. Objectives:

1. To characterize the role of ANG on neutrophil biology and study ANG binding proteins
    a. To evaluate the effect of ANG on isolated mice and human neutrophil chemotaxis and activation in response to fMLP and LPS respectively.
    b. To image putative ANG binding proteins for co-localization like $\alpha_v\beta_3$ integrin, F_1F_0 ATP synthase, hsp-27 and angiomotin in activated neutrophils using confocal imaging.
2. To study the role of ANG on leukocyte recruitment in cremaster muscle.
3. To characterize the ANG function in LPS induced mice model of acute lung injury and to see real-time lung dynamics and evaluate the role of ANG in mice imaged through DEI and phase-contrast imaging.

2.3. Rationale for the Conducted Experiments

i.) Chemotaxis of activated neutrophils is an essential early step in host defense towards the site of injury. Activated neutrophils live longer and are responsible for collateral tissue damage and multiple complications in the injured organs (Witko-Sarsat, Rieu et al. 2000, Witko-Sarsat 2010) through release of inflammatory products like proteinases, cationic

polypeptides, cytokines and reactive oxygen species (ROS) (Witko-Sarsat, Rieu et al. 2000, Dallegri, Ottonello 1997, Haslett 1999, Haslett, Savill et al. 1989, Witko-Sarsat 2010). As a first step towards understanding the effect of ANG on neutrophil chemotaxis, I chose to observe the uptake and molecular actions of ANG on isolated mice and human neutrophils towards bacterial chemotactic peptide, fMLP. The uptake of ANG by normal and activated neutrophils was explored through evaluation of various putative ANG receptors such as $\alpha_v\beta_3$ integrin, F_1F_0 ATP synthase, hsp-27, and angiomotin. Because there are very little data on the actions of ANG on the chemotaxis of neutrophils, I examined the actions on cell signaling, cytoskeletal reorganization, cell activation and apoptosis through the use of various methods.

ii.) There is a need to evaluate new molecules to modulate the behavior of neutrophils *in vivo* to fine-tune inflammatory responses. In second set of experiments, I examined actions of ANG on leukocyte migration under flow conditions through measurement of various steps such as tethering, rolling, crawling, and transmigration that are involved in the migration of neutrophils (Ley, Laudanna et al. 2007), (Liu, Kubes 2003). I imaged the neutrophil recruitment in a cremaster model of TNFα-induced neutrophil migration. This technique has been standardized for unbiased quantification of leukocyte migration *in-vivo* (Cara, Kubes 2003).

iii.) Acute lung injury is characterized by the migration of activated neutrophils into lung vasculature and alveoli (Matute-Bello, Martin 2008, Perl, Lomas-Neira et al. 2008). These activated neutrophils live longer and cause significant tissue damage through inflammatory products like proteinases, cationic polypeptides, cytokines and reactive oxygen species (ROS) (Witko-Sarsat, Rieu et al. 2000, Dallegri, Ottonello 1997, Haslett

1999, Haslett, Savill et al. 1989, Witko-Sarsat 2010). The paradox of neutrophil biology is highlighted by the fact that although activated neutrophils are essential for clearing of bacteria, the tissue damage caused by them is believed to be the cause of organ failure, morbidity and mortality. ANG levels are reportedly increased in acute respiratory distress syndrome patients (Hamacher, Lucas et al. 2002, Lucas, Lijnen et al. 2002), which along with high levels of TNF-α have been implicated in *in vitro* endothelial cell cytotoxicity that is indicative of its potential role in ARDS-related EC injury (Hamacher, Lucas et al. 2002). Currently, there are no data on the effects of ANG in acute lung injury. Therefore, role of ANG was investigated in mouse model of lipopolysaccharide-induced acute lung injury. Intranasal bacterial endotoxin was utilized, which is a well established and non-invasive model of lung inflammation (Szarka, Wang et al. 1997).

iv.) Lastly, I imaged real-time lung dynamics using state-of-the art synchrotron radiation facility at Canadian Light Source (CLS), housed at University of Saskatchewan. This study was undertaken with two objectives in mind, one to establish an imaging system for live mice lung imaging and secondly to evaluate the role of ANG in this imaging system. Lungs are an excellent choice for DEI due to its soft tissue, air-filled alveoli that scatter light. This scattering is a metric of the projected number of air filled alveoli. This allows time-dependent imaging in a mouse avoiding need of higher number of animals required for understanding ALI dynamics in a conventional model. Diffraction enhanced imaging (DEI) and phase contrast imaging modalities were utilized for this study. The basic mice model of ALI was same as in the above stated *in-vivo* ALI study. At the end of imaging, lungs were collected for histology to re-affirm my findings.

CHAPTER 3
ANGIOSTATIN INHIBITS NEUTROPHIL MIGRATION AND ACTIVATION

3.1. Abstract

Angiostatin is an anti-angiogenic molecule. I studied the role of angiostatin in neutrophil recruitment *iv-vivo* and *iv-vitro*. Angiostatin inhibited MAPK signalling, cytoskeletal reorganization and formation of leading edge in neutrophils activated with fMLP and LPS. Angiostatin blocked formation of reactive oxygen species, activated caspase-3 and induced apoptosis in pre- as well as post-LPS-activated neutrophils. Finally, the data show reduced adhesion and emigration of neutrophils in post-capillary venules in TNFα-treated cremaster muscle.

3.2. Introduction

Many acute inflammatory conditions such as peritonitis, pneumonia, sepsis, or sterile injury are marked by chemotaxis of activated neutrophils, an essential early step in host defense, towards the site of injury. Activated neutrophils live longer and are responsible for collateral tissue damage and multiple complications in the injured organs (Witko-Sarsat, Rieu et al. 2000, Witko-Sarsat 2010). Therefore, one of the critical needs is to identify molecules to regulate neutrophil migration and to silence activated neutrophils to prevent exuberant tissue damage. Directed neutrophil migration is explained through signal-centred and pseudopod-centred theories. Both these theories approach directionality through specific signalling molecules or development of one of the random pseudopods up the chemoattractant gradient (Insall 2010, Insall, Machesky 2009). At a molecular level, filamentous (F) actin aggregation supports extension of a major pseudopod also known as the leading edge. Chemoattractants bind to G-protein coupled receptors that signal through βγ subunits via GTP bound small G-proteins like Rho, Rac, cdc42. Two functionally antagonistic enzymes, guanine nucleotide exchange factors

(GEFs) such as DOCK2 and GTPase activating protein (GAP) like p190 Rho GAP regulate GTP levels for its continuous recycling during adhesion-deadhesion in neutrophil chemotaxis. During these events the microtubule complex destabilizes through hsp-27 phosphorylation in favour of a major pseudopod (Jog, Jala et al. 2007, Hino, Hosoya 2003). Actin and microtubule filaments, therefore, are the primary cytoskeketal filaments involved in neutrophil chemotaxis.

Angiostatin (ANG) binds to several cell surface proteins 7, 8 such as ATP synthase F_1F_0, heat shock proteins (hsp)-27 (Dudani, Mehic et al. 2007), annexin II (Syed, Martin et al. 2007),(Sharma, Rothman et al. 2006), $\alpha_V\beta_3$ integrin (Tarui, Miles et al. 2001) and angiomotin (AMOT) (Troyanovsky, Levchenko et al. 2001b) induces anoikis and apoptosis, and inhibits endothelial and epithelial cell migration. Integrin $\alpha_v\beta_3$ is of particular interest in this context as it is expressed on the apical and basal surfaces of endothelial and epithelial cells (Singh, Fu et al. 2000). AMOT can bind to Rho GAP through coiled-coil or PDZ domains and induce a polarised scaffold in haptokinetic cells. ANG inhibits peripheral blood leukocyte recruitment and angiogenesis in a mouse model of acute peritonitis (Chavakis, Athanasopoulos et al. 2005). The detailed and precise molecular mechanisms of effects of angiostatin on neutrophil biology are not known. I report the novel data that angiostatin silences activated neutrophils through inhibition of MAPK cell signals, cytoskeletal reorganization, reactive oxygen species formation and induction of activated caspase-3. Angiostatin also inhibits neutrophil migration in an *iv-vivo* model of inflammation.

3.3. Materials and Methods

Lipopolysaccharide, LPS 0127:B8 (L4516) , Cytochalasin D (C2618), FluoroTag FITC Conjugation Kit (FITC1) and Methyl-β-cyclodextrin (C4555) were obtained from Sigma Chemicals, (St. Louis, MO, USA); angiostatin K1-4 was from Haematologic Technologies Inc.,

(Essex Junction, VT, USA); recombinant murine TNFα, R&D Systems, (Minneapolis, MN, USA), Vectashield Hard Set Mounting Media with DAPI from Vector Laboratories, (Burlingame, CA, USA). Rhodamine phalloidin, reduced mitotracker orange (M7511), IMAGE-iT LIVE Green ROS Detection Kit (I36007), Alexa fluor 633 conjugated secondary goat anti-rabbit (A2107) and anti-mouse (A21052) antibodies were purchased from Invitrogen, (Carlsbad, CA, USA). Alexa 555 anti-α-tubulin (05-829X-555), β_3 blocking antibody clone LM609 (MAB1976H) were from Millipore, (Billerica, MA, USA). Mouse anti ATP synthase β subunit primary antibody (ab5432) was purchased from Abcam, (Cambridge, MA, USA). Donkey anti-goat allophyocyanin conjugated secondary antibody (sc-3860), goat anti-mouse β_3 subunit (sc-6627), goat anti-angiomotin s-20 (sc-82494) and rabbit anti-phospho HSP-27 ser82 (sc-101700) were from Santa Cruz Biotechnology Inc., (Santa Cruz, CA, USA). Rabbit anti-phospho p38 MAPK (4511) and anti-phospho p44/42 MAPK (4370) antibody were from New England Biolabs Inc., (Ipswich, MA, USA). Rabbit anti-cleaved caspase-3 antibody (IMG 5700) was from Imigenex, (San Diego, CA, USA). Mouse anti-flotillin-1 (610820) and anti-flotillin-2 (610384) was from BD biosciences, (San Jose, CA, USA). All other chemicals (if not specified) were purchased from Sigma Chemicals.

3.3.1. Animal Care Ethics and Human Research Ethics

All the animals and protocols (protocol # 20070065) were approved by Research Ethics Board of University of Saskatchewan, Saskatoon, Canada. Male C57BL/6 mice were procured from Animal Resource Centre and housed at Animal Care Unit at University of Saskatchewan. The study of neutrophils from healthy human volunteers was approved (#10-103), and informed consent was obtained from all subjects.

3.3.2. FITC Conjugation of ANG

Fluorotag kit from Sigma was utilized for ANG conjugation to FITC in order to visualize ANG in neutrophils. An F/P ratio (i.e. FITC to protein ratio) of 4:1 was achieved after conjugation with a final FITC-ANG concentration of 26.7 μg/ml according to small scale production protocol. Extinction coefficient of unconjugated ANG as per manufacturer data sheet is 1.74 at 1 mg/ml.

3.3.3. Isolation of Mice and Human Neutrophils

Briefly, peripheral blood was withdrawn by cardiac puncture after ketamine/xylazine anaesthesia from mice and from intercubital vein of healthy humans. Blood was carefully overlayed onto a discontinuous gradient of Histopaque-1119, 1083 and 1077 according to an established protocol (Nuzzi, Lokuta et al. 2007). After centrifugation at 700g, the neutrophil rich layer at the interface of Histopaque 1119 and 1083 was aspirated. Mice red blood cells (RBCs) were lysed with ACK buffer for 3 minutes whereas human RBCs were subjected to hypotonic lysis and the neutrophil pellet was used for further experiments. The procedure yielded > 95% viable neutrophils upon trypan blue exclusion and staining cytospins for differential leukocyte count.

3.3.4. Confocal Microscopy

Confocal images were taken using Leica TCS SP5 (Germany). Images were acquired using a 63X/1.20 oil objective (Leica Plan Apochromat). Neutrophils were equilibrated for one hour before subjecting them to pre-treatment with PBS, 12.5 μg/ml ANG/FITC-ANG or 100 μM cytochalasin D for 30 minutes after a cocktail of the respective tagging dyes like rhodamine phalloidin in combination with saponin had been added. In case of immunofluorescence, neutrophils were adhered to 12mm circle coverslips coated with fetal bovine serum (FBS) or vitronectin for 5 minutes. Thereafter, neutrophils (0.8×10^6/ml) were stimulated with 1 μM

fMLP for 1 minute or 1 µg/ml LPS for 30 minutes, 4 hours or 8 hours to initiate formation of leading edges or stimulation of MAPKinases or caspase-3 cleavage, respectively. SB230963 was added at 500 nMol/l, U0126 at 1 µMol/l and MCD was added at 1mMol/l for 30 minutes according to the experiment. Neutrophils were immediately fixed with 4% paraformaldehyde for 15 minutes and labelled for standard immunofluorescence labeling (Nuzzi, Lokuta et al. 2007). The slides were mounted with vector hard setting mounting media that contained DAPI for identification of nuclear morphology.

For the ROS assay, neutrophils were pre- or post-treated with ANG where necessary followed by 1 µg/ml LPS for 30 minutes and incubated with dye for further 30 minutes before coverslipping and confocal imaging.

For activated caspase-3 staining, neutrophils were either incubated with ANG for 30 minutes followed by LPS 1µg/ml incubations for varying time periods from 2, 4, 6, 8 to 16 hours or 1 µg/ml LPS was incubated for 2 hours followed by 4 hour ANG treatment.

3.3.5. Western Blots

Isolated human neutrophils were subjected to a 30 min treatment with vehicle, ANG, SB 230963 or U0126 before activating them with 1 µg/ml LPS for 30 minutes. The reaction was terminated by adding cold lysis buffer followed by extraction and centrifugation. Equal protein across groups was loaded and subjected to electrophoresis in 12% SDS-PAGE (180 V), transferred onto nitrocellulose membrane (100 V, 60 min.), blocked with 5% BSA-0.1% PBST and immunoblotted for phoshorylated p38 MAPK, p44/42 MAPK or phsp-27. Membranes were washed with 2.5% BSA-0.05% PBST and developed with chemiluminescence using GE ECL blot detection reagent.

3.3.6. Intravital Cremaster Muscle Preparation

To evaluate the effects of ANG on leukocyte adhesion and emigration *iv-vivo*, I performed intravital microscopy of the cremaster muscle. Mice were divided into four groups: negative control saline treated (n=10), positive control TNFα treated (n=9), ANG treated (n=5) and TNFα + ANG treated (n=5). TNFα was injected intrascrotally at a concentration 0.5 μg/0.05 ml, 3 hours prior to recording. For TNFα + ANG group, ANG was employed along with TNFα at a dose of 260 μg/mice intrascrotally in a 0.1ml volume. Mice were anaesthetized at a dose of 100 mg/kg ketamine + 10 mg/kg xylazine intraperitoneally. The cremaster muscle was carefully exteriorised to avoid activation and tied onto a custom made cremaster board (University of Saskatchewan, Engineering shop). The muscle was neither stretched too far nor was it let loose on the stage. After 30 minute stabilization, an unbranched post-capillary venule of 25-40 μm diameter was recorded for 5 minutes at 3 h, 3.5 h, 4 h, 4.5 h and 5h time points after specific treatment. An infra-red lamp maintained the body temperature in case of any anaesthetic-induced hypothermia. During the entire experiment, the muscle was superfused with bicarbonate buffer continuously bubbled with air to maintain a pH of 7.4. A BX51 Olympus microscope with a Gibraltar stage was utilized for capturing brightfield images with 10X and 20X objectives coupled to cannon high definition digital video recording. At the end of the experiment, heparinised peripheral blood was withdrawn by cardiac puncture for total and differential leukocyte counts, and cremaster tissue was fixed in 4% paraformadehyde for H&E staining.

For image analysis, the recorded video sequences were projected onto a monitor and analysed off-line for rolling flux (cells/min), rolling velocity (μm/s), adherent cells per 100 μm vessel segment length and emigrated cells per 100 μm vessel length that include any cells that

had emigrated below or above the vessel in the cremaster preparation. Rolling flux is described as the average number of leukocytes crossing a fixed reference line perpendicular to the axis of flow in one minute. Rolling velocity is calculated by measuring the time required for the first twenty rolling leukocytes to cross a distance of 100 μm along the vessel. Adhesion is defined as the number of leukocytes adhering to the vessel wall for a minimum of 30 seconds within a vessel segment of 100 μm in length. Emigration is defined as the number of cells that can be observed outside the vessel and in the interstitial space within the field of observation at 20X.

3.4. Statistical Analysis

Data from intravital experiments are expressed as means ± SEMs. Shapiro-wilk test was employed for assessing normality of data and equivalence of variance within groups was ascertained by Barlett's test utilizing Stata/SE 10.0 software (Texas, US). Results were analysed by application of one-way ANOVA and unpaired t-test to assess differences between two groups followed by Bonferroni's all group comparison utilizing Graphpad software. A minimum p level of 0.05 was pre-set to establish statistical difference.

3.5. Results

3.5.1. FITC-ANG is internalized only by activated neutrophils and colocalizes with β_3 integrin and lipid raft markers

Immunolocalization of ANG, to visualize its cellular interaction and uptake, is impossible because the available ANG antibody also reacts with plasminogen and other angiostatin forms. I circumvented this problem by conjugating ANG to FITC (fluorescein isothiocyanate) to directly demonstrate surface and cytosolic localization of ANG in the fMLP activated but not resting neutrophils (Figure 7a).

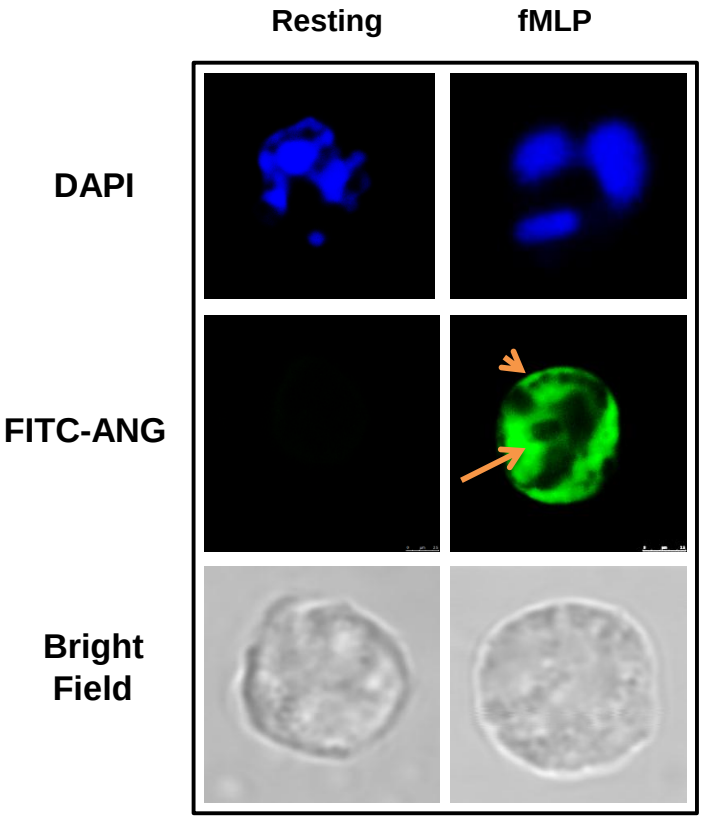

Figure 7a: Localization of FITC-ANG in mice neutrophils. (n=3). Suspended mouse neutrophils (0.8 X 10^6 cells/ml) were pretreated with PBS or 12.5 µg/ml FITC-ANG for 30 min. and then treated with PBS or 1µM fMLP for 1 min. and then fixed with 4% paraformaldehyde for 15 min. before making cytospin slides and then coverslipped using hard-set DAPI mounting media. Note the absence of staining for FITC-ANG in resting neutrophils. Short arrow head indicates the membrane staining and long arrow indicates internalization of FITC-ANG in fMLP activated neutrophils.

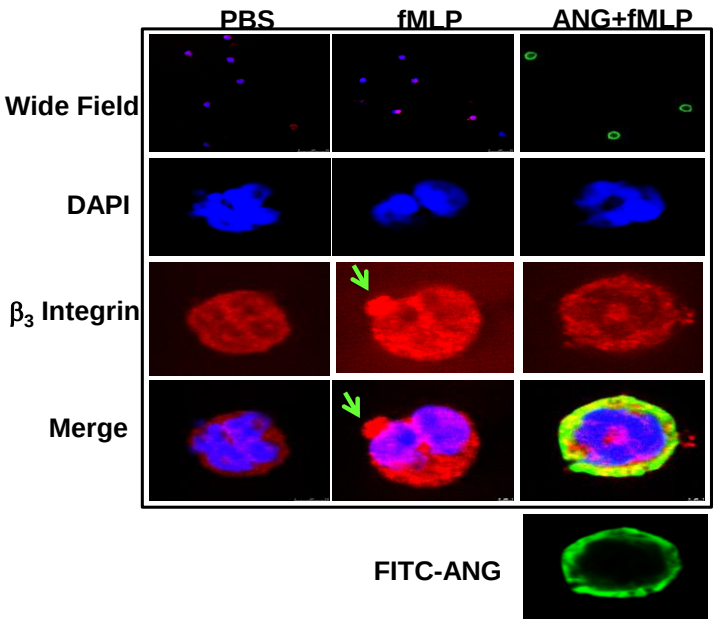

Figure 7b: Localization of β_3 integrin subunit (in red) and FITC-ANG (in green) in PBS or 1µM fMLP (1 min.) stimulated mouse neutrophils (0.8 X 10^6 cells/ml) adhered on FBS coated coverslips. Note attenuation of polarised distribution in ANG group. (n=3) Arrows indicate the polarised distribution of β_3 integrin subunit. Please note that merge for the last treatment group, i.e. ANG+fMLP, shows merge of DAPI (blue), β_3 integrin subunit (red) and FITC-ANG (green).

β_3 integrin is, a receptor of ANG, localized in a Ca2+ dependent manner to the leading edge during chemotaxis on vitronectin (Hendey, Lawson et al. 1996, Lawson, Maxfield 1995). I noticed expression pattern of β_3 integrin in fMLP-stimulated mice neutrophils on vitronectin similar to that of ANG. Also, ANG colocalized with and abolished polarized distribution of β_3 integrins (Figure 7b).

I examined the role of lipid rafts in the uptake of FITC-ANG. Lipid rafts are cell signalling platforms and have a proven role in endocytosis (Singh, Marks et al. 2010). I examined redistribution of lipid raft markers, flotillin-1 and flotillin-2, in fMLP and LPS stimulated human neutrophils along with reduced mitotracker dye as a marker of neutrophil activation. The dye fluoresces upon oxidation and stains mitochondria based on the membrane potential. fMLP as well as LPS light up the reduced dye indicating neutrophil activation (Figure 7c). ANG attenuates the expression of reduced mitotracker in neutrophils activated with fMLP or LPS. Expression of FITC-ANG superimposed on flotillin-2 and flotillin-1 in fMLP or LPS activated neutrophil which suggests a role for lipid rafts in endocytosis of ANG in activated human neutrophils (Figure 7c). To further examine the role of lipid rafts in uptake of FITC-ANG, human neutrophils were pre-incubated with 1 mM methyl-β-cyclodextrin (MCD) that disrupts lipid rafts by depleting cholesterol followed by activation with fMLP. MCD completely inhibited the uptake of FITC-ANG and actin aggregation was restored (Figure 7d).

3.5.2. ANG abolishes formation of leading edges in response to fMLP in neutrophils

Because chemotaxis involves formation of leading edges, also known as pseudopods (Insall 2010), I examined the cytoskeletal dynamics in fMLP-activated mouse and human neutrophils with or without ANG. ANG pre-treatment prevented reorganization of actin

filaments and formation of polarized head (Figure 8a and Figure 8b). Mouse neutrophils treated with cytochalasin D also failed to develop the leading edge (Figure 8a) in response to fMLP. Because ANG has been reported to bind $\alpha_V\beta_3$ integrin (Tarui, Miles et al. 2001), I treated human neutrophils with a humanised function blocking $\alpha_V\beta_3$ antibody (clone LM609) to block the integrin binding with ANG. LM609 blocked actions of ANG and led to polarization evidenced by actin staining pattern (Figure 8b).

3.5.3. ANG stabilises and colocalizes with microtubule network in fMLP-stimulated neutrophils

Microtubules are destabilized in fMLP stimulated neutrophils (Eddy, Pierini et al. 2002). ANG stabilized and co-localized with α-tubulin (tubulin) in fMLP stimulated human neutrophils (Figure 8c and Movie 1). Phosphorylated heat shock protein-27 (phsp-27) and angiomotin (AMOT) are known to interact with ANG (Dudani, Mehic et al. 2007, Wells, Fawcett et al. 2006). As reported by others (Jog, Jala et al. 2007, Hino, Hosoya 2003), I observed colocalization of phsp-27 with tubulin in resting as well as fMLP stimulated human neutrophils, and that fMLP produces a strong polarization of phsp-27 and tubulin. ANG treatment reduced the expression of phsp-27 after fMLP stimulation and stabilized the tubulin network in contrast to the microtubules in fMLP stimulated human neutrophils (Figure 9a). Western blots showed reduced expression of phsp-27 in ANG-treated LPS-activated human neutrophil (Figure 9b).

AMOT is recognised, from a yeast two-hybrid screen, as an ANG binding protein. While it is widely expressed in endothelial and epithelial cells, its transcript is expressed in neutrophils too (BENELLI, MORINI et al. 2002).

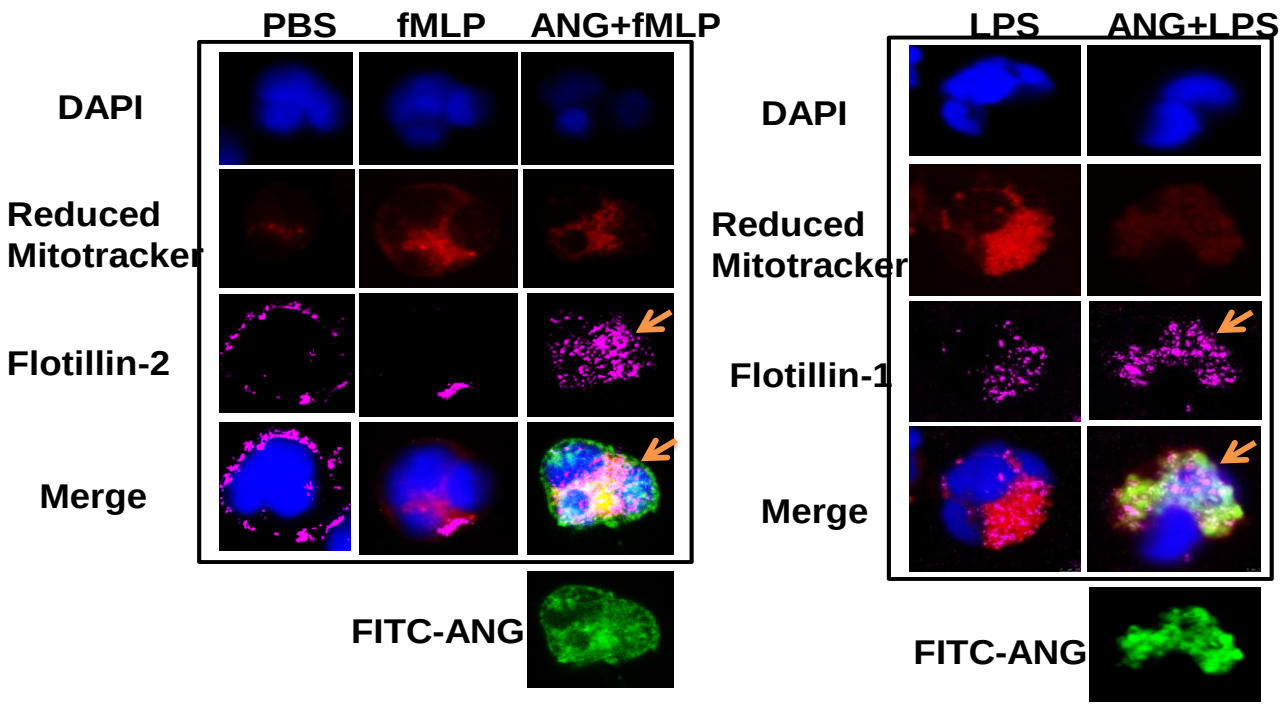

Figure 7c: Immunofluorescence of flotillin-1 and flotillin-2 (in fuschia), reduced mitotracker (in red) and FITC-ANG (in green) in 1µg/ml LPS (30 min.) and 1µM fMLP (1 min.) stimulated human neutrophils (0.8 X 10^6 cells/ml) adhered on FBS coated coverslips. Note attenuation of signal for reduced mitotracker in FITC-ANG incubated cells. FITC-ANG colocalizes with lipid raft markers, flotillin-1 and flotillin-2. (n=3). Arrows indicate flotillin distribution upon ANG and fMLP or LPS treatment. Please note that merge for the last treatment group i.e. ANG+fMLP or LPS show merge of DAPI (blue), reduced mitotracker (red), flotillin (fuschia) and FITC-ANG (green).

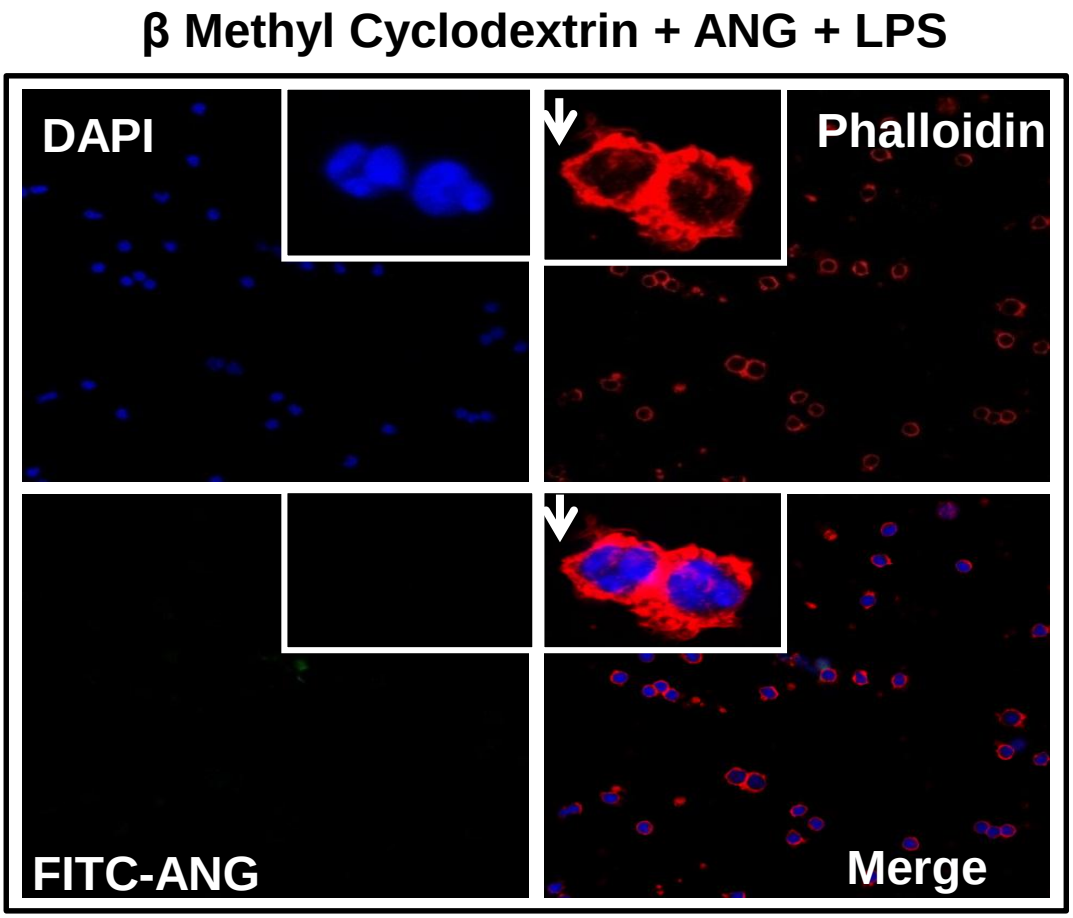

Figure 7d: Localization of Alexa 555 phalloidin (in red) and FITC-ANG (in green) in 1µM fMLP (1 min.) stimulated human neutrophils (0.8 X 10^6 cells/ml) pretreated with 1mM MCD (30 min.) adhered on FBS coated coverslips. MCD treatment abolished uptake of FITC-ANG but does affect cortical actin aggregation and leading edge formation. Arrows indicate leading edge. (n=3)

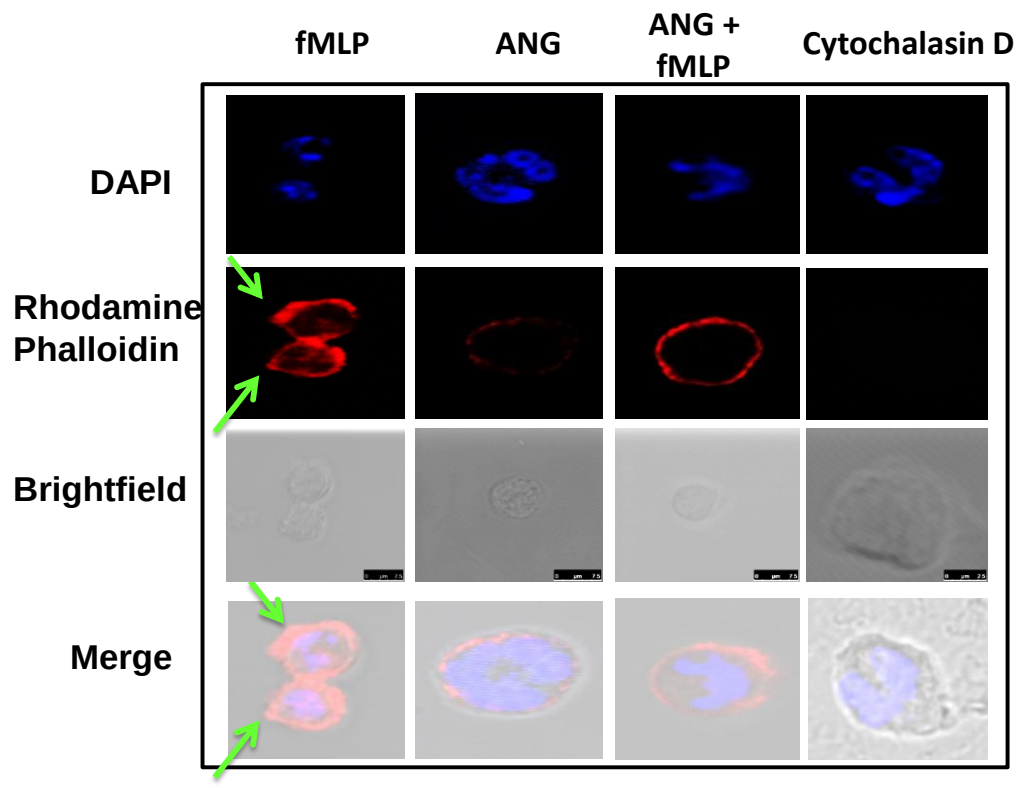

Figure 8a: Effect of ANG on actin cytoskeleton in mice neutrophils. Suspended mouse neutrophils (0.8 X 10^6 cells/ml) were pretreated with PBS or 12.5 µg/ml FITC-ANG or 100µM cytochalasin D for 30 min. and then treated with PBS or 1µM fMLP for 1 min. and then fixed with 4% paraformaldehyde for 15 min. before making cytospin slides and then coverslipped using hard-set DAPI mounting media. Actin is stained in red. Arrows indicate actin aggregation of neutrophils. Note attenuation of polarized head in 1µM fMLP incubated cells treated with ANG. (n=3)

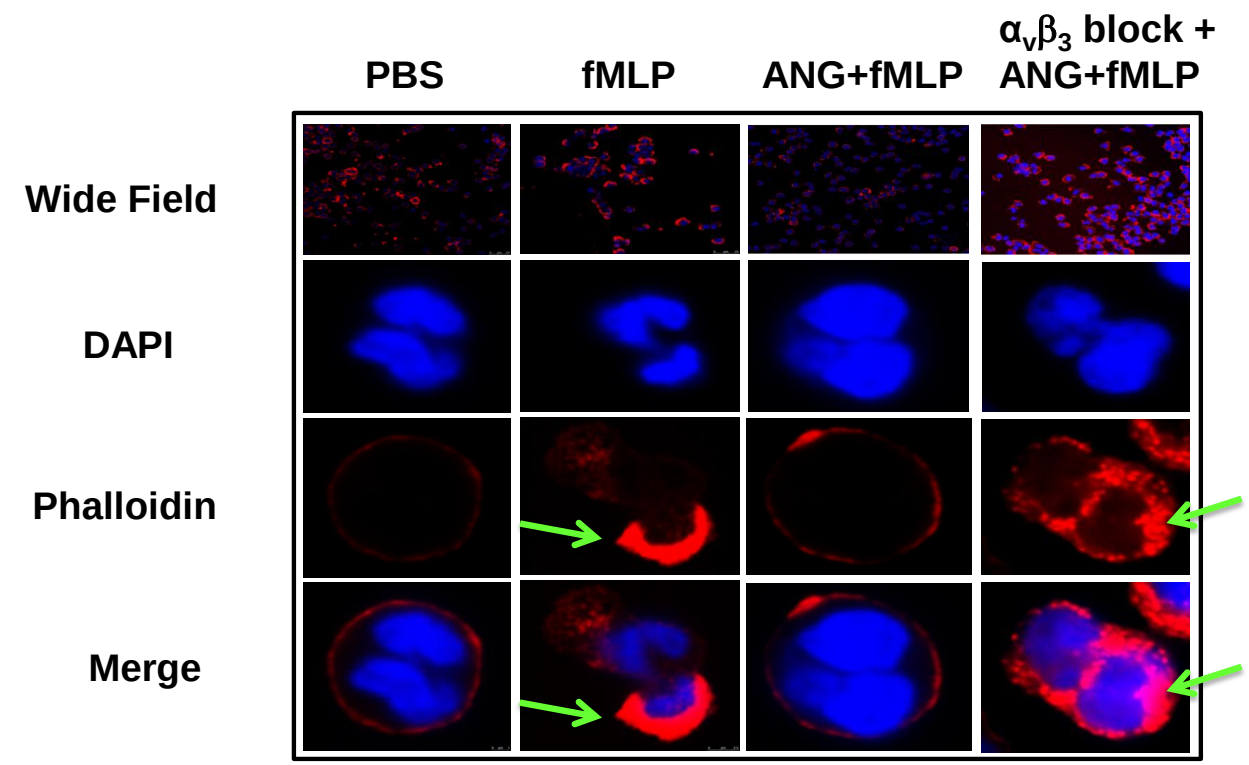

Figure 8b: Localization of actin (in red) and FITC-ANG (in green) in PBS or 1µM fMLP (1 min.) stimulated human neutrophils (0.8 X 10^6 cells/ml) adhered on FBS coated coverslips. Note attenuation of polarized head in fMLP incubated cells treated with 12.5µg/ml ANG. ANG could not abolish aggregation in $\alpha_v\beta_3$ LM609 (1:100 dilution) pretreated neutrophils. Arrows indicate actin aggregation. (n=3)

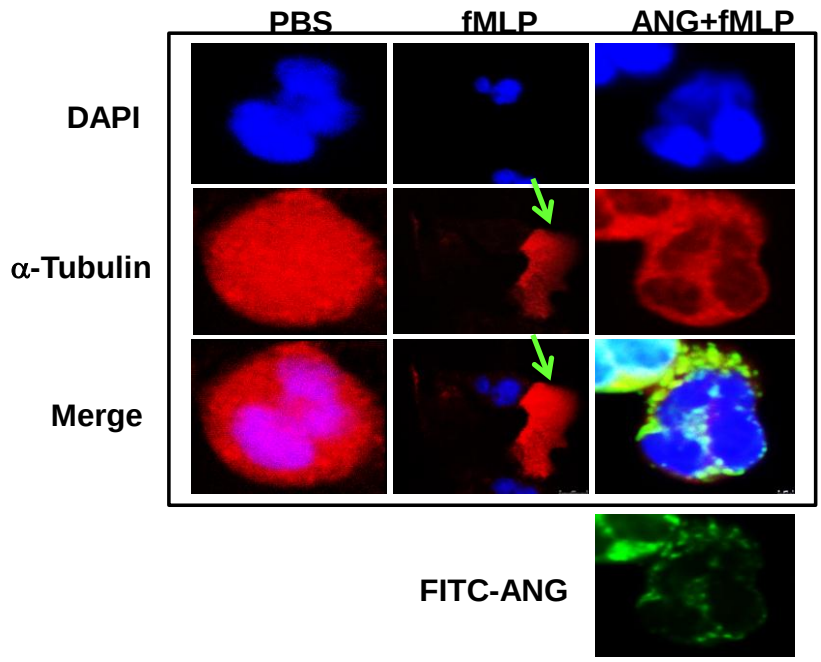

Figure 8c: Localization of α-tubulin (in red) and FITC-ANG (in green) in PBS or 1μM fMLP (1 min.) stimulated human neutrophils adhered on FBS coated coverslips. Note stabilization as well as colocalization of tubulin network with 12.5μg/ml FITC-ANG incubated cells. Arrows indicate destabilized α-tubulin (n=3). Please note that merge for the last treatment group i.e. ANG+fMLP shows merge of DAPI (blue), α-tubulin (red) and FITC-ANG (green).

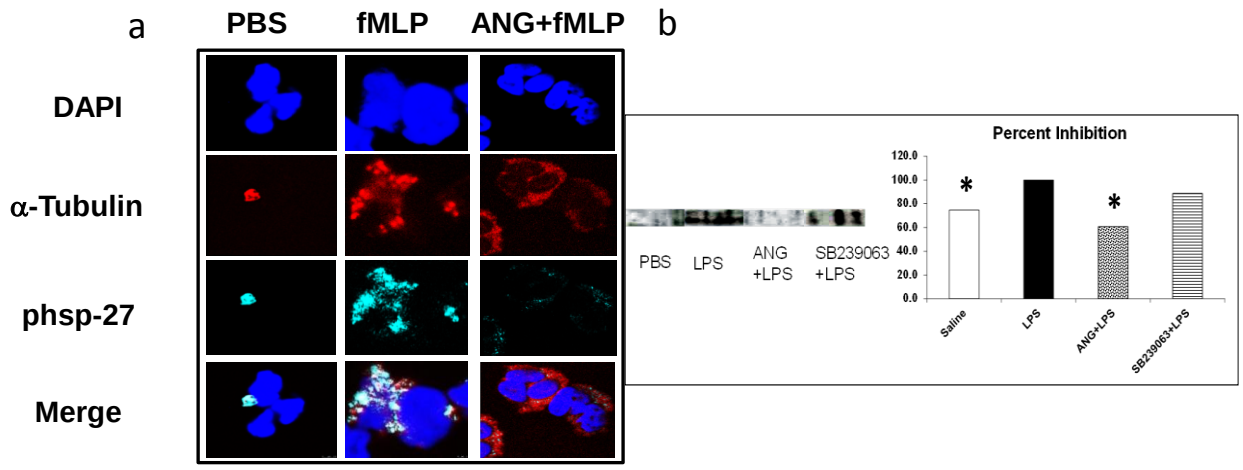

Figure 9a: Immunofluorescence of phosphorylated hsp-27 (phsp-27) (in cyan) and α-tubulin (in red) in fMLP (1 min.) stimulated human neutrophils (0.8 X 10^6 cells/ml) adhered on vitronectin coated coverslips. Note stabilization of tubulin network with 12.5µg/ml ANG+fMLP treated neutrophils. (n=3)

Figure 9b: Expression of phsp-27 in human neutrophil lysates subjected to SDS electrophoresis. Human neutrophils (2 X 10^6/ml) were activated with 1µg/ml LPS for 30 min. Note attenuation of phsp-27 in 12.5µg/ml ANG as well as 500nM SB239063 treated neutrophils. The graph depicts percent inhibition of the expressed protein where LPS represents 100% of the protein. Statistical differences at $p < 0.05$ are indicated by asterisks (*).

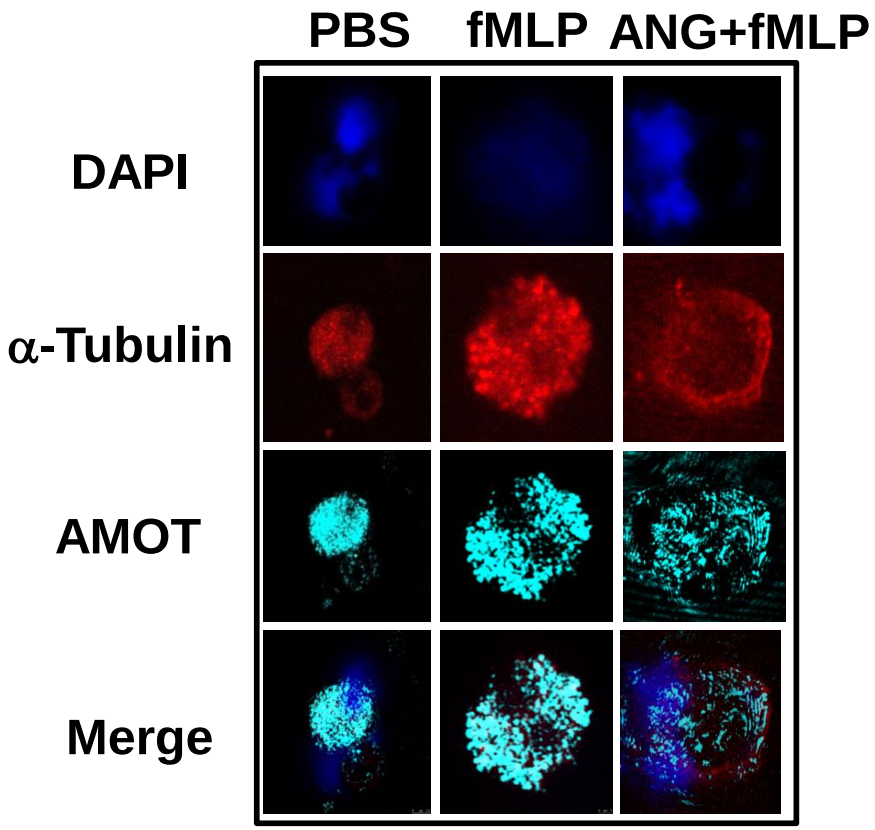

Figure 9c: Immunofluorescence of angiomotin (AMOT) (in cyan) and α-tubulin (in red) in 1μM fMLP (1 min.) stimulated human neutrophils (0.8 X 10^6 cells/ml) adhered on vitronectin coated coverslips. Note stabilization of tubulin network with ANG+fMLP treated cells. (n=3)

Moreover, AMOT possesses various conserved domains such as the coiled-coil, PDZ binding, proline rich and ANG binding domain (Bratt, Wilson et al. 2002, Bratt, Wilson et al. 2003). AMOT co-localized with the tubulin network in resting as well as fMLP-treated human neutrophils (Fig. 9c).

fMLP induces polarization of AMOT as well as the alpha-tubulin (Figure 9c). ANG pretreatment stabilized the tubulin and reduced expression of AMOT (Figure 9c). Collectively, ANG's effects on phsp-27, alpha-tubulin and AMOT may result in inhibition of chemotaxis and promote maintenance of cell shape in activated neutrophils.

3.5.4. ANG co-localizes with mitochondria in vitronectin adhered neutrophils

Neutrophil activation involves mitochondrial reorganization in order to orchestrate chemotaxis, phagocytosis and ROS production (Fossati, Moulding et al. 2003). Mitochondrial ATP synthase, upon translocation to the plasma membrane, is proposed to bind ANG (Lee, Muschal et al. 2009a). Reduced mitotracker dye, which binds to mitochondria in the presence of reactive oxygen species, stained active mitochondria in fMLP or LPS-activated mouse and human neutrophils in suspension or those adhered to fetal bovine serum or vitronectin (Figure 10a). FITC-ANG attenuated the expression of reduced mitotracker dye in suspended or adhered neutrophils treated with LPS or fMLP (Figure 10a). Mouse neutrophils stimulated with LPS and adhered to vitronectin showed partial co-localization of ANG with reduced mitotracker dye (Figure 10a; Movie 2). Furthermore, ANG attenuated F_1F_0 ATP synthase expression in LPS–stimulated human neutrophils (Figure 10b, 10c).

3.5.5. ANG shuts down p38MAPK signalling and reactive oxygen species formation (ROS)

I investigated the impact of ANG on MAPK because p38 MAPKinase is implicated in cell migration signalling (Niggli 2003, Spisani, Falzarano et al. 2005) and p44/42 MAPKinase or ERK1/2 is involved in activation of NADPH oxidase required for generation of reactive oxygen species (ROS) (Markvicheva, Gorokhovatskii et al. 2010). Mouse as well as human neutrophils activated with LPS show strong expression for phosphorylated p38 and p44/42 MAPKinases (Figures 11a, 11b, 11d) and ANG attenuates their expression (Figures 11a, 11b, 11d). Western blots also showed that ANG treatment attenuated the expression of phosphorylated p38 and p44/42 MAPK (Figures 11c and 11e). p38 and p44/42 MAPKinase inhibitors SB239063 and U0126, respectively, reduced the expression of respective MAPK (Figures 11c and 11e) in LPS-stimulated human neutrophils.

Furthermore, ANG attenuated ROS production in LPS-treated human neutrophils (Figures 12a and 12b) hence confirming my earlier observation where ANG attenuates reduced mitotracker dye which is a preliminary dye for determining the redox status (Figure 10a). ROS production was observed in neutrophils by using carboxy-H2DCFDA (5-(and 6-)carboxy-2',7'-dichlorodihydrofluorescein diacetate), a reliable fluorogenic marker for reactive oxygen species in live cells. ROS production was reduced in neutrophils even when they were activated with LPS before treatment with ANG (Figures 12a and 12b).

3.5.6. ANG induces apoptosis in LPS-activated human neutrophils

LPS is known to prolong neutrophil survival by delaying their constitutive apoptosis (Aoshiba, Yasui et al. 1999). To determine whether ANG induces apoptosis in LPS-activated neutrophils, I incubated human neutrophils with LPS with or without ANG pre-treatment and stained them for cleaved caspase-3 as an indicator of apoptosis.

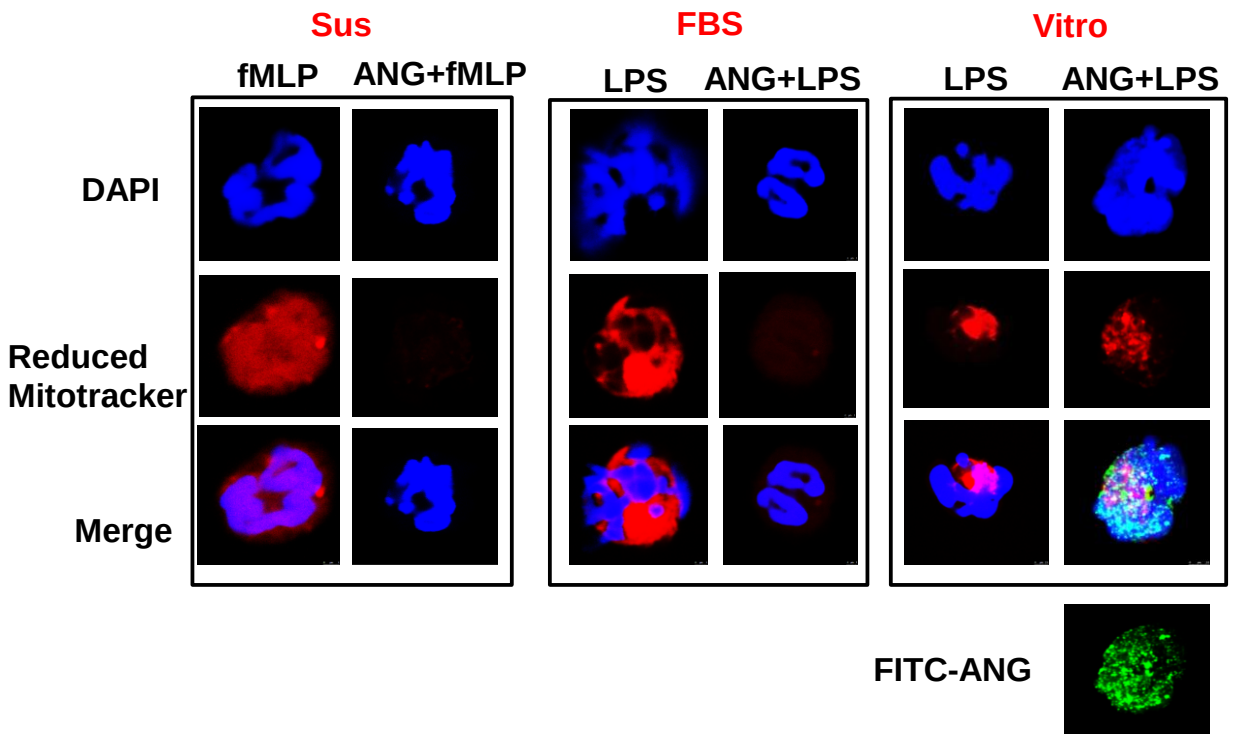

Figure 10a: Localization of reduced mitotracker (in red) and FITC-ANG (in green) in 1µg/ml LPS (30 min.) or 1µM fMLP (1 min.) stimulated mouse neutrophils (0.8 X 10^6 cells/ml) in suspension (sus), adhered on fetal bovine serum (FBS) or vitronectin (vitro) coated coverslips. Notice attenuation of mitochondrial activation after 12.5µg/ml FITC-ANG pre-incubation. (n=3). Please note that merge for the last treatment group i.e. ANG+LPS on vitronectin coated coverslips shows merge of DAPI (blue), reduced mitotracker (red) and FITC-ANG (green).

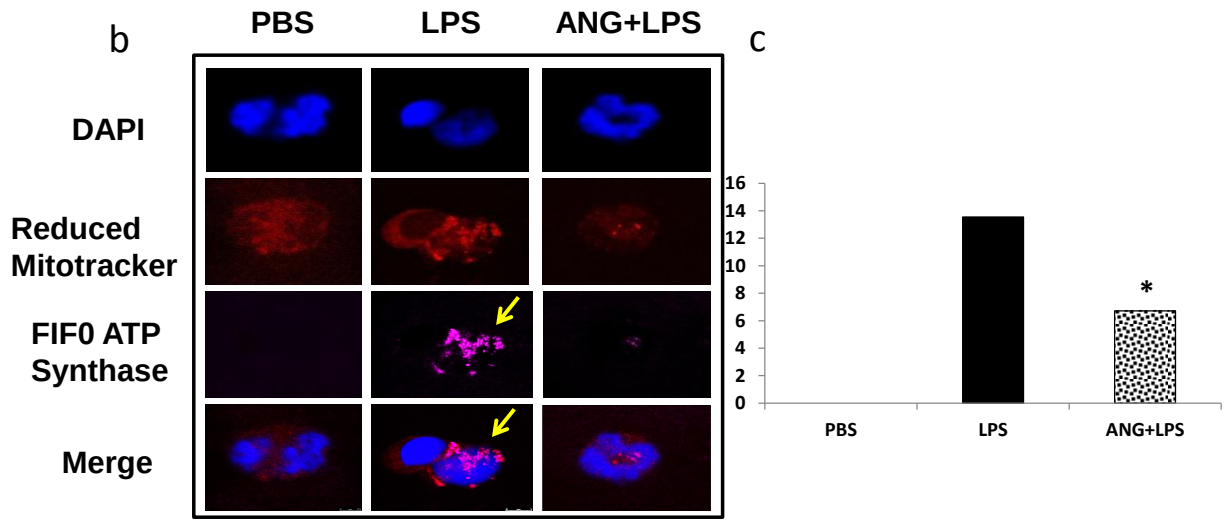

Figure 10b: Immunofluorescence of F_1F_0 ATP synthase β subunit (in fuschia) and reduced mitotracker (in red) in LPS (30 min.) stimulated human neutrophils (0.8 X 10^6 cells/ml) adhered on FBS coated coverslips. Note attenuation of signal for ATP synthase as well as reduced mitotracker in ANG incubated cells. Arrows indicate expression of F_1F_0 ATP synthase. (n=3)

Figure 10c: Fluorescence intensity measurements of F_1F_0 ATP synthase (fuschia channel) in PBS, LPS and ANG+LPS treatment groups as indicated in the confocal experiment described above (n=3). Average intensities, for the fuschia channel, from 100 neutrophils per slide were measured by Image J software. Statistical differences at $p < 0.05$ are indicated by asterisks (*).

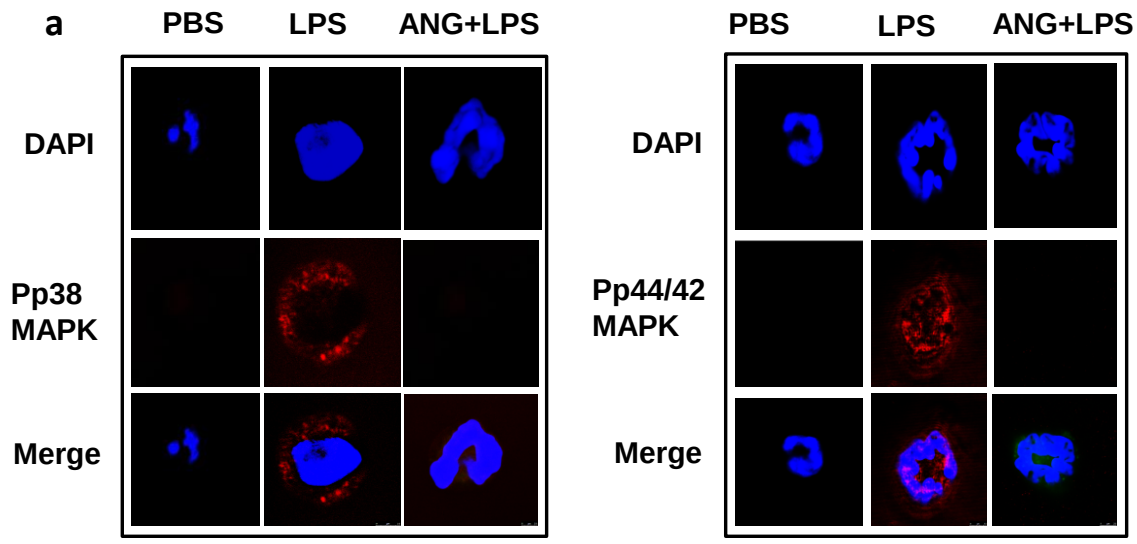

Figure 11a: Immunofluorescence of phosphorylated p38 MAPKinase and phosphorylated p42/44 MAPKinase (in red) in PBS or 1µg/ml LPS (30 min.) stimulated mouse neutrophils (0.8 X 10^6 cells/ml) adhered on FBS coated coverslips. Note attenuation of the signal in 12.5µg/ml ANG incubated cells. (n=3)

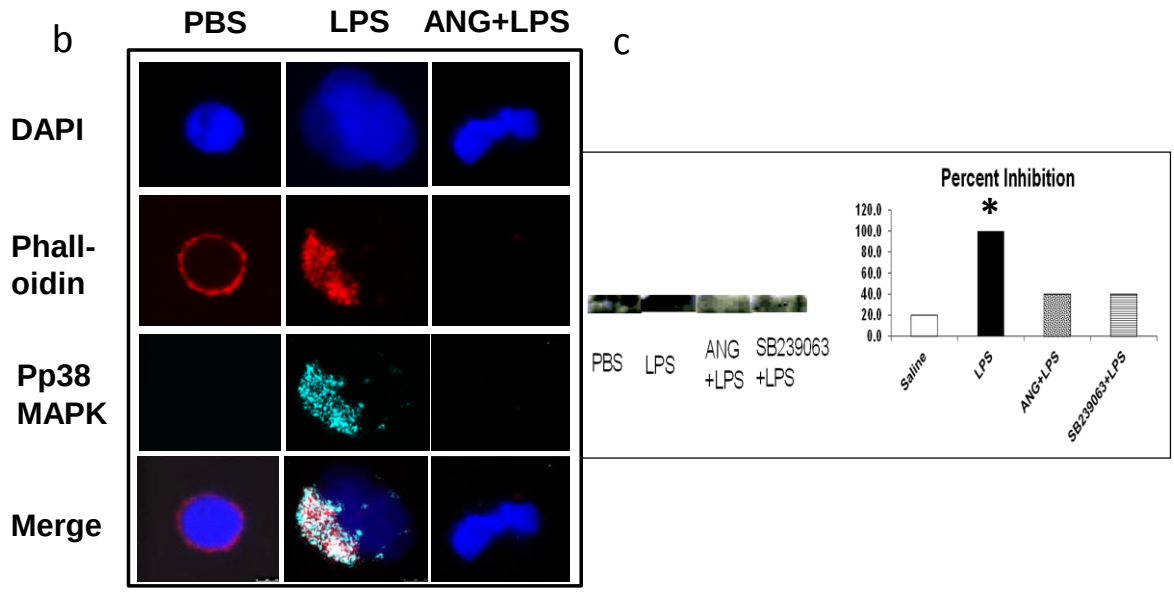

Figure 11b: Immunofluorescence of phosphorylated p38 MAPKinase (Pp38 MAPK) (in cyan), actin (in red) and ANG (in green) in PBS or 1µg/ml LPS (30 min.) stimulated human neutrophils (0.8 X 10^6 cells/ml) adhered on FBS coated coverslips. Note attenuation of the signal in ANG incubated cells. (n=3)

Figure 11c: Expression of Pp38 MAPK in human neutrophil lysates subjected to SDS electrophoresis. Neutrophils (2 X 10^6 cells/ml) were activated with 1 µg/ml LPS for 30 min. Note attenuation of p38MAPK in 12.5 µg/ml ANG as well as 500nM SB239063 pre-treated (30 min.) neutrophils. The graph depicts percent inhibition of the expressed protein where LPS represents 100% of the protein. Statistical differences at $p < 0.05$ are indicated by asterisks (*).

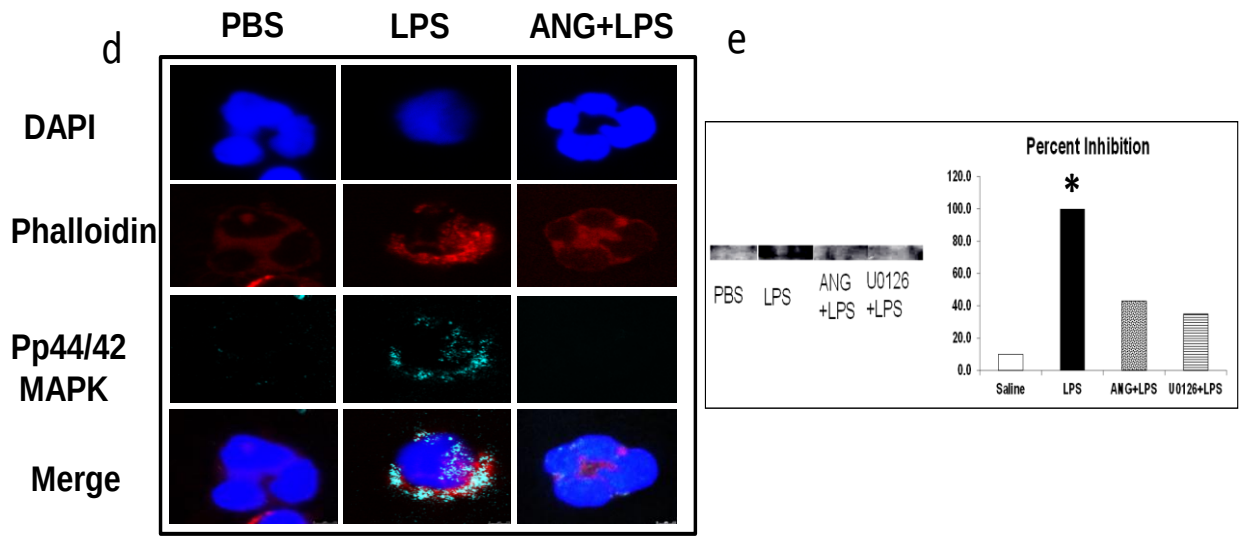

Figure 11d: Immunofluorescence of phosphorylated p42/44 MAPKinase (Pp44/42 MAPK) (in cyan) and actin (in red) in PBS or LPS (30 min.) stimulated human neutrophils (0.8 X 10^6 cells/ml) adhered on FBS coated coverslips. Note attenuation of the signal in 12.5µg/ml ANG incubated cells. (n=3)

Figure 11e: Expression of Pp44/42 MAPK in human neutrophil lysates subjected to SDS electrophoresis. Neutrophils (2 X 10^6 cells/ml) were activated with 1 µg/ml LPS for 30 min. Note attenuation of Pp44/42 MAPK in 12.5µg/ml ANG as well as 1µM U0126 pre-treated (30min.) neutrophils. The graph depicts percent inhibition of the expressed protein where LPS represents 100% of the protein. Statistical differences at $p < 0.05$ are indicated by asterisks (*).

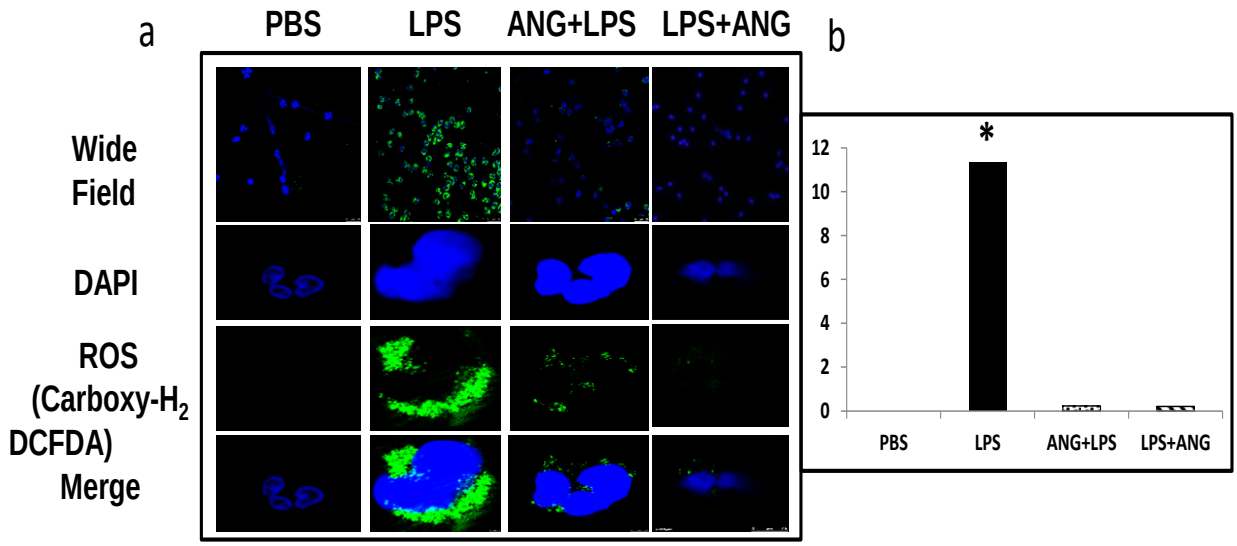

Figure 12a: Localization of reactive oxygen species (ROS) detected by carboxy-H_2 DCFDA (in green) in 1µg/ml LPS (30 min.) stimulated human neutrophils (0.8 X 10^6 cells/ml). Note attenuation of ROS in 12.5µg/ml ANG incubated cells. (n=3)

Figure 12b: Fluorescence intensity measurements of carboxy-H_2 DCFDA (green channel) in PBS, LPS ANG+LPS and LPS+ANG treatment groups as indicated in the confocal experiment described above (n=3). Average intensities, for the green channel, from 100 neutrophils per slide were measured by Image J software. Statistical differences at $p < 0.05$ are indicated by asterisks (*).

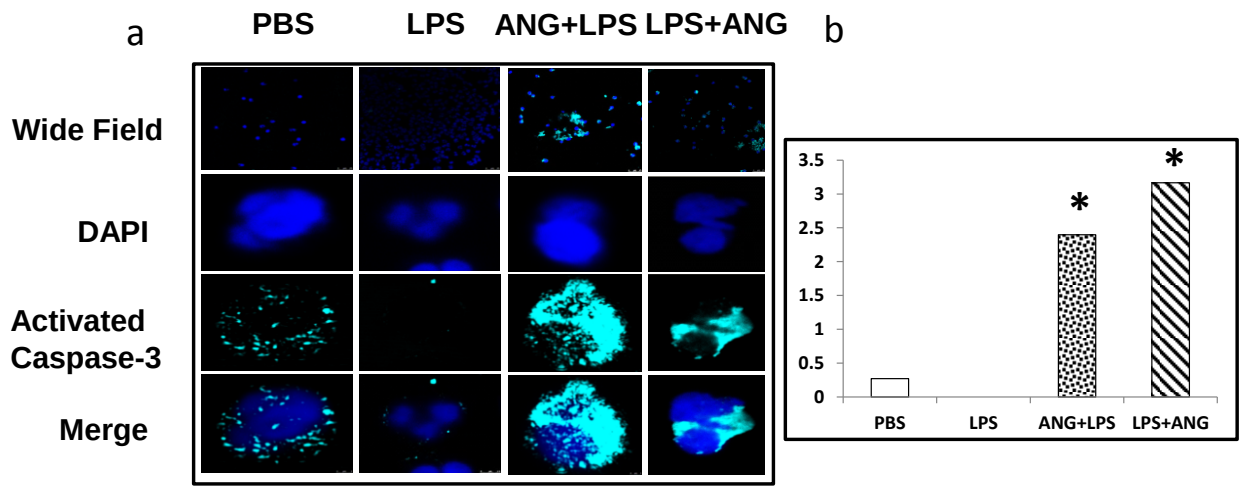

Figure 13a: Immunofluorescence of cleaved caspase-3 (in cyan in PBS, 1µg/ml LPS (4 hrs.), ANG+LPS or LPS+ANG stimulated human neutrophils (0.8 X 10^6 cells/ml) adhered on FBS coated coverslips. Note activation of cleaved caspase-3 in cytosol of 12.5µg/ml ANG pre- amd post-LPS treatments. (n=3).

Figure 13b: Fluorescence intensity measurements of activated caspase-3 (cyan channel) in PBS, LPS ANG+LPS and LPS+ANG treatment groups as indicated in the confocal experiment described above (n=3). Average intensities, for the cyan channel, from 100 neutrophils per slide were measured by Image J software. Statistical differences at $p < 0.05$ are indicated by asterisks (*).

While ANG per se does not induce apoptosis, it stimulated an intense expression of activated caspase-3 in LPS-stimulated human neutrophils at a 4 hour time point compared to both control and LPS-activated neutrophils (Figures 13a and 13b). Interestingly, ANG induced the expression of activated caspase-3 even in those neutrophils that were pre-treated with LPS (Figures 13a and 13b).

3.5.7. ANG inhibits adhesion and transendothelial migration in TNFα-activated cremaster muscle

Lastly, I did translational evaluation of function of ANG in transendothelial migration of leukocytes under flow conditions in cremaster muscle venules. The rolling flux was significantly reduced in TNFα group at all time-points compared to the control groups as well as ANG treatment groups (Figure 14a). Adhesion and emigration was significantly higher in TNFα group compared to all other groups. ANG treatment group had significantly higher number of adhered and emigrated cells compared to saline and ANG only groups but was less when compared to TNFα group (Figures 14c and 14d). Control groups such as saline or ANG only had significantly higher rolling velocity compared to TNFα or ANG treatment groups (Figure 14b). TNFα upregulates chemokine expression, produces inflammation in the cremaster muscle with significantly lower rolling flux, velocity and a markedly high index of adhesion and emigration (Wong, Heit et al. 2010). ANG treatment produces significantly higher rolling flux and velocity and a significantly lower adhesion and emigration. H&E data (Figure 15) support my off-line video analysis (Movie 3, 4, 5, 6). The dose of TNFα employed in my studies did not produce systemic effects as indicated by similar leukocyte counts in the peripheral blood (data not shown).

3.6 **Discussion**

ANG is upregulated in acute respiratory distress syndrome (Lucas, Lijnen et al. 2002), and neutrophils can also produce ANG (Scapini, Nesi et al. 2002). Neutrophils upon activation are credited with elimination of bacteria as well as causing significant tissue damage. I provide novel data that ANG inhibits neutrophil migration, induces silence by deactivating ROS production and activating apoptotic pathway, and inhibits their recruitment *iv-vivo*.

ANG does not bind to resting neutrophils but binds to and is endocytosed by fMLP-activated neutrophils. ANG co-localized with the lipid raft markers flotillin-1 and flotillin-2 in LPS and fMLP stimulated neutrophils. Disruption of lipid rafts with MCD inhibited ANG uptake, indicating that ANG binding and internalization are mediated via lipid rafts. β_3 integrin, a known ligand for ANG, colocalized with ANG in a nonpolar fashion. Integrins can recycle to and from lipid rafts during chemotaxis (Hendey, Lawson et al. 1996, Fabbri, Di Meglio et al. 2005). Integrin blocking experiments were done to study the interaction of ANG with β_3 integrin. Unexpectedly, integrin blocking did not prevent ANG endocytosis, but restored polarization of neutrophils in the presence of ANG and fMLP. There are three possible explanations for this partial reversal of ANG's effects with blockade of β_3¬ integrin. First, LM609 is an allosteric inhibitor of $\alpha_V\beta_3$ integrin but ANG interacts with RGD binding site on this integrin. Second, it has been recently shown that integrins are dispensable for neutrophil migration (Lammermann, Bader et al. 2008). Based upon lipid raft blocking experiment, I speculate that other membrane proteins like flotillin and caveolin-rich microdomains are possibly involved in endocytosis of ANG (Fabbri, Di Meglio et al. 2005, Castel, Pagan et al. 2001). Third, ANG and LM609 may not be stoichometrically balanced so that the block was not sufficient.

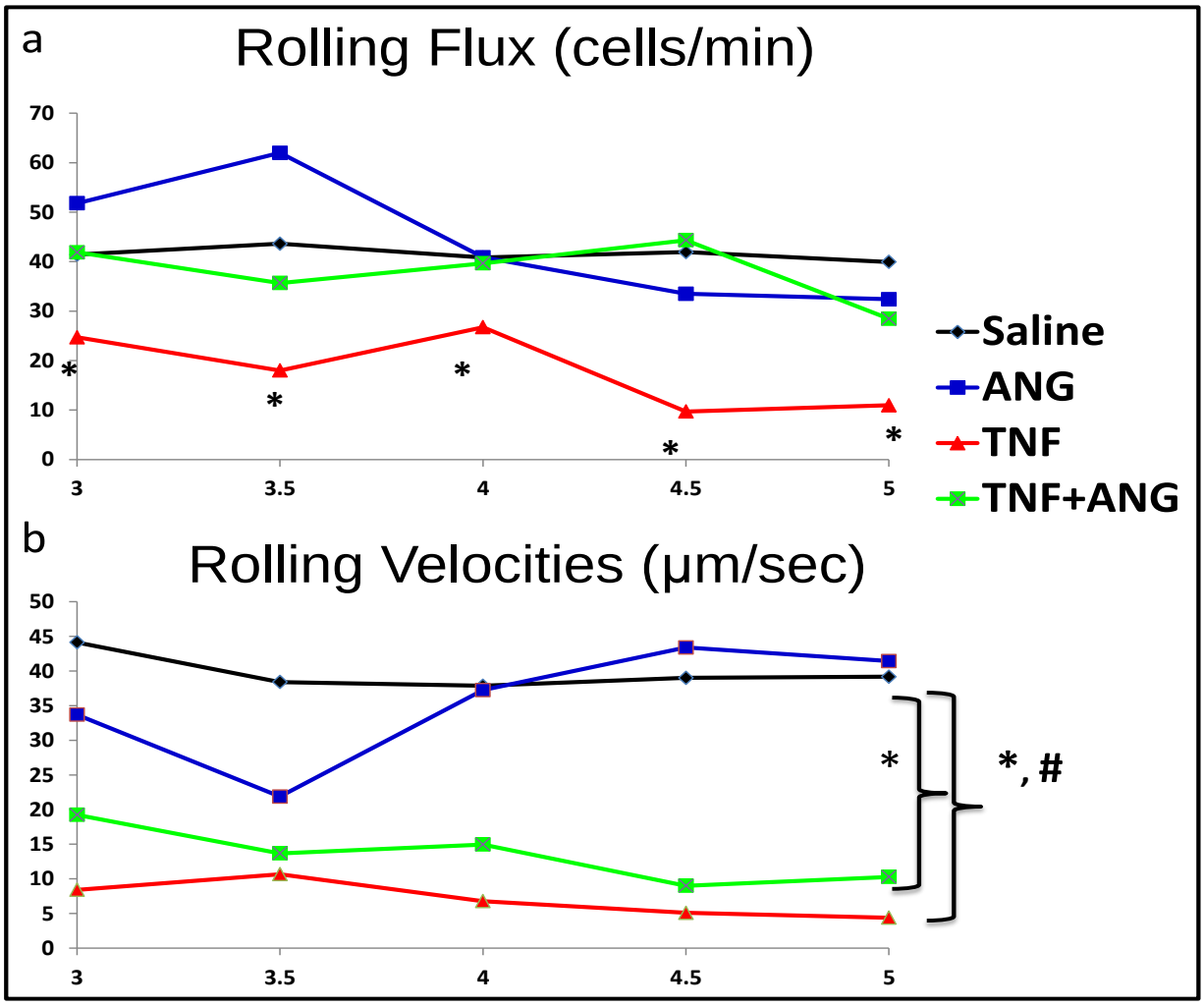

Figure 14a: Rolling Flux (cells/minute) of leukocytes in post-capillary venules of cremaster tissue at 3, 3.5, 4, 4.5 and 5 hours, along X-axis, after intrascrotal injection of saline (n=10), ANG (260µg/mice) (n=5), TNFα (0.05µg/mice) (n=9) and TNFα (0.05µg/mice)+ANG (260µg/mice) (n=5). Statistical differences at $p < 0.05$ are indicated by asterisks (*).

Figure 14b: Rolling velocities (µm/second) of first twenty rolling leukocytes in post-capillary venules of cremaster tissue at 3, 3.5, 4, 4.5 and 5 hours, along X-axis, after intrascrotal injection of saline (n=10), ANG (260µg/mice) (n=5), TNFα (0.05µg/mice) (n=9) and TNFα (0.05µg/mice)+ANG (260µg/mice) (n=5). Statistical differences at $p < 0.05$ are indicated by asterisks (*) and hash (#).

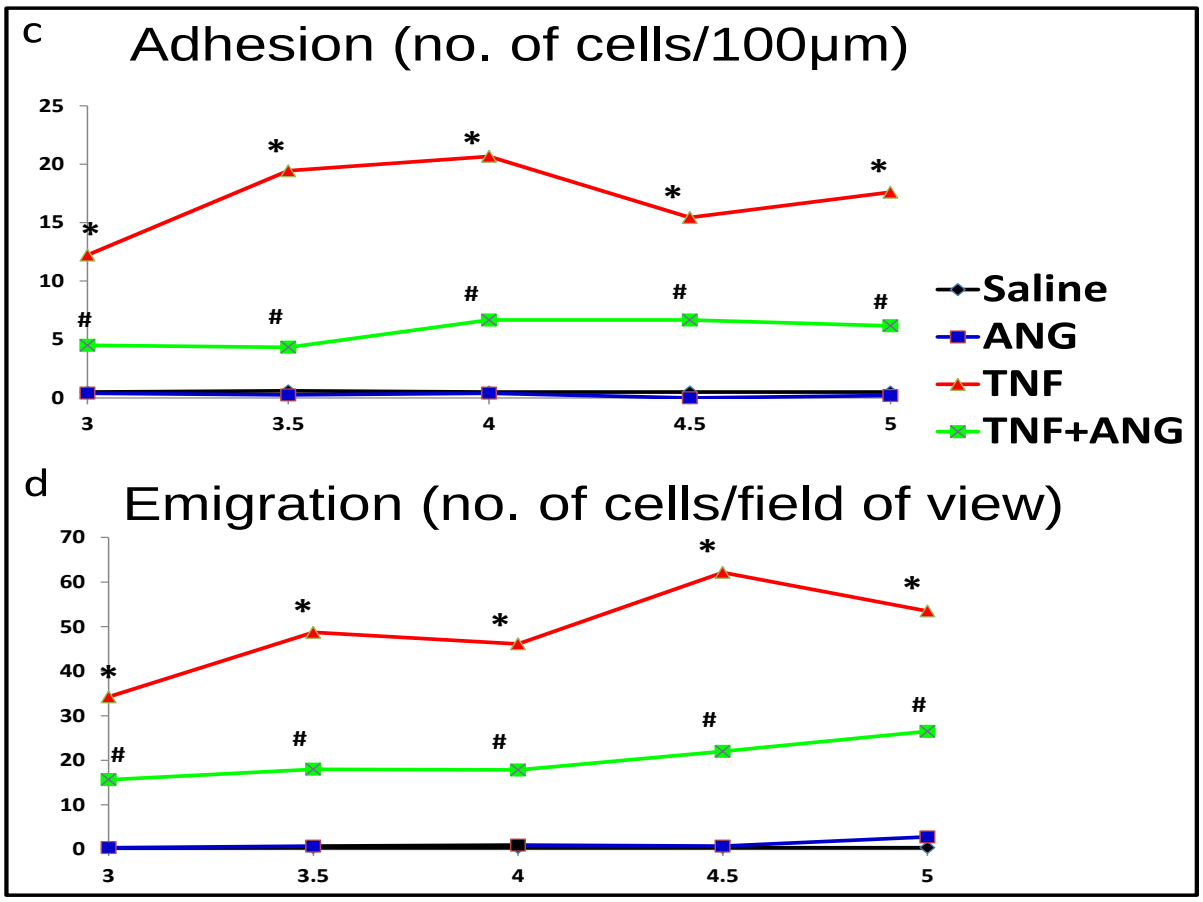

Figure 14c: Adhesion (number of cells per 100µm vessel length) of leukocytes in post-capillary venules of cremaster tissue at 3, 3.5, 4, 4.5 and 5 hours, along X-axis, after intrascrotal injection of saline (n=10), ANG (260µg/mice) (n=5), TNFα (0.05µg/mice) (n=9) and TNFα (0.05µg/mice)+ANG (260µg/mice) (n=5). Statistical differences at $p < 0.05$ are indicated by asterisks (*) and hash (#).

Figure 14d: Emigration (number of cells per field of view i.e. two screens wide) of leukocytes above and below the post-capillary venules of cremaster tissue at 3, 3.5, 4, 4.5 and 5 hours, along X-axis, after intrascrotal injection of saline (n=10), ANG (260µg/mice) (n=5), TNFα (0.05µg/mice) (n=9) and TNFα (0.05µg/mice)+ANG (260µg/mice) (n=5). Statistical differences at $p < 0.05$ are indicated by asterisks (*) and hash (#).

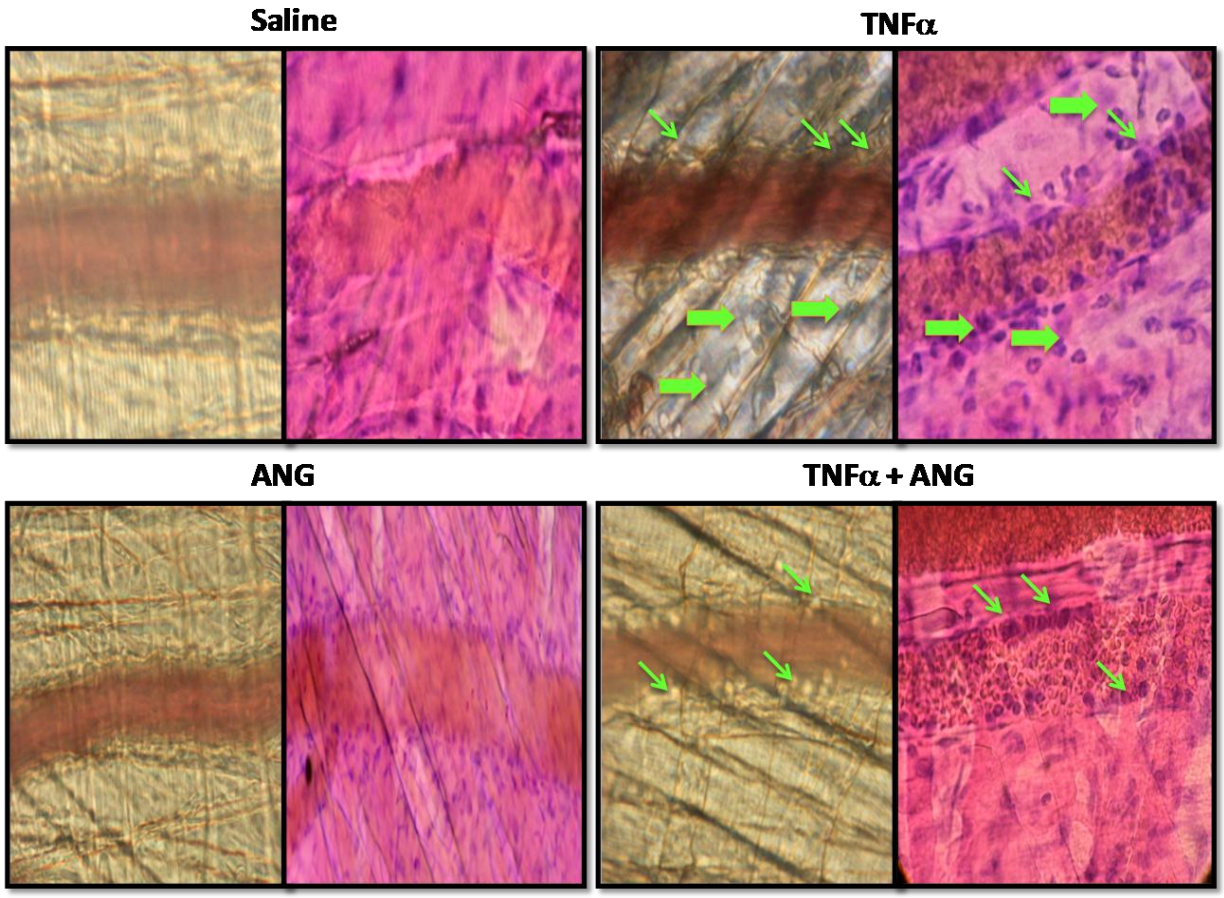

Figure 15: Representative differential interference contrast and H&E stained images of cremaster tissue hours after after intrascrotal injection of saline (n=10), ANG (260µg/mice) (n=5), TNFα (0.05µg/mice) (n=9) and TNFα (0.05µg/mice)+ANG (260µg/mice) (n=5).

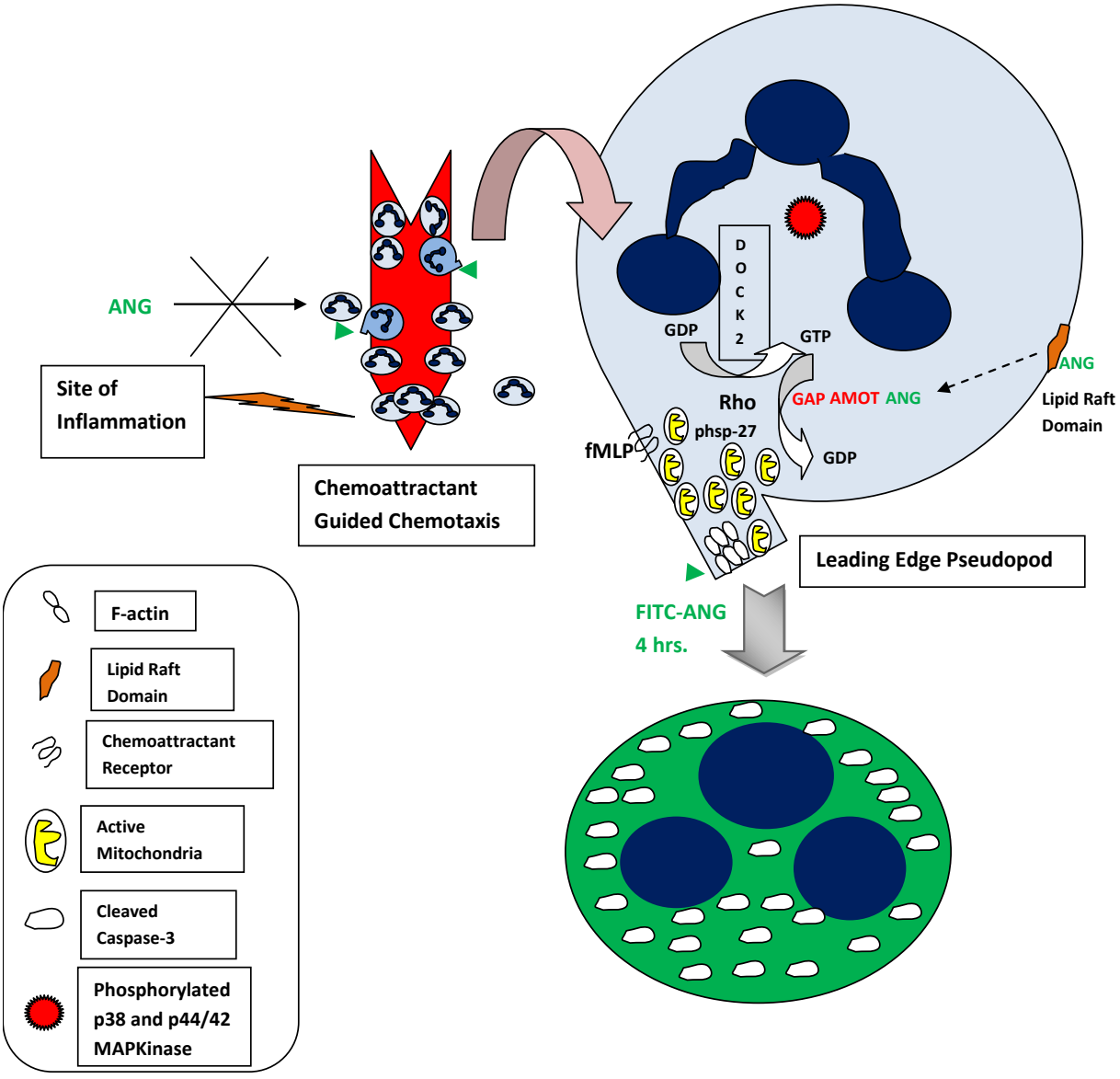

Figure 16: Schematic diagram for mechanism of action of angiostatin (ANG) in acute inflammation. ANG inhibits and adhesion as well as neutrophil trans-endothelial migration in an acute inflammation setting by inhibiting the leading edge actin dynamics. Dashed arrows depict hypothesized ANG binding to angiomotin (AMOT) that inhibits guanosine triphophate (GTP) recycling required for F-actin aggregation at the leading edge, thereby, inhibiting neutrophil chemotaxis. Note the apoptotic nuclear morphology (depicted in green) in LPS stimulated neutrophil incubated with ANG at a 4hr. time point. For further explanation, refer text.

Polarisation in response to chemoattractants is a primal event in chemotaxis. *Iv-vitro* confocal microscopy on mouse as well as human neutrophils revealed that ANG abolished polarisation as well as activation of neutrophils in response to fMLP and LPS. Hsp-27 induces actin capping and phosphorlyation of hsp-27 is essential for maintaining polarised heads (Jog, Jala et al. 2007). Immunoprecipitation revealed that hsp-27 binds to both α and β tubulin and inhibits tubulin polymerization (Hino, Hosoya 2003, Hino, Kurogi et al. 2000). ANG colocalises with this protein and blocked formation of polarized heads. It is however, still unclear if inhibition of hsp-27 phosphorylation is a direct effect of ANG or due to inactivation of MAPKinases.

The PDZ domain of AMOT can bind to cdc-42 Rho GTPase Activating Protein (GAP), Rich1 and produce a hypermigratory state in endothelial and epithelial cells. p190 Rho GAP is a RhoGAP that uncouples GTP from small G-protein Rho in order to recycle the small G-proteins during early establishment of polarity (Wells, Fawcett et al. 2006). AMOT is also known to be a scaffolding protein for Rich1 in endothelial and epithelial cells (Wells, Fawcett et al. 2006). Because of ANG's colocalization with AMOT and tubulin in human neutrophils, I speculate that ANG ultimately interferes with microtubular rearrangement. It has been shown earlier that ANG can bind to actin in cultured macrophages and endothelial cells (Dudani, Mehic et al. 2007, Perri, Annabi et al. 2007). I found AMOT as a probable candidate for ANG mode of action during inhibition of chemotaxis.

I did not observe co-localization of ATP synthase, another putative ANG binding protein, with ANG. However, ANG diminishes ATP synthase expression and the function of mitochondria which is in concordance with an earlier observation where ANG upregulates antiangiogenic and proapoptotic pathways via mitochondrial proteins (Lee, Muschal et al. 2009a). Mitochondria aggregate near the plasma membrane, as indicated by flotillin-1 and

flotillin-2 co-expression with mitochondria in LPS activated human neutrophils. Mitochondria activated by LPS generate ROS through p44/42 MAPKinase phosphorylation (Markvicheva, Gorokhovatskii et al. 2010, Espinosa, Leiva et al. 2006, Zhong, Jiang et al. 2003). Respriatory burst is also mediated by integrin β_3 signalling (Yan, Novak 1999). ANG abolished the ROS response in neutrophils possibly through binding to $\alpha_V\beta_3$ integrin. Downstream molecules for chemotaxis regulation are in part mediated by phosphorylation of p38 MAPKinase (Kutsuna, Suzuki et al. 2004). TLR agonists such as endotoxin activate neutrophils to stimulate downstream MAPKinase pathways and thus regulate their migration and survival (Sabroe, Dower et al. 2005), as well as production of ROS. The produced ROS contribute critically to collateral tissue damage in the host. Neutrophil MAPKinase signalling in response to fMLP or LPS is silenced by ANG. ANG treatment of neutrophils either before or after the LPS exposure abolishes ROS production and induced expression of caspase-3 to limit neutrophil survival.

Once the *iv-vitro* effects of ANG were observed in isolated neutrophils, I was interested in looking at ANG's effect on leukocyte migration under flow conditions. ANG inhibits leukocyte recruitment in Boyden's chamber (BENELLI, MORINI et al. 2002). My intravital experiments show that ANG also blocks neutrophil adhesion and emigration *iv-vivo* under flow conditions.

Taken together (Figure 16), the data show that ANG deactivates neutrophils, limits their survival and inhibits their *iv-vivo* migration in inflamed blood vessels. Hypothesis was proven true. Based on these data, ANG may act as a novel inhibitor of acute inflammation.

CHAPTER 4
FUNCTION OF ANGIOSTATIN IN ACUTE LUNG INJURY

4.1. At a Glance Commentary

The current study shows that subcutaneous angiostatin treatment inhibits neutrophilia and fluid accumulation in mice acute lung injury model as assessed by conventional cytological, biochemical and histological techniques as well as by novel synchrotron diffraction enhanced imaging followed over 9 hours utilising diffraction enhanced imaging. I also show reduced neutrophil activation in lung microvessels. As angiostatin treatment does not affect cytokines and chemokines analysed by us, but reduces neutrophil infiltration and activation in mice lungs, it offers novel inhibition of neutrophil migration during acute lung injury.

4.2. Abstract

Rationale: Acute lung injury is marked by profound neutrophil influx along with fluid accumulation that impairs lung function at the cost of high mortality. Neutrophils are activated and are programmed for anti-apoptosis during this phase in order to be competent phagocytes over the next couple of hours. Toxic mediators due to neutrophil over-activation leads to tissue damage that in turn impairs lung function. Angiostatin is an endogenous antiangiogenic molecule highly expressed in lavage fluid of patients with acute respiratory distress syndrome that has recently been shown to inhibit neutrophil infiltration in mice peritonitis. *Objective:* My aim was to investigate the role of angiostatin in acute lung injury. *Methods:* I used bacterial lipopolysaccharide induced acute lung injury model for bronchoalveolar lavage and lung analysis. In addition, I imaged mice lungs with synchrotron diffraction enhanced imaging to assess lung area and contrast ratios over 9 hours. *Measurements and Main Results:* Subcutaneous angiostatin reduces neutrophil influx, protein accumulation, lung Gr1+ neutrophils and myeloperoxidase activity, phosphorylated p38 MAPK without affecting the levels of MIP-1α,

IL-1β, KC and MCP-1 in lavage and lung homogenates. Diffraction enhanced imaging shows that angiostatin causes a time-dependent improvement in lung area and lung contrast ratios that reflect reduction in lung edema. *Conclusion:* Overall, the study shows that angiostatin is a novel inhibitor of acute lung injury in mice.

Key Words: acute lung injury; angiostatin; DEI

4.3. **Introduction**

Inflammation is the host response to microbial or chemical stimuli and typically involves migration of inflammatory cells such as neutrophils or polymorphonuclear cells (PMNs) in the affected organ (Jain, Bellingan 2007, Mizgerd 2008). Acute lung injury is characterized by the migration of activated neutrophils into lung vasculature and alveoli (Matute-Bello, Martin 2008, Perl, Lomas-Neira et al. 2008). These activated neutrophils live longer and cause significant tissue damage through inflammatory products like proteinases, cationic polypeptides, cytokines and reactive oxygen species (ROS) (Witko-Sarsat, Rieu et al. 2000, Dallegri, Ottonello 1997, Haslett 1999, Haslett, Savill et al. 1989). The paradox of neutrophil biology is highlighted by the fact that although activated neutrophils are essential for clearing of bacteria, the tissue damage caused by them is believed to be the cause of organ failure, morbidity and mortality. Hence, there is a need to understand the processes that regulate neutrophil activation and their lifespan in acute lung injury.

Angiostatin (ANG), a potent anti-angiogenic molecule, is the cleavage product of plasminogen and is composed of the either the first four or three-Kringle (K) domains (Wahl, Kenan et al. 2005, O'Reilly, Holmgren et al. 1994). K-5 of plasminogen also shows similar activity (Lu, Dhanabal et al. 1999). Figure 4 depicts conversion of plasminogen to plasmin, reduction of plasmin by phopshoglycerate kinase followed by serine proteinase dependent release of *Kringle* (K) 1-4½ and finally matrix metalloprotease-dependent trimming of K 1-4½ to K 1-4 or K1-3 (Lay, Jiang et al. 2000). Proteolysis of membrane-bound plasmin generates angiostatic molecules *in-vitro* and *in-vivo* (Falcone, Khan et al. 1998). Western blots from cutaneous wound model detect ANG forms and plasminogen as early as day 1 and day 3 after generation of the wounds (i.e., at the initial phase of wound healing) and expression of ANG

forms peaked during the last phase of wound healing, and almost disappeared after wound healing was complete (Chavakis, Athanasopoulos et al. 2005). ANG released from PMNs mediate the initial angiogenic switch in mouse model of multi-stage carcinoma (BENELLI, MORINI et al. 2002, Scapini, Nesi et al. 2002, Nozawa, Chiu et al. 2006). Platelets are also well known to produce ANG from uPA (JURASZ, SANTOS-MARTINEZ et al. 2006).

ANG binds to several cell surface proteins (Wahl, Kenan et al. 2005, Tabruyn, Griffioen 2007) such as ATP synthase F_1F_0, heat shock proteins (hsp) 27 and 70, annexin II (Syed, Martin et al. 2007, Sharma, Rothman et al. 2006), $\alpha_V\beta_3$ integrin (Tarui, Miles et al. 2001) and angiomotin (Troyanovsky, Levchenko et al. 2001a) to produce anoikis, apoptosis and cell migration. ANG binds to adhesion proteins such as integrin $\alpha_v\beta_3$ expressed on the apical and basal surfaces of endothelial and epithelial cells (Singh, Fu et al. 2000). ANG also induces the expression of adhesion molecules (ICAM-1, E-selectin) (Luo, Lin et al. 1998, Chen, Huang et al. 2008), and through interaction with Mac-1 ($\alpha_M\beta_2$) integrin as well as reduced activation of NF-κB and related tissue factor expression inhibits peripheral blood leukocyte recruitment and angiogenesis in a mouse model of acute peritonitis (Chavakis, Athanasopoulos et al. 2005). ANG levels are reportedly increased in acute respiratory distress syndrome and septic patients (Hamacher, Lucas et al. 2002, Lucas, Lijnen et al. 2002, Singh, Janardhan et al. 2005), which along with high levels of TNF-α have been implicated in *in-vitro* endothelial cell cytotoxicity that is indicative of its potential role in ARDS-related EC injury (Hamacher, Lucas et al. 2002). These data indicate a potential role of ANG in cell activation and inflammation.

Currently, there are no data on the effects of ANG in acute lung injury. Because increased levels of ANG have been reported in the lungs of ARDS and septic patients (Hamacher, Lucas et al. 2002, Lucas, Lijnen et al. 2002, Singh, Janardhan et al. 2005), I investigated the role of ANG in

mouse model of lipopolysaccharide-induced acute lung injury. I also imaged mice lungs with diffraction enhanced imaging using synchrotron radiation. Conventional invasive techniques are helpful in delineating the molecular mechanism of a pathophysiological event but they do not represent the mass dynamics of a disease progression as has been underlined in acute lung injury. Dynamic imaging of small lung airways remains a challenge despite wide strides in imaging relatively static tissue beds. X-rays are still the only available diagnosis for lung pathologies that utilise absorption to highlight the hard tissue from soft tissue. However, this does not resolve soft tissues like lungs. The unique properties of synchrotron radiation, in particular its brightness, make synchrotron radiation ideal for these experiments. With this configuration and a high-speed detector, it is possible to acquire dynamic images with relative ease. Diffraction Enhanced Imaging (DEI) derives contrast from an object's X-ray absorption, refraction gradient and small angle scatter properties (extinction) (Chapman, Pisano et al. 1998, Chapman, Nesch et al. 2006, Chapman, Thomlinson et al. 1997).

4.4. Materials and Methods

All the animal experiments were conducted in accordance with the institutional guidelines and following approval from the University of Saskatchewan Animal Ethics Board. Six to eight weeks old male C57BL6 mice purchased from Animal Resource Center of the University of Saskatchewan. *E. coli* 0127:B8 lipopolysaccharide (LPS; Sigma Chemicals, St. Louis, MO, USA), ANG K1-4 (Haematologic Technologies Inc., Essex Junction, VT, USA), mouse Ly-6G Ly-6C (Gr-1) antibody (BD Biosciences, San Jose, CA, USA), human vWF, secondary anti-rat and anti-rabbit HRP (horseradish peroxidase) conjugated antibody (Dako, Carpinteria, CA, USA), Vector® VIP peroxidase substrate kit (Vector Laboratories, Burlingame, CA, USA) were purchased commercially.

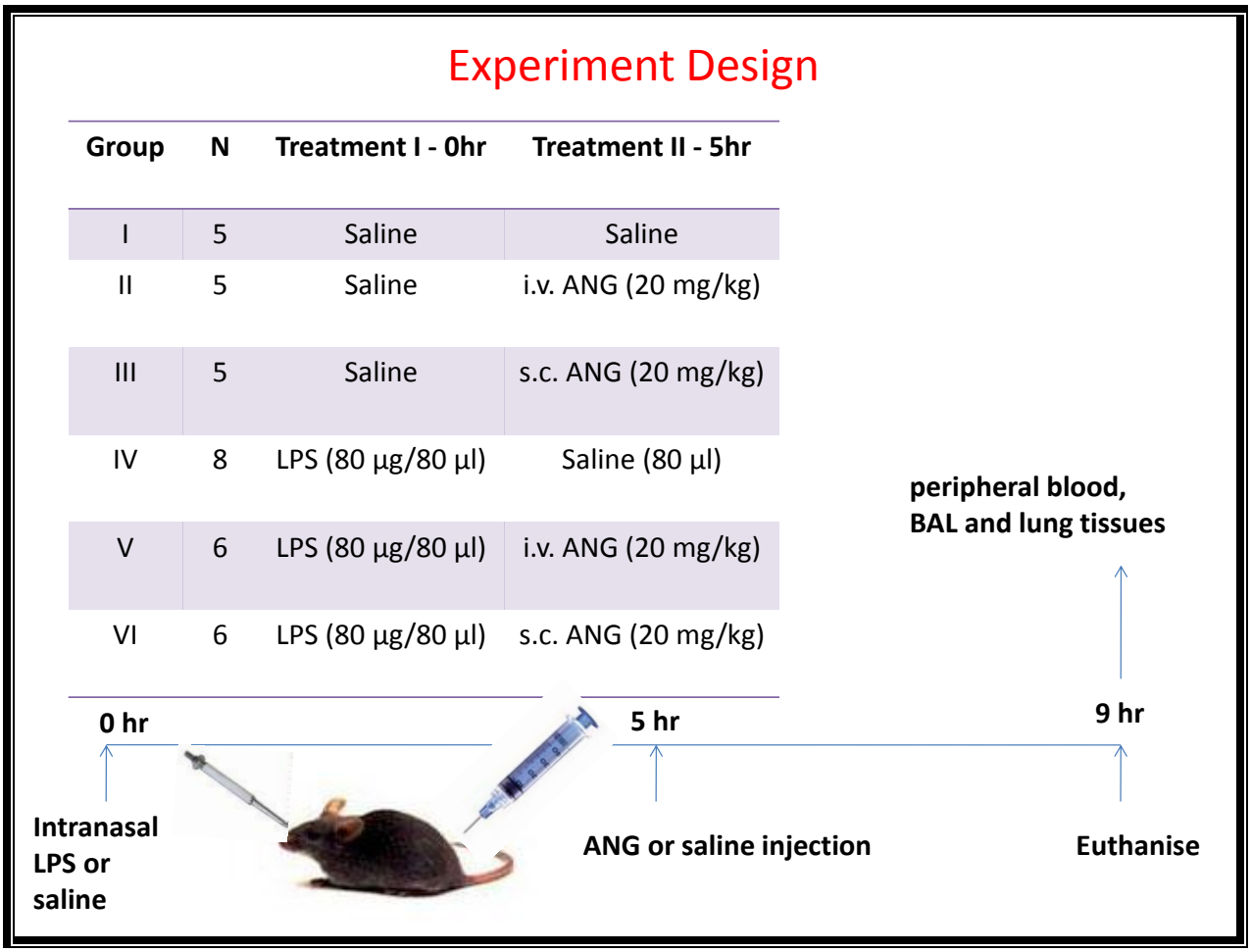

Figure 17: Experimental protocol indicating the design of six treatment groups.

4.4.1. Intranasal LPS-Induced Mouse Acute Lung Injury Model

I used an intra-nasal LPS instillation mouse model of acute lung inflammation (Szarka, Wang et al. 1997). The angiostatin post-treatment protocol and dose were standardized after a series of preliminary experiments and the treatment groups are shown in Figure 17. Peripheral blood was collected through cardiac puncture for differential and total peripheral leukocyte counts, and lungs were lavaged with a total of 1.5 ml of ice-cold Hank's balanced salt solution (HBSS). The right lung bronchus was ligated and fixed the left lung *in-situ* with four percent paraformaldehyde (PF) for one hour after which the right lung was snap frozen.

4.4.2. Bronchoalveolar Lavage (BAL)

BAL was centrifuged at 700*g* (2500 rpm) and supernatant stored at -80°C for protein estimation and cytokine assay. Cells were resuspended at 10^6/ml to make cytospin for differential count.

4.4.3. Peripheral Blood Leukocyte counts

Total and differential leukocyte counts (TLC and DLC) were done after RBC hemolysis with 2% acetic acid and blood smear stained with Diffquick®.

4.4.4. Lung MPO Assay

Lung homogenates were centrifuged in 50 mM HEPES (pH 8.0) at 900g (3000 rpm) for 20 minutes at 4°C. The pellet was resuspended in 0.5% CTAC (cetyl trimethylammonium chloride) solution and rehomogenised. MPO colorimetric assay was performed (Schierwagen, Bylund-Fellenius et al. 1990) using 3,3´,5,5´-tetramethylbenzidine (TMB) as substrate for H_2O_2 under low pH conditions. Results were expressed as MPO units per mg of lung tissue.

4.4.5. Protein assay

Bradford's reagent was used to assess total lung as well as BAL protein (Bio-Rad, Hercules, CA, USA).

4.4.6. Cytokine assay

Sandwich ELISA was performed on lung homogenates for MCP-1 (monocyte chemoaatractant protein-1), KC (keratinocyte chemoattractant), IL-1β (interleukin-1 beta), MIP-1α (macrophage inflammatory protein-1 alpha) using ELISA kits from R&D systems, US.

4.4.7. Lung H&E Staining

The OCT embedded left lung was cut into four micron sections and stained with hematoxylin and eosin to assess structural changes in various groups.

4.4.8. Anti-Gr-1 and Phosphorylated p38 MAPK Immunohistochemistry

Briefly, cryosections were subjected to endogeneous peroxide removal followed by antibody blocking, primary rat anti-mouse Gr-1 or anti-phosphop38MAPK and secondary anti-rat HRP conjugated antibody treatments. Negative controls and positive controls were included for every section that comprised of no primary antibody and vWF (von Willbrand factor) stain, respectively. Semi-quantitative scoring (0 = no staining; 1 = light staining; 2 = moderate staining; and 3 = heavy staining) was performed on five sections/treatment group.

4.4.9. Western Blots

Lung homogenates were processed to detect plasminogen and ANG proteins. Briefly, homogenates extracted with equal volume of 2X Laemmli Sample Buffer Concentrate (Sigma) were electrophoresed in 12% SDS-PAGE at 180V followed by electro-transferred to nitrocellulose membranes at 100V for 60 minutes. The resulting membranes were, thereafter, blocked (5% skim milk in 0.1% PBS-T for 60 minutes), incubated with rat monoclonal plasminogen antibody (ab61387) overnight at four degrees, washed three times with PBS-T for 5

minutes each and exposed to HRP-conjugated anti-rat IgG antibody for 60 minutes. The membrane was treated with ECL (enhanced chemiluminescence system) solutions (GE Amersham Western Blotting Detection Reagents) and developed with special ECL sensitive films (GE, UK). The probed membranes were restored with blot-restore solution (Millipore, CA, US) to be re-probed with β-actin that served as a house-keeping gene product. The blots were subjected to densitometric quantification.

4.4.10. DEI Imaging

For DEI imaging, mice were mounted vertically on a custom-made plexiglass board and monitored from the control room during imaging. Exposure times per frame for phase contrast imaging 1 s corresponding to a surface entrance dose of approximately 1Gy per frame.
For the DEI imaging the scans took approximately 50 seconds with a total dose per scan of about 0.4mGy (about 1/10 of a mammogram exposure). Lungs were imaged at the synchrotron facility of Canadian Light Source at University of Saskatchewan, Canada on beamline BMIT. A Si (2,2,0) double-crystal monochromator was used to select a narrow bandwidth of the bending magnet radiation. 16.5 keV x-rays were chosen to provide both good phase and absorption contrast from the mice lungs. All objects were positioned in hutch POE-2 of beamline BMIT, approximately 24 m downstream of the synchrotron source. The Si (4,4,0) planes were used in the double crystal monochromator to select 40keV with a matching Si (4,4,0) analyzer after the object, but before the detector. Photonic Science detector XDR-90 (Photonic Science, UK) was placed 3.0 m downstream. This detector had 18.7micron square pixel size with a field of view of approximately 50mm (horizontal) x 75mm (vertical). Images on both sides of the rocking curve as well as on top of the curve were recorded. Images were recorded at 2 hr intervals for 9 hrs

with a Hamamatsu phosphor charge-coupled device (CCD) camera (C9300-124). At the end of imaging, mice were euthanized for collection of lungs and stained them with H&E.

4.4.11. DEI Image Analysis

Following image acquisition, ImageJ software (National Institutes of Health; rsbweb.nih.gov/ij/) was used to correct for dark current and non-uniform beam intensity effects. This was achieved by the usual method of recording a flat field with identical illumination to the experimental image but with no object and a dark image with the x-ray shutter closed. Identical exposure times were used for the experimental and the correction images. Both the experimental image and the flat field image were first corrected by subtracting the dark image and then the dark corrected experimental image was divided by the dark corrected flat field image. Normalized DEI images were further processed for calculation of percent increase in lung area (cm^2) and in contrast ratios of top images w.r.t. respective 0 hr images.

4.5. Statistical Analysis

Results were analysed by application of one-way ANOVA and unpaired *t*-test to assess differences between two groups followed by Bonferroni's all group comparison utilizing Graphpad software. The treatment significance was set at $P< 0.05$.

4.6 Results

4.6.1. BAL Cell Counts

LPS caused a significant rise in BAL total as well as neutrophil cell counts (Figures 18a and 18d). Intravenous ANG treatment of LPS-treated mice resulted in significant increase in BAL leukocytes compared to the LPS only group. However, the subcutaneous treatment of LPS-treated mice with ANG significantly reduced the numbers of neutrophils in the BAL (Figure 18a). Subcutaneous ANG treatment of LPS-challenged mice caused a significant increase in

apoptotic neutrophils in their BAL (Figure 18c) compared to the LPS and LPS+ANG intravenous groups. Mice treated with only ANG, irrespective of the route, did not alter the BAL cell counts, which were primarily comprised of alveolar macrophages (Figure 18a).

4.6.2. BAL Protein

BAL protein concentration, as an indicator of vascular permeability, was increased in LPS-treated mice (343.7±11.3 μg/ml) compared to saline treatment (156±42.8 μg/ml). The subcutaneous but not intravenous ANG treatment caused a significant reduction in protein concentration (303.4±15.7 μg/ml) compared to the LPS-treated mice (Figure 18b). All LPS groups had significantly higher protein concentration compared to the control groups (saline only, intravenous ANG only and subcutaneous ANG only).

4.6.3. Peripheral Blood Leukocyte counts

While TLC didn't differ among treatment groups, monocytes were decreased and neutrophils were increased in all the LPS-challenged animals compared to the negative controls (Figure 19).

4.6.4. Lung MPO Assay

MPO, a surrogate indicator of neutrophils, was significantly lower in the saline group compared to all LPS treatments irrespective of the ANG treatments (Figure 20). However, LPS-challenged mice treated with ANG, both subcutaneous and intravenous, showed significantly lower MPO compared to the LPS only animals.

4.6.5. Anti-Gr-1 Immunohistochemistry

To evaluate the neutrophils still trapped in the lung tissues, I stained lung sections with Gr-1 antibody. Figure 22a shows clear airways and alveolar septa whereas in figure 22b intense staining for neutrophils is seen in perivascular, peribronchiolar areas along with alveolar septa of

the LPS-treated mice. Figures 21c and 21d represent the LPS + intravenous ANG and LPS + subcutaneous ANG treatments, respectively, and show moderate degree Gr-1 staining mainly in alveolar septa. I was able to obtain a similar trend of Gr-1 staining in immunohistochemical slides (Figure 21e). vWF staining, normally used as an immunohistochemical control (Figure 22b) showed marked increase in the lungs from LPS+ intravenous ANG group.

4.6.6. Expression of IL-1β, MIP-1α, MCP-1 and KC

I assayed IL-1β, MIP-1α, MCP-1 and KC in BAL for their well-established roles in ALI and found them to be significantly increased in LPS-treated groups compared to saline treatment (Figure 23). However, there were no differences among the LPS-treated animals with or without ANG, irrespective of the administration route. Also, mRNA levels of these cytokines and chemokines in lung tissue were not different among endotoxin-treated animals (Figure 24).

4.6.7. Lung H&E Staining

Lung sections from the saline group showed normal alveolar septa (Figure 25a) while those from the LPS-treated mice had septal congestion, and neutrophil accumulation in the septa and the perivascular and peribronchial areas (Figure 25b). Compared to the lungs sections from the LPS + intravenous ANG mice (Figure 25c), those from subcutaneous ANG+ LPS mice contained markedly reduced lung inflammation (Figure 25d). Although all the lungs were lavaged, I still observed neutrophils in the alveoli of lung sections from the LPS and LPS+intravenous ANG mice that indicate robust migration of neutrophils. Mice treated with only ANG, either intravenous or subcutaneous, show normal lung histology similar to the saline only group.

4.6.8. Phosphorylated p38 MAPK Immunohistochemistry

Lung sections from all of the LPS- treated mice showed staining in leukocytes trapped in the alveolar septae and blood vessels (Figure 26).

4.6.9. Western Blots

Plasminogen bands at 105kDa were detected in all groups. ANG forms were detectable in LPS-treated lung homogenates as well as BAL (Figures 27a, 27b). Densitometry showed a forty fold increase in ANG expression in LPS-treated lavage samples (Figure 27a) and a tenfold increase in corresponding lung homogenates compared to saline treated samples (Figure 27b).

4.6.10. DEI Imaging

Figure 28 shows absorption (top) images of mice lung. Due to fewer animals used, I discuss trends observed across groups over time. Increase in lung area is an index of increased lung weight due to edema following endotoxin instillation. Saline treated mice lungs do not gain in area over time when compared to 40% increase in LPS treated mice (Figure 29a). Subcutaneous ANG treatment at 5 hrs attenuates increase in lung area.

Contrast ratios are proportional to the light scattered by lungs and therefore reflect number of air-filled alveoli. The contrast ratios for LPS treated mice lungs show a low percent increase over time, with a maximum of 138% (Figure 29b) when compared to LPS + subcutaneous ANG treated mice, with a rapid increase to a maximum of 447% (Figure 29b). The lower contrast ratios for LPS mice are explained due to lesser number of air-filled alveoli due to fluid accumulation that leads to lesser scatter.

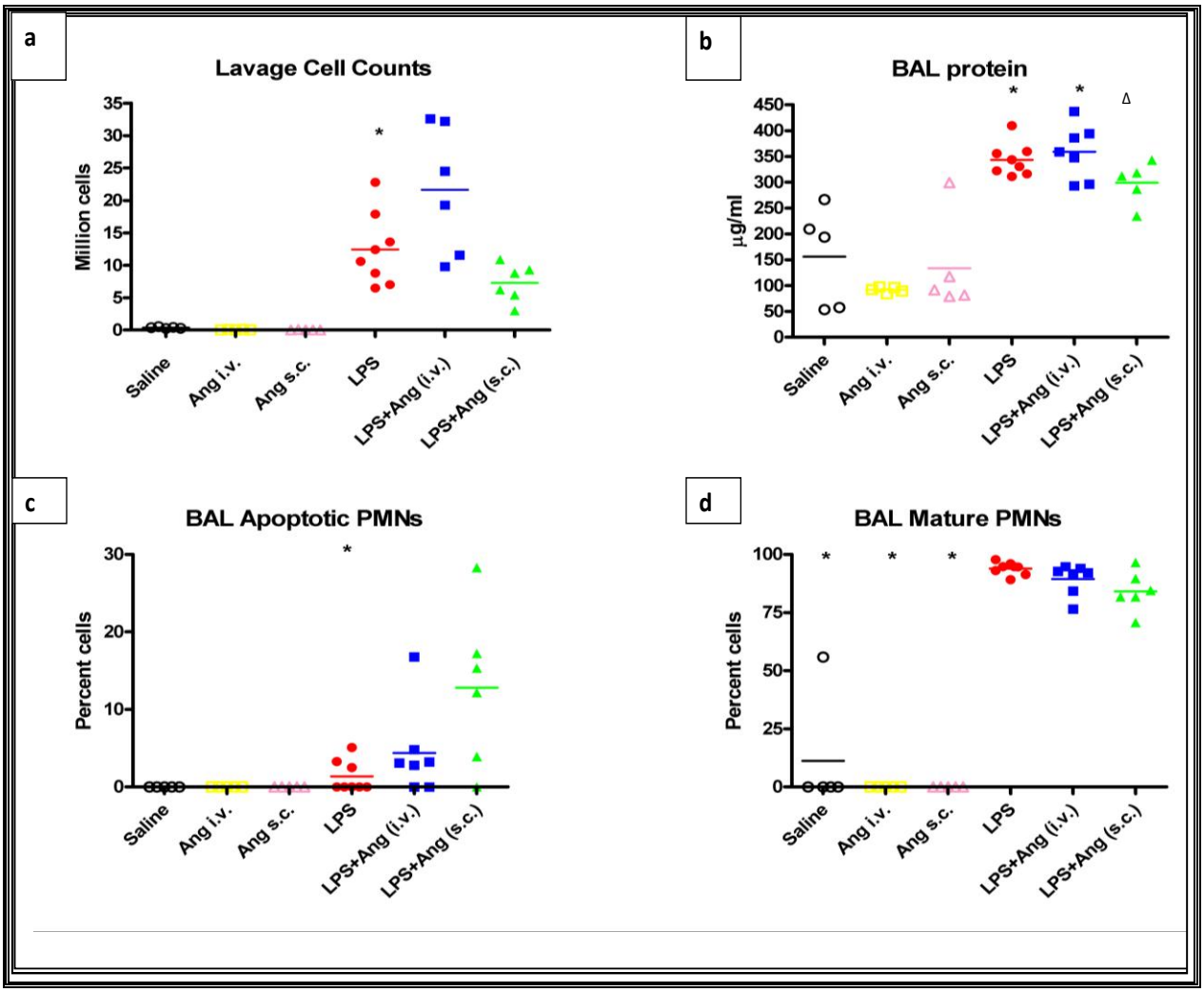

Figure 18: Bronchoalveolar lavage (BAL) a) total leukocyte counts, b) BAL protein content (µg/ml), c) BAL apoptotic PMNs and d) BAL Mature PMNs in the six treatment groups. Statistical differences at $p < 0.05$ are indicated by asterisks (*) and open triangles (Δ).

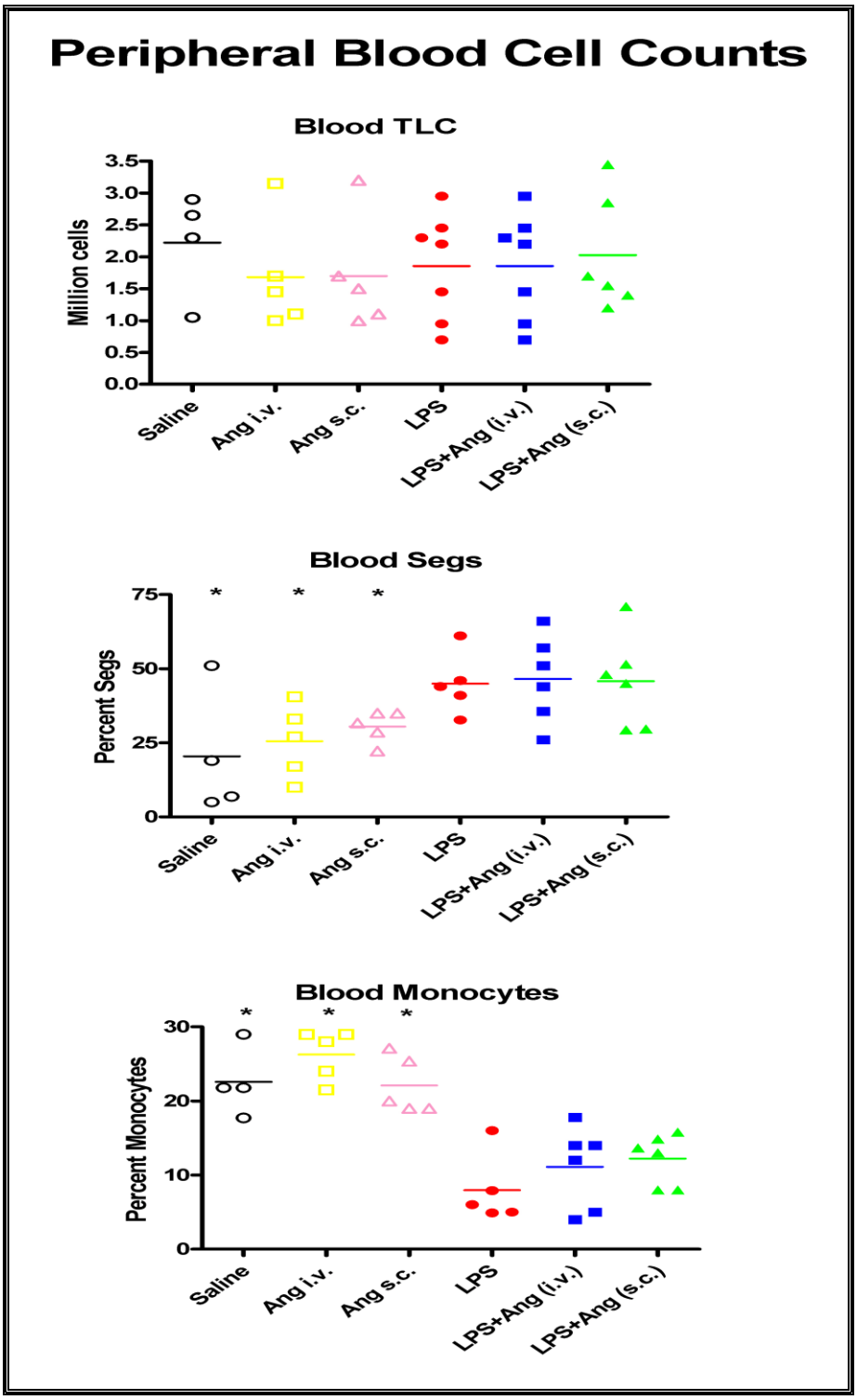

Figure 19: Peripheral blood total and differential leukocyte counts in the six treatment groups. Statistical differences at $p < 0.05$ are indicated by asterisks (*).

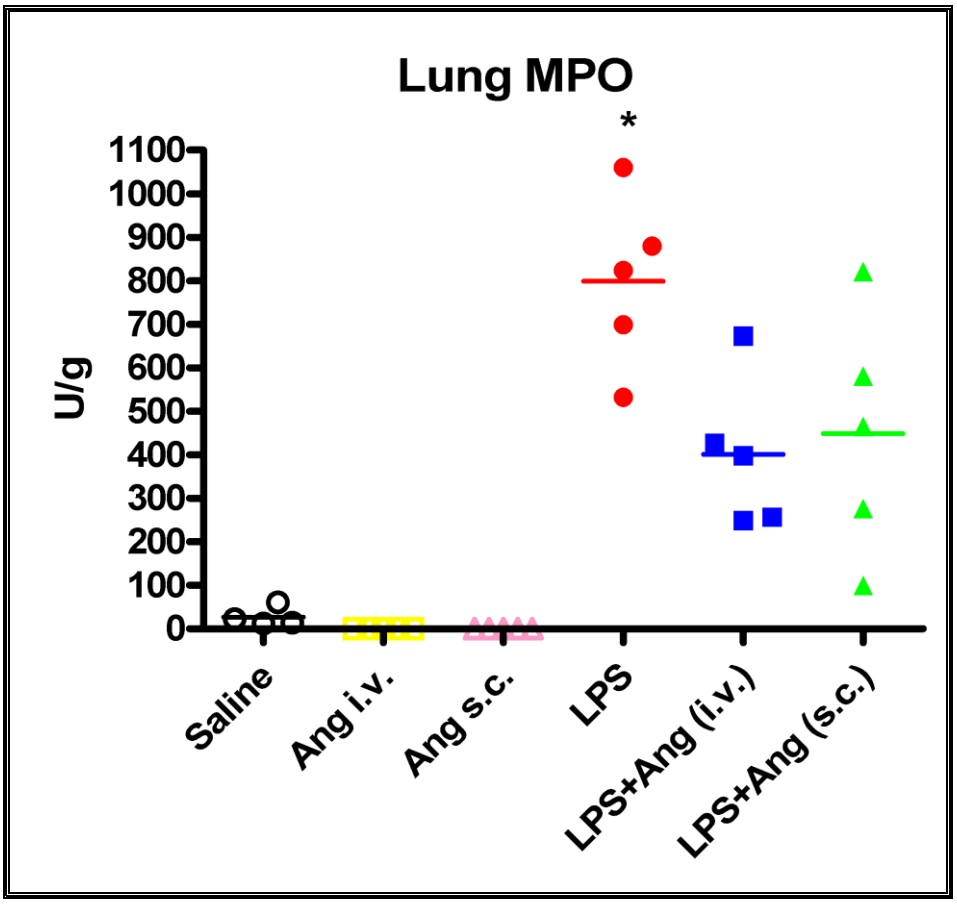

Figure 20: Lung MPO per unit gram of lung protein in the six treatment groups. Statistical differences at $p < 0.05$ are indicated by asterisks (*).

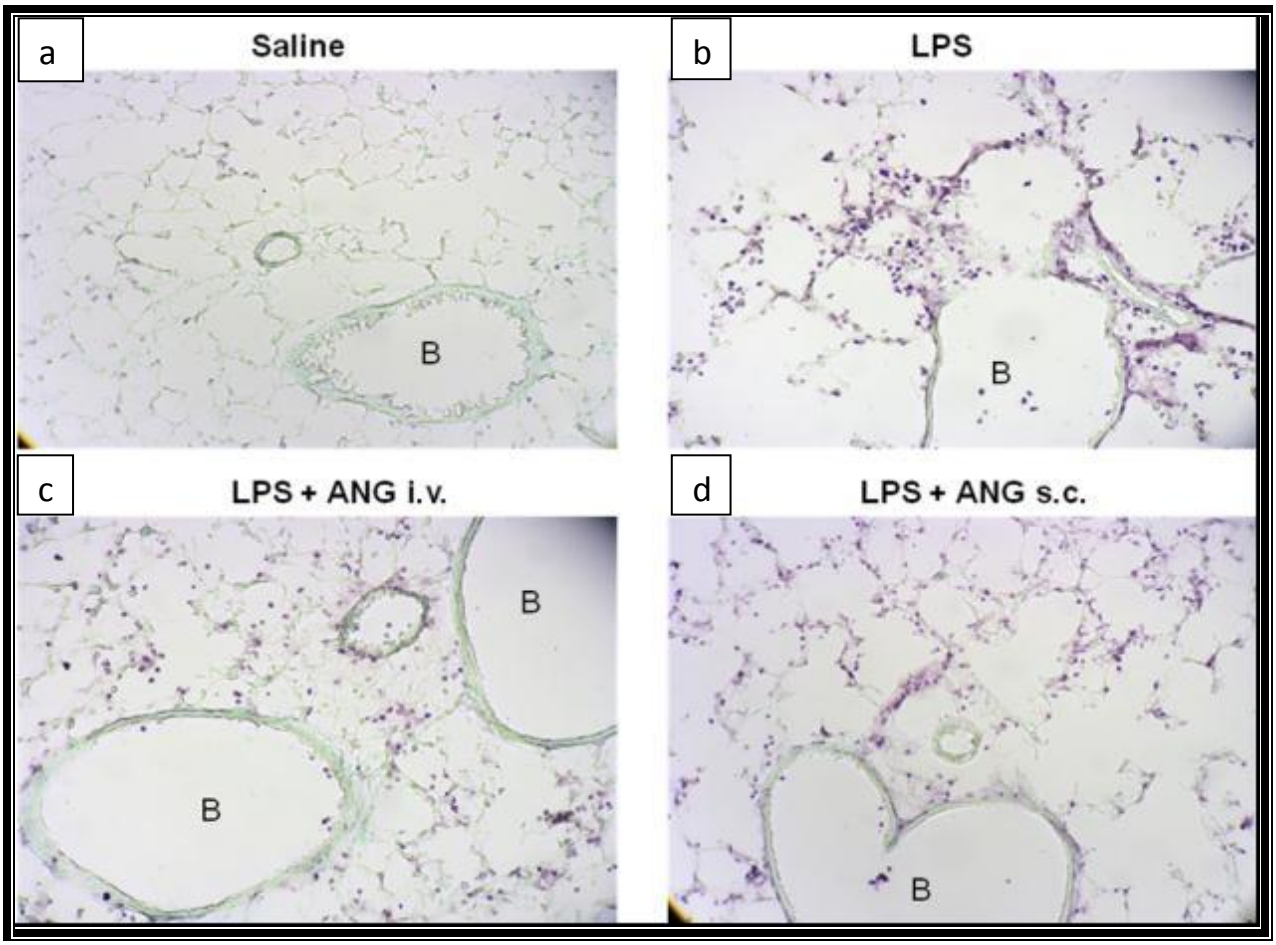

Figure 21: 10X magnified Gr-1 stained sections from lavaged lungs in a) control saline treated mice show almost negative Gr-1 immunostaining while b) shows signs of heavy staining and hence acute inflammation in LPS treated animals after 9 hours. c) shows moderate staining after LPS and ANG intravenous treatment whereas d) also shows moderate staining of lung after LPS and ANG subcutaneous treatment.

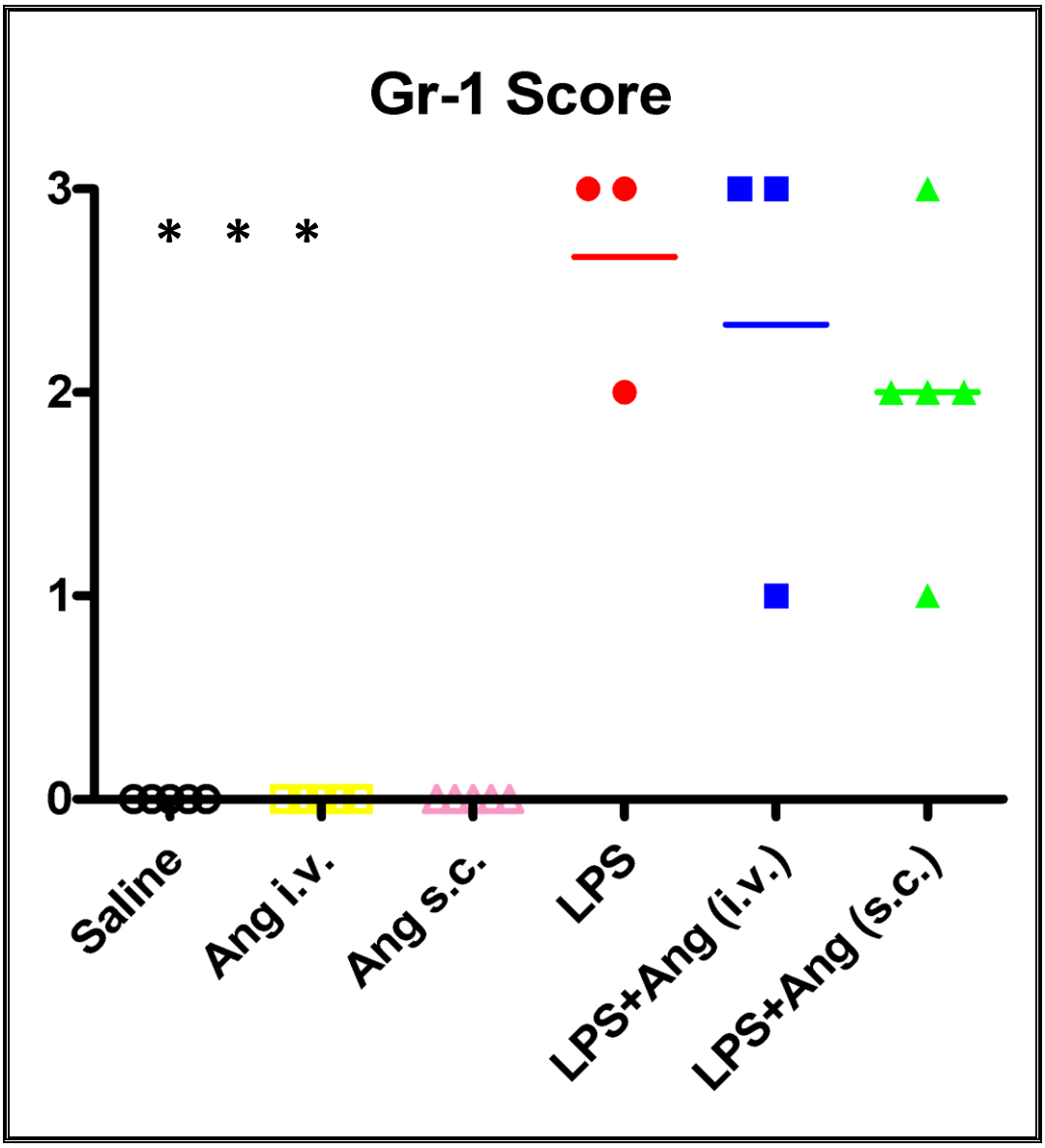

Figure 21e: Semiquantitative representation of Gr-1 lung immunohistochemical staining in the six treatment groups. Statistical differences at $p < 0.05$ are indicated by asterisks (*).

0 = no staining; 1 = light staining; 2 = moderate staining; and 3 = heavy staining

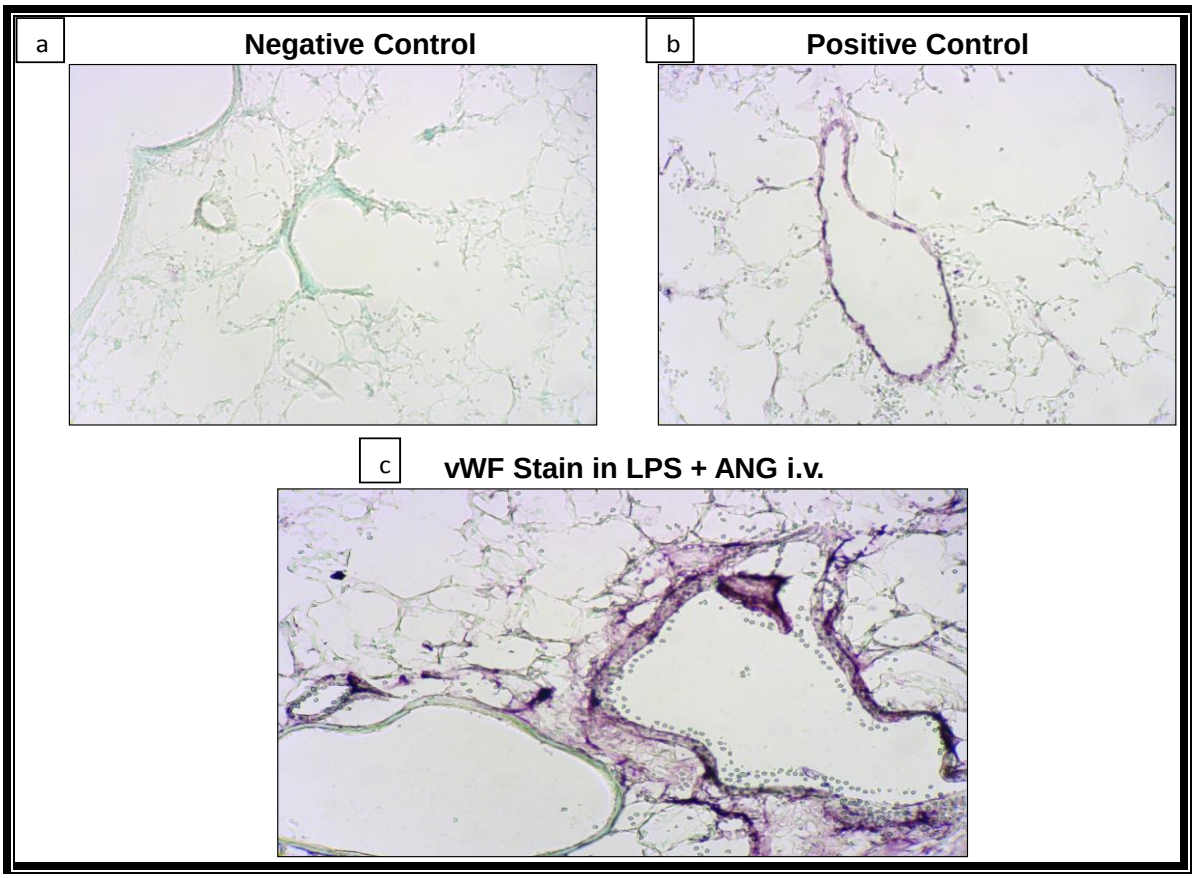

Figure 22: a) vWf stained 10X magnified mice lung sections used as positive control b) Primary antibody excluded to serve as a negative control for IHC protocol c) vWf staining in LPS + intravenous Angiostatin group. Note the bead like structures that are probably platelets in this group and excessive vWf staining indicating damage to the vessel.

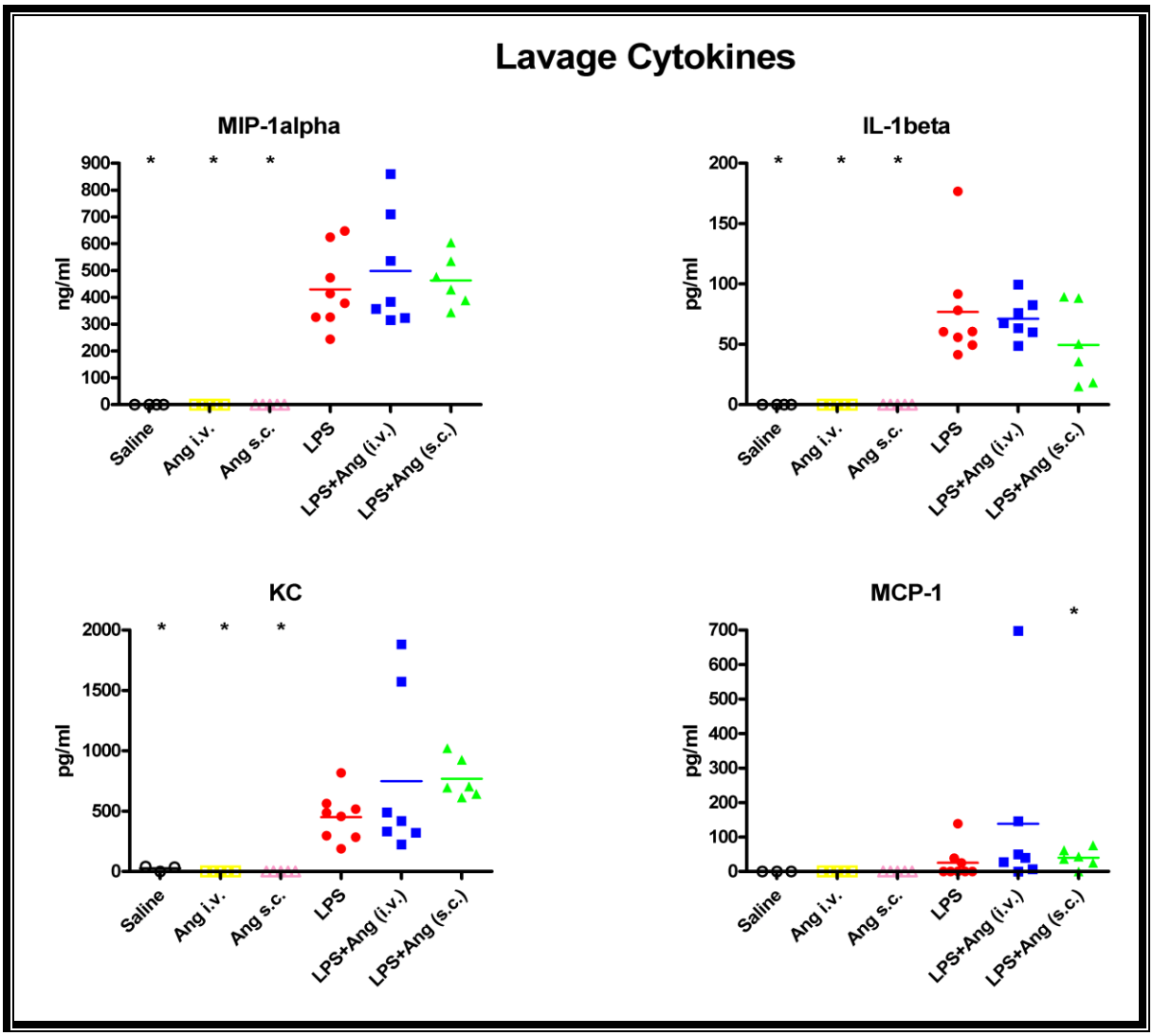

Figure 23: Lavage cytokine and chemokine concentrations in the six treatment groups.

Statistical differences at $p < 0.05$ are indicated by asterisks (*).

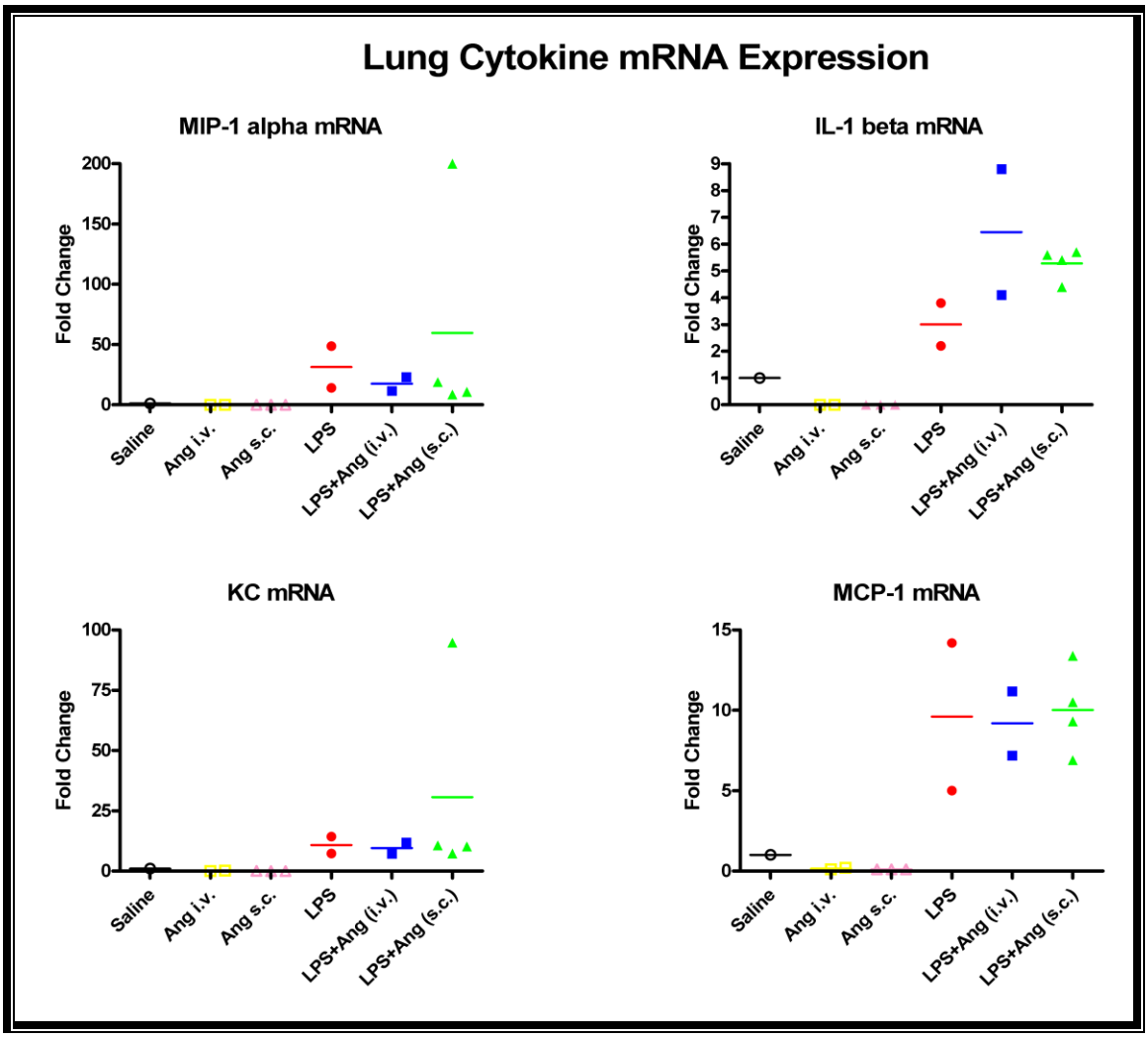

Figure 24: Lung cytokine and chemokine mRNA fold change in the six treatment groups. Statistical differences at $p < 0.05$ are indicated by asterisks (*).

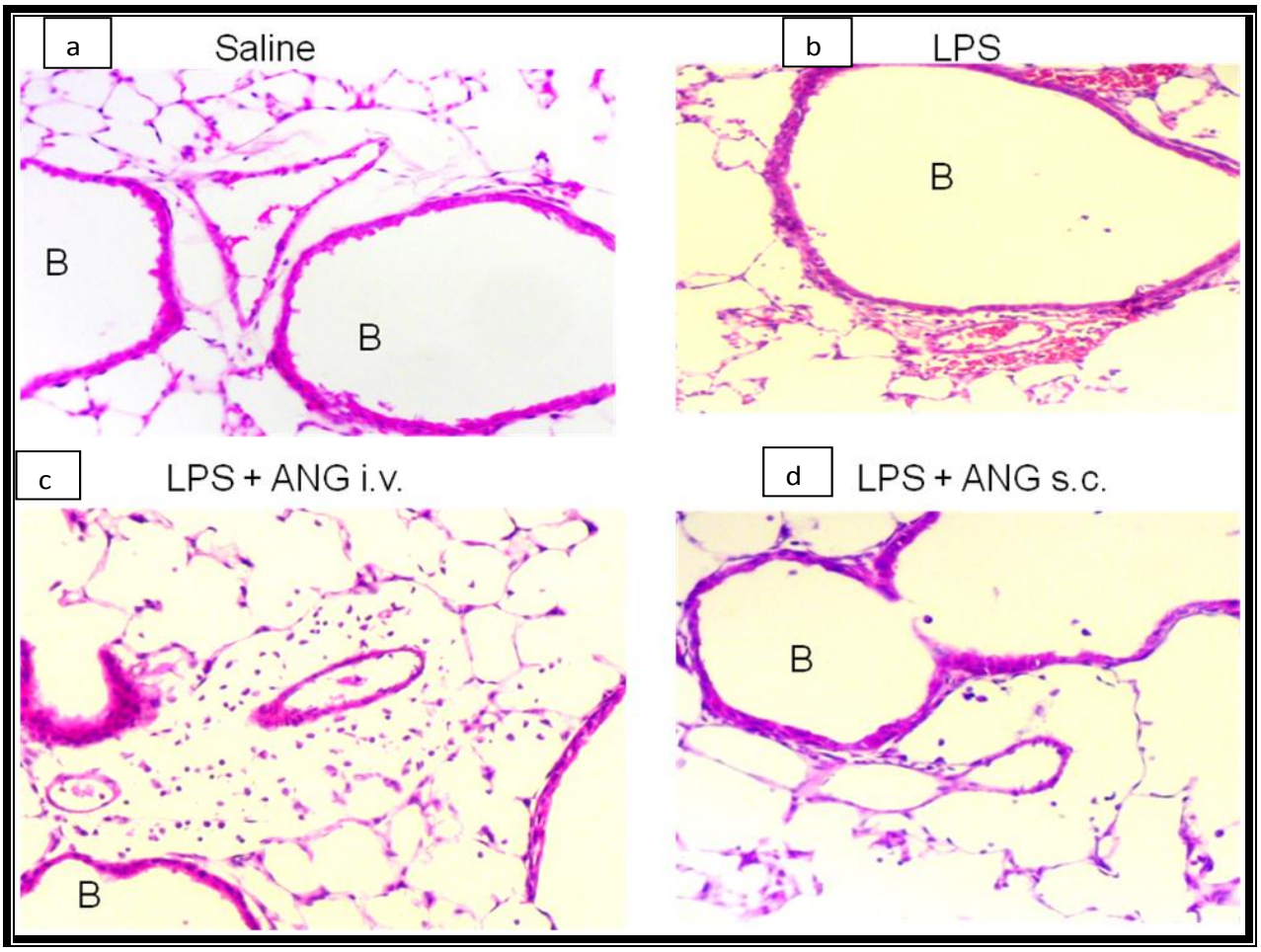

Figure 25: 10X magnified hematoxylin-eosin stained sections from lavaged lungs in a) control saline treated mice show normal histology while b) shows signs of acute inflammation in LPS treated animals after 9 hours c) shows signs of acute inflammation after LPS and ANG treatment whereas d) shows near normal looking lung after LPS + ANG subcutaneous treatment.

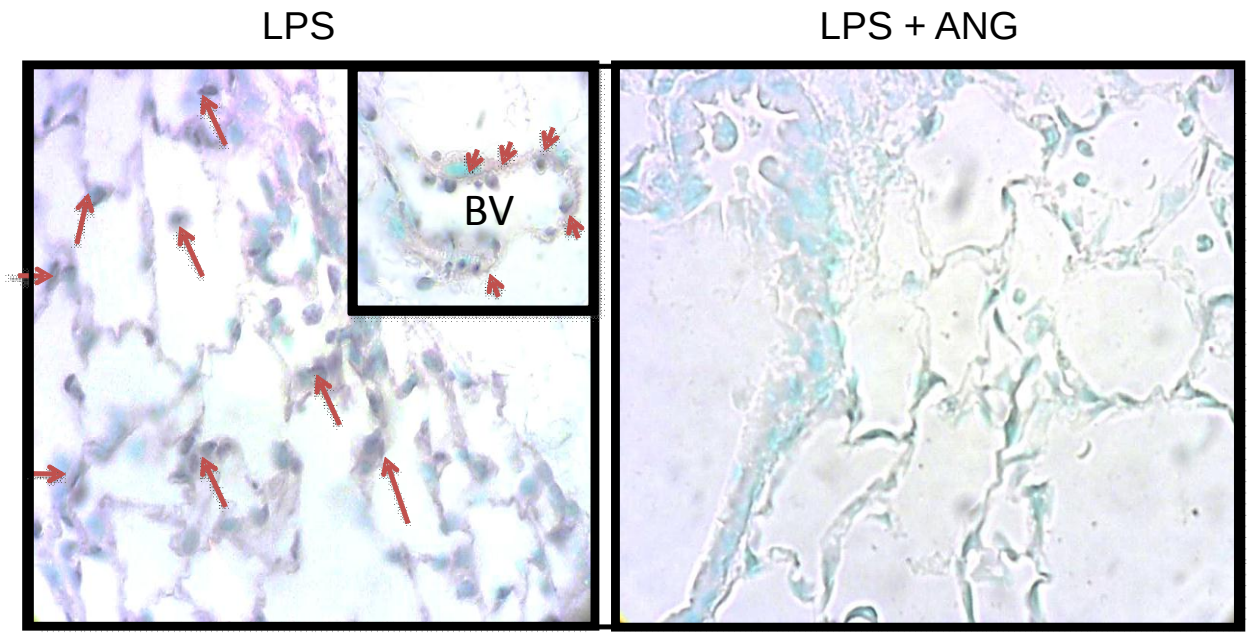

Figure 26: 10X magnified phospho-p38 MAPK stained sections from lavaged lungs in a) LPS treated mice show positive immunostaining in leukocytes trapped in the alveolar septae as well as in blood vessel (BV) while b) Subcutaneous ANG treated lung section shows no signs of staining . Arrows indicate positively stained leukocytes in LPS treated mice lung section.

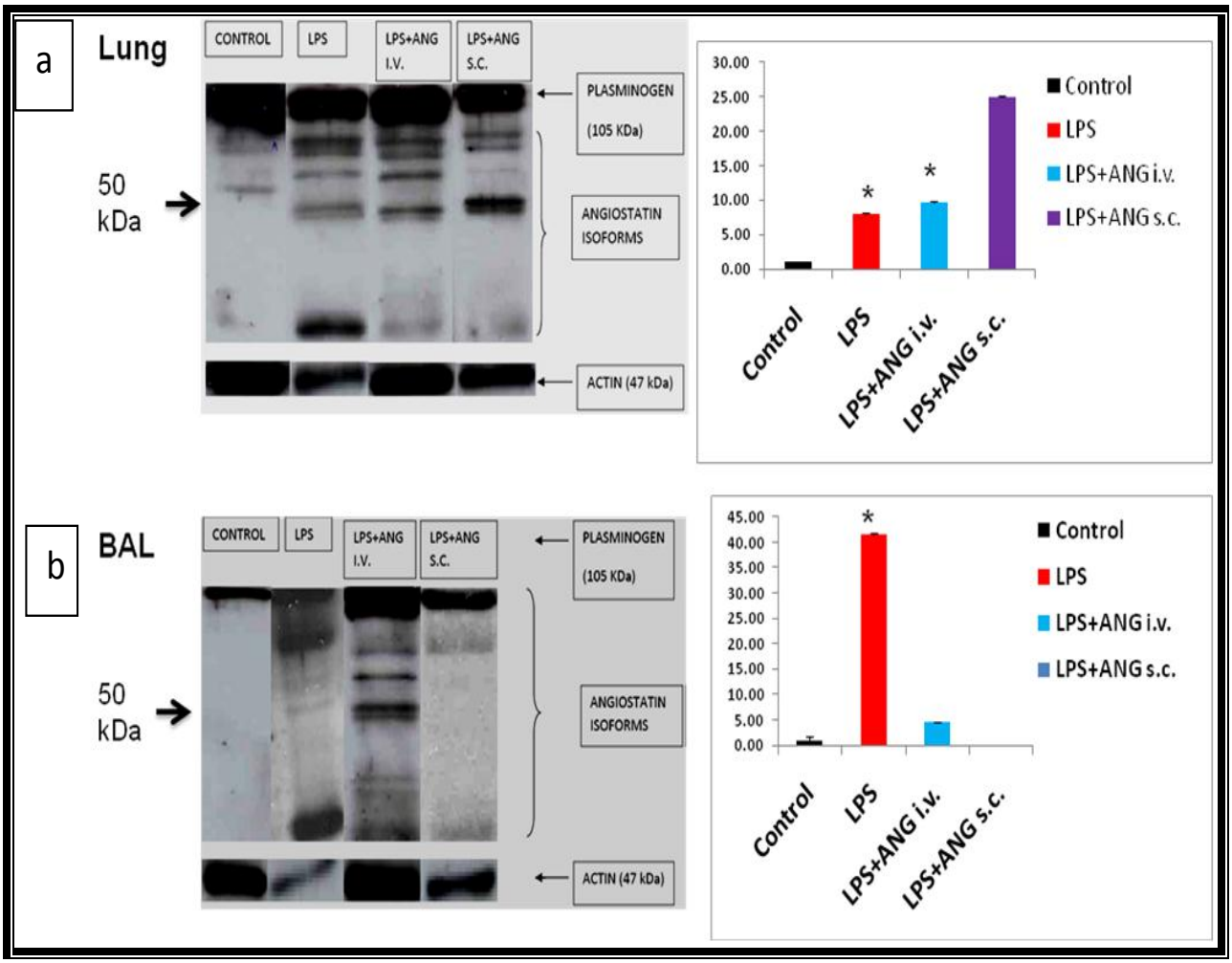

Figure 27: Representative western blots of plasminogen and angiostatin isoforms and densitometric analysis for 50kDa ANG in a) lung homogenates and b) bronchoalveolar lavage fluid. Also shown corresponding beta-actin expression. Y-axis represents fold difference normalized for actin expression. Statistical differences at $p < 0.05$ are indicated by asterisks (*).

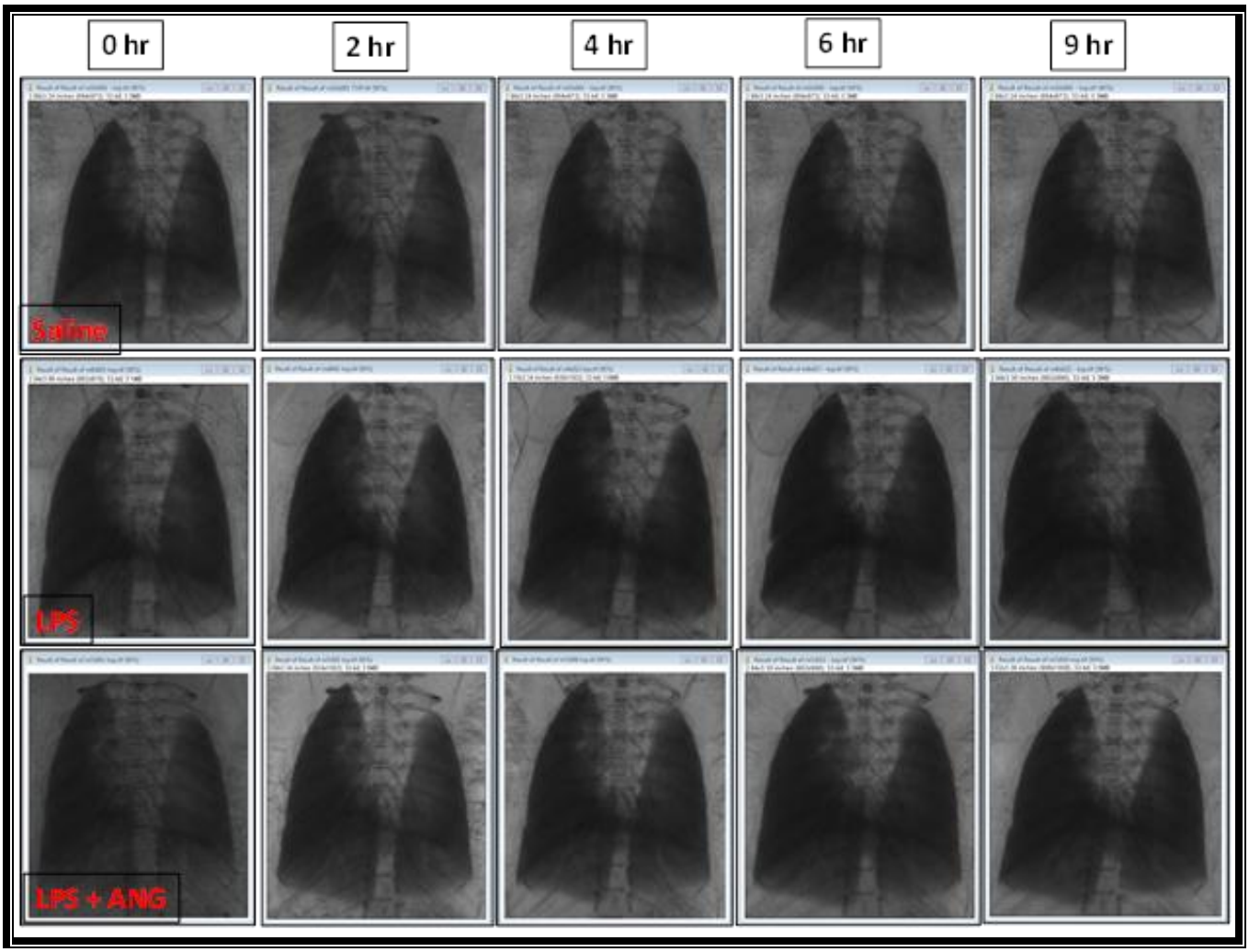

Figure 28: Representative normalized DEI images, taken on top of the rocking curve, of saline, LPS and LPS + ANG treated mice lungs followed over 9hrs.

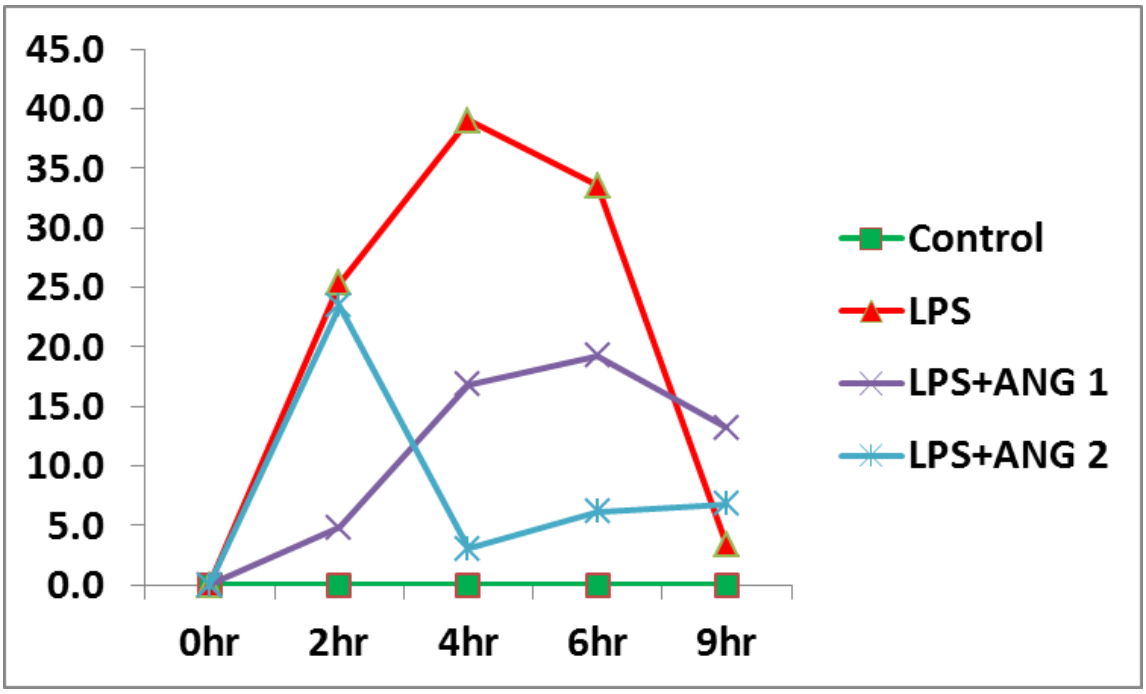

Figure 29a: Percent increase in lung area of DEI images from saline, LPS and LPS + subcutaneous ANG treated mice lungs followed over 9 hrs.

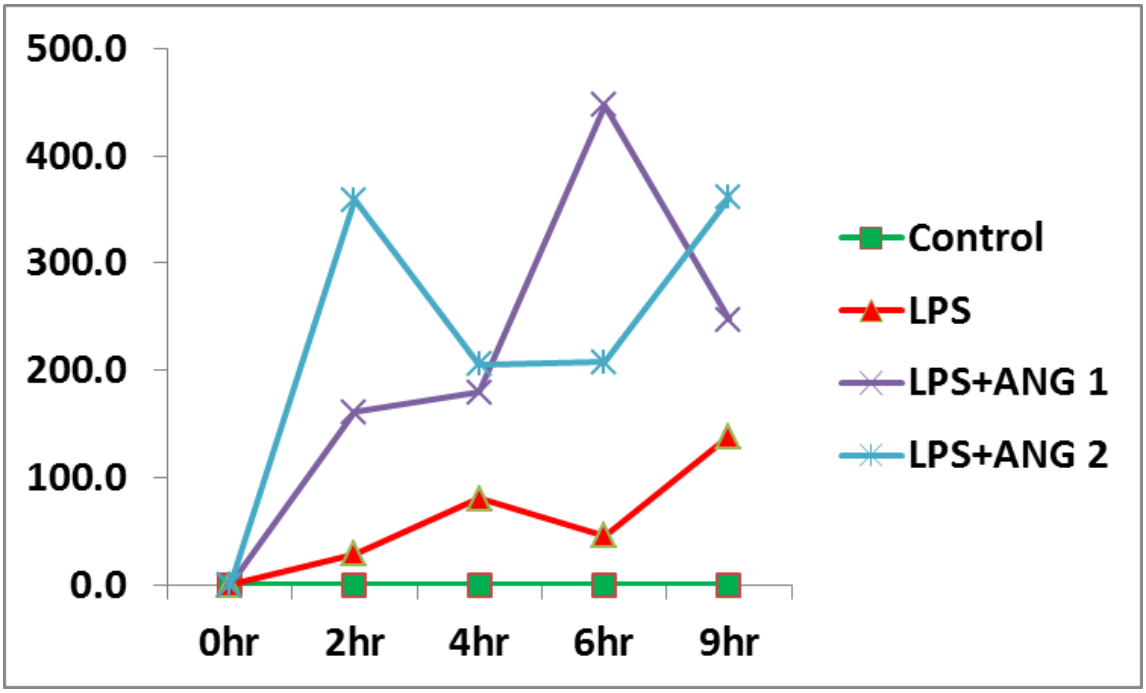

Figure 29b: Percent increase in contrast ratios of DEI images from saline, LPS and LPS + subcutaneous ANG treated mice lungs followed over 9 hrs.

4.7. Discussion

I report the first data on the anti-inflammatory role of ANG in a mouse model of acute lung injury. The data show that subcutaneous but not intravenous treatment with ANG reduces histologic signs of lung inflammation, decreases neutrophil migration into the lungs and edema formation. ANG reduced leukocyte expression of p38 MAPK. These data are of significance because of the critical double-edged role of neutrophils in acute lung injury and because of lack of any major therapeutic breakthroughs for ALI.

I used a well-established model of LPS-induced lung inflammation. The intranasal instillation of *E. coli* LPS resulted in significant increase in leukocytes in BAL and the lung tissues. The subcutaneous ANG treatment of the LPS-treated mice caused a significant reduction in neutrophil numbers in the BAL and reduced MPO concentrations in lung homogenates. Histologically, there was reduced septal congestion and near absence of inflammatory cells in the perivascular and peribronchial areas of the LPS + subcutaneous ANG mice compared to the LPS only group. In contrast, the intravenous ANG treatment of the LPS-treated mice caused an increase in BAL neutrophil numbers compared to the LPS group. The reasons for these strikingly different outcomes with subcutaneous and intravenous treatments with ANG are not known and were not investigated in my experiments. I do speculate, however, that the differences could be due to preferences in the uptake and metabolism of ANG or robust binding to its receptors on various vascular cells. Interestingly, mice treated with ANG only irrespective of the route did not induce lung inflammation or migration of neutrophils into the lung. Nevertheless, significant reduction of neutrophil migration and lung tissue inflammation by ANG is an important observation.

Neutrophil migration is induced through a complex interplay of adhesion molecules, cytokines and chemokines (Ley, Laudanna et al. 2007). Chemokines such as KC, MCP-1 and MIP-1 are known mediators of neutrophil migration in the lung (Wagner, Roth 2000) while IL-1β is a major player in the LPS-induced lung inflammation. While LPS treatment of mice resulted in significant increase in the concentrations of these mediators, there was no effect of ANG administration on their expression. ANG attenuated p38 MAPK phosphorylation in leukocytes in spite of its lack of effect on cytokines and chemokines analysed in this study. These data suggest that ANG does not affect neutrophil migration through inflammatory molecules analysed in this study. Further LPS + intravenous ANG group shows a distinct staining pattern for vWF that is marked by long strings surrounded by beaded structures, probably platelets. A recent report shows such binding of integrin $\alpha_v\beta_3$ to vWF under sheer stress (Huang, Roth et al. 2009a). Platelet activation can induce neutrophil recruitment in acute lung injury that might be the case in LPS + intravenous ANG group (Andonegui, Bonder et al. 2003, Clark, Ma et al. 2007, Andonegui, Kerfoot et al. 2005). It is possible that ANG shows its effects through direct binding to one of the ligands such as integrin $\alpha_v\beta_3$, which is expressed by neutrophils and endothelial cells in the normal and the inflamed lungs (Singh, Fu et al. 2000, Janardhan, Appleyard et al. 2004). In LPS + intravenous ANG group it is possible that ANG quickly binds to endothelial cells due to mode of its administration. There is speculation that integrin $\alpha_v\beta_3$ may play a role in neutrophil migration in the lung; however, direct evidence is yet to emerge. Based on my unpublished data, ANG may block integrin $\alpha_v\beta_3$ to inhibit actin aggregation to interfere with neutrophil motility in acute lung injury. However, this still may not explain the differential effects of subcutaneously versus intravenously administered ANG. This discrepancy in BAL neutrophil counts and lung MPO levels might be attributed to more cells

getting trapped in the pulmonary capillaries in the subcutaneous group avoiding their transmigration in the alveolar spaces. ANG does increase the expression of ICAM-1 and E-selectin (Luo, Lin et al. 1998, Chen, Huang et al. 2008) that might cause neutrophils to be trapped at the endothelial membrane. ANG binds to and inhibits F_1F_0 ATP synthase under conditions of low pH to cause ATP deficiency and consequently caspase-mediated apoptosis (Wahl, Kenan et al. 2005, Veitonmäki, Cao et al. 2004). Moreover, neutrophils express ATP synthase mRNA (BENELLI, MORINI et al. 2002). Unpublished data from our laboratory have also shown attenuation of F_1F_0 ATP synthase in ANG+LPS treated neutrophils *in-vitro* along with an enhanced apoptosis as witnessed by induction of activated caspase-3. Therefore, apoptotic neutrophils observed in ANG treated LPS animals could be attributed to inhibition of ATP synthase. A recent study has shown that ANG does not suppress spontaneous apoptosis by activating prosurvival pathways in neutrophils but it is yet to be tested if ANG induces neutrophil apoptosis by itself (Pluskota, Soloviev et al. 2008). My study also establishes a significantly higher expression of ANG in acute lung injury as depicted by western blots of lavage fluid and lung homogenates.

These experiments were my first attempt to visualize live mice lungs under normal or inflamed conditions over a span of 9 hrs. Lung area is proportional to lung weight and therefore an increase in area reflects increase in lung weight due to edema. ANG treatment attenuates increase in lung area that is increased in LPS treated mice. The DEI images obtained over both sides of the rocking curve are indicative of the scatter produced by lungs. Therefore, in future I would like to go further down the rocking curve in order obtain a fuller description of the ultra-small angle x-ray scattering (USAXS). This scattering is a metric of the projected number of air filled alveoli. Thus, a larger amount of scatter implies a larger number of air filled alveoli. This

scatter is reflected in the width of the scattering distribution measured with DEI. To obtain good scatter width information then requires that more images should be taken as a function of rocking angle. This subtle fact was not discovered until after the experimental run was completed. Contrast ratios of top images are proportional to the number of air filled alveoli. Therefore, LPS treatment causes attenuates any increase in contrast ratios when compared to basal line lungs or ANG treated lungs. These findings indicate that ANG causes improvement in lung function over time.

Conclusion

Hypothesis was proven true. To conclude, it can be stated that ANG, when administered through the subcutaneous route, diminishes neutrophilia whereas the intravenous route enhances this. From the result of lung myeloperoxidase and granulocyte specific staining, it seems that ANG inhibits the transmigration step of neutrophil migration rather than rolling and activation. ANG also shuts down leukocyte activation in lung sections as indicated by phospho-p38 MAPK immunohistochemistry. However, ANG does not affect cytokine release. ANG also improves lung function and edema over time as assessed by DEI.

Chapter 5
GENERAL DISCUSSION AND FUTURE DIRECTIONS

5.1. General Discussion

The main aim of my research was to investigate the function of ANG in neutrophil migration during ALI. Therefore, my experiments were designed to investigate the effect of ANG on neutrophil chemotaxis and activation, leukocyte migration under flow conditions and in LPS- induced ALI. The data reported in this thesis advance our knowledge about the ways to modulate neutrophil biology in inflamed tissues and also allude to the use of new imaging modalities to observe dynamics of lung inflammation.

ANG is upregulated in acute respiratory distress syndrome (Lucas, Lijnen et al. 2002), and neutrophils can also produce ANG (Scapini, Nesi et al. 2002). Neutrophils upon activation are credited with elimination of bacteria as well as causing significant tissue damage. The complexity however arises from the ability of excessive migration of activated neutrophils into an organ to protect the host but causation of tissue damage through production of ROS and cytotoxic molecules. The *in-vitro* study provides novel data that ANG inhibits neutrophil migration, induces silence by deactivating ROS production and activating apoptotic pathway, and inhibits their recruitment *in-vivo*.

To explore the molecular actions of ANG on neutrophils, first I developed a method through the use of FITC-NG to image ANG uptake by neutrophils. ANG does not bind to resting neutrophils but binds to and is endocytosed by fMLP-activated neutrophils. ANG co-localized with the lipid raft markers flotillin-1 and flotillin-2 in LPS and fMLP stimulated neutrophils. Disruption of lipid rafts with MCD inhibited ANG uptake, indicating that ANG binding and internalization are mediated via lipid rafts. β_3 integrin, a known ligand for ANG, colocalized with ANG in a nonpolar fashion. Integrins can recycle to and from lipid rafts during chemotaxis

(Hendey, Lawson et al. 1996, Fabbri, Di Meglio et al. 2005). Integrin blocking experiments were done to study the interaction of ANG with β_3 integrin. Unexpectedly, integrin blocking did not prevent ANG endocytosis, but restored polarization of neutrophils in the presence of ANG and fMLP. The data show that the integrin may not be the only receptor responsible for the uptake and actions of ANG in neutrophils.

Polarisation in response to chemoattractants is a primal event in chemotaxis and entails intimate reorganization of cytoskeleton. *In-vitro* confocal microscopy on mouse as well as human neutrophils revealed that ANG abolished polarisation as well as activation of neutrophils in response to fMLP and LPS. Hsp-27 induces actin capping and phosphorlyation of hsp-27 is essential for maintaining polarised heads (Jog, Jala et al. 2007). Immunoprecipitation revealed that hsp-27 binds to both α and β tubulin and inhibits tubulin polymerization (Hino, Hosoya 2003, Hino, Kurogi et al. 2000). ANG colocalises with this protein and blocked formation of polarized heads. It is however, still unclear if inhibition of hsp-27 phosphorylation is a direct effect of ANG or due to inactivation of MAPKinases.

The PDZ domain of AMOT can bind to cdc-42 Rho GTPase Activating Protein (GAP), Rich1 and produce a hypermigratory state in endothelial and epithelial cells. p190 Rho GAP is a RhoGAP that uncouples GTP from small G-protein Rho in order to recycle the small G-proteins during early establishment of polarity (Wells, Fawcett et al. 2006). AMOT is also known to be a scaffolding protein for Rich1 in endothelial and epithelial cells (Wells, Fawcett et al. 2006). Because of ANG's colocalization with AMOT and tubulin in human neutrophils, I speculate that ANG ultimately interferes with microtubular rearrangement. It has been shown earlier that ANG can bind to actin in cultured macrophages and endothelial cells (Dudani, Mehic et al. 2007, Perri,

Annabi et al. 2007). I found AMOT as a probable candidate for ANG mode of action during inhibition of chemotaxis.

While ANG didn't co-localize with ATP synthase, it diminished ATP synthase expression and the function of mitochondria which is in concordance with an earlier observation where ANG upregulates antiangiogenic and proapoptotic pathways via mitochondrial proteins (Lee, Muschal et al. 2009a). Mitochondria aggregate near the plasma membrane, as indicated by flotillin-1 and flotillin-2 co-expression with mitochondria in LPS activated human neutrophils. Mitochondria activated by LPS generate ROS through p44/42 MAPKinase phosphorylation (Markvicheva, Gorokhovatskii et al. 2010, Espinosa, Leiva et al. 2006, Zhong, Jiang et al. 2003). Respriatory burst, mediated by integrin β_3 signalling (Yan, Novak 1999), was abolished by ANG possibly through binding to $\alpha_V\beta_3$ integrin. Downstream molecules for chemotaxis regulation, ROS production and lifespan are in part mediated by phosphorylation of p38 MAPKinase (Kutsuna, Suzuki et al. 2004), which are activated by LPS. ANG inhibited MAPK signaling in activated neutrophils to abolishe ROS production and induced expression of caspase-3 to limit neutrophil survival.

The *in-vivo* studies are the first data on the anti-inflammatory role of ANG in a mouse model of acute lung injury. The data show that subcutaneous but not intravenous treatment with ANG reduces histologic signs of lung inflammation, decreases neutrophil migration into the lungs and edema formation. ANG reduced leukocyte expression of p38 MAPK. Based on the in vitro data and the reduced leukocyte expression of p38MAPK, I believe that ANG inhibits leucocyte cytoskeletal rearrangement and other downstream effects through blocking of p38MAPK. Although I don't have direct evidence, but based on the endothelial and neutrophil expression of integrin $\alpha_v\beta_3$, it is possible that ANG uses the integrin as a receptor. The precise of

role of interaction of the integrin with ANG may be explored through the use of $\beta_3^{-/-}$ mice. The direct physical interaction of ANG with one of its receptors and effects on cytoskeletal rearrangement may be the reason for reduced neutrophil migration in inflamed lungs because the concentrations of measured cytokines and chemokins were not altered by ANG treatment. An intriguing observation was that the intravenous ANG treatment of the LPS-treated mice caused an increase in BAL neutrophil numbers compared to the LPS group. The reasons for these strikingly different outcomes with subcutaneous and intravenous treatments with ANG are not known and were not investigated in my experiments. I do speculate however that the differences could be due to preferences in the uptake and metabolism of ANG or robust binding to its receptors on various vascular cells. Further LPS + intravenous ANG group shows a distinct staining pattern for vWF that is marked by long strings surrounded by beaded structures, probably platelets. A recent report shows such binding of integrin $\alpha_v\beta_3$ to vWF under sheer stress (Huang, Roth et al. 2009b). Platelet activation can induce neutrophil recruitment in acute lung injury that might be the case in LPS + intravenous ANG group (Andonegui, Bonder et al. 2003, Clark, Ma et al. 2007, Andonegui, Kerfoot et al. 2005). Interestingly, mice treated with ANG only irrespective of the route did not induce lung inflammation or migration of neutrophils into the lung. Nevertheless these data are of significance because of the critical double-edged role of neutrophils in acute lung injury and because of lack of any major therapeutic breakthroughs for ALI.

It is possible that ANG shows its effects through direct binding to one of the ligands such as integrin $\alpha_v\beta_3$, which is expressed by neutrophils and endothelial cells in the normal and the inflamed lungs (Singh, Fu et al. 2000, Janardhan, Appleyard et al. 2004). In LPS + intravenous ANG group it is possible that ANG quickly binds to endothelial cells due to mode of its

administration. There is speculation that integrin $\alpha_v\beta_3$ may play a role in neutrophil migration in the lung; however, direct evidence is yet to emerge. Based on *in-vitro* data from the first study, ANG may block integrin $\alpha_v\beta_3$ to inhibit actin aggregation to interfere with neutrophil motility in acute lung injury. However, this still may not explain the differential effects of subcutaneously versus intravenously administered ANG. This discrepancy in BAL neutrophil counts and lung MPO levels might be attributed to more cells getting trapped in the pulmonary capillaries in the subcutaneous group avoiding their transmigration in the alveolar spaces. ANG does increase the expression of ICAM-1 and E-selectin (Luo, Lin et al. 1998, Chen, Huang et al. 2008) that might cause neutrophils to be trapped at the endothelial membrane. ANG binds to and inhibits F_1F_0 ATP synthase under conditions of low pH to cause ATP deficiency and consequently caspase-mediated apoptosis (Wahl, Kenan et al. 2005, Veitonmäki, Cao et al. 2004). Moreover, neutrophils express ATP synthase mRNA (BENELLI, MORINI et al. 2002). Therefore, apoptotic neutrophils observed in ANG treated LPS animals could be attributed to inhibition of ATP synthase. A recent study has shown that ANG does not suppress spontaneous apoptosis by activating prosurvival pathways in neutrophils but it is yet to be tested if ANG induces neutrophil apoptosis by itself (Pluskota, Soloviev et al. 2008). My study also establishes a significantly higher expression of ANG in acute lung injury as depicted by western blots of lavage fluid and lung homogenates.

The synchrotron experiments were my first attempt to visualize live mice lungs under normal or inflamed conditions over a span of 9 hrs. My intital results of DEI image analysis show an improvement in lung congestion produced by subcutaneous ANG treatment as indicated by a decrease in lung area and an increase in contrast ratio over 9 hours. The DEI images obtained over both sides of the rocking curve are indicative of the scatter produced by lungs.

Therefore, in future, I would like to go further down the rocking curve in order obtain a fuller description of the ultra-small angle x-ray scattering (USAXS). This scattering is a metric of the projected number of air filled alveoli. Thus, a larger amount of scatter implies a larger number of air filled alveoli. This scatter is reflected in the width of the scattering distribution measured with DEI. To obtain good scatter width information then requires that more images should be taken as a function of rocking angle. This subtle fact was not discovered until after the experimental run was completed. Certainly, DEI has the capacity to quantitatively image lungs over time non-invasively; a property that makes this experimental approach unique. Conventional invasive techniques are helpful in delineating the molecular mechanism of a pathophysiological event but they do not represent the mass dynamics of a disease progression as has been underlined in acute lung injury. Further scope of improvement for phase contrast imaging lies in changing the object to detector distance in order to optimize the speckle pattern of lung images. High radiation dose is a limiting factor in high resolution phase contrast imaging coupled with a complicated post-analysis of the speckle pattern. This leaves DEI as a promising technique for real-time lung imaging.

5.2. Conclusions and Future Directions

Taken together my *in-vitro* experiments have established (Figure 15) that ANG deactivates neutrophils, limits their survival and inhibits *in-vivo* migration of leukocytes in inflamed blood vessels. Based on these data, ANG may act as a novel inhibitor of acute inflammation.

The *in-vivo* studies show that ANG, through subcutaneous route, diminishes neutrophilia whereas the intravenous route enhances this. From, the result of lung myeloperoxidase and

granulocyte specific staining, it seems that ANG inhibits the transmigration step of neutrophil migration rather than rolling and activation. ANG also shuts down the leukocyte activation in lung sections as indicated by phospho-p38 MAPK staining. However, ANG does not affect cytokine release. I have standardized the protocol for DEI imaging of mice lungs in ALI. My study offers promising non-invasive evaluation of alveolar dynamics in real-time. However, there is need to take images further down the rocking curve in order to establish metrics between scatter produced by lungs and the number of air-filled alveoli. Therefore, the proposed hypotheses were proven true.

In the present studies, co-localization experiments have indicated possible binding sites with tubulin and $\alpha_v\beta_3$ integrin but these do offer conclusive evidence. Therefore, there is a need to direct future studies in order to elucidate the binding proteins of ANG in neutrophils. For future experiments, it would be interesting to first look at real-time uptake of FITC-ANG in cremaster vascular bed. Based upon the cells that take up ANG *in-vivo*, the next experiment should be directed at identifying the primary binding sites of ANG *in-vivo*. In order to establish a precise signaling cascade for ANG's anti-inflammatory actions, phosphoproteomics using SILAC (stable-isotope labelling with amino-acids in cell culture) and functional assays for neutrophil migration and actin dynamics in specific knock-outs for ANG's putative binding proteins would be conclusive.

Based upon my intravital cremaster muscle experiments, it is likely that ANG is acting through endothelial cells to inhibit leukocyte adherence and emigration. As $\alpha_v\beta_3$ integrin and angiomotin are expressed on endothelial cells that are the binding sites established in

angiogenesis models, it would be interesting to see if conditional β_3 or angiomotin knockout mice show an increased neutrophil recruitment upon TNFα activation.

VITA

1 PATENT

1. European Patent dated 7 June, 2007 (Patent No.: WO/2007/063356 A2) entitled MONOSACCHARIDE DERIVATIVES: An inventor Applicants: Ranbaxy Laboratories Limited, Sattigeri, J.V., Arora, S.K., Salman, M., Palle, V.P., Nagarajan, M., Shirumalla, R.K., **Aulakh, G.K.**, Ray, A.

5 PUBLICATIONS

2. Charavaryamath, C., Keet, T., **Aulakh, G.K.**, Townsend, H.C.G. and Singh, B. Lung responses to secondary endotoxin challenge in rats exposed to pig barn air. 2008. *Journal of Occupational Medicine and Toxicology*, **3:** 24.
3. **Aulakh, G.K.**, Sodhi, R.K. and Singh, M. An update on non-peptide angiotensin receptor antagonists and related RAAS modulators. 2007. *Life Sciences,* **81:** 615-639.
4. Sodhi, R.K., **Aulakh, G.K.** and Singh, M. Cell Suicide and Caspases. 2007. *Vascular Pharmacology*, **46(6):** 383-393.
5. Shirumalla, R.K., Naruganahalli, K.S., Dastidar, S.G., Sattigeri, V., **Kaur, G**., Deb, C., Gupta, J.B., Salman, M. and Ray, A. RBx 7796: A novel inhibitor of 5-lipoxygenase. 2006. *Inflammation Research,* **55:** 517-527.
6. Bali, A., Bansal, Y., Sugumaran, M., Saggu, J.S., Balakumar, P., **Kaur, G**., Bansal, G., Sharma, A. and Singh, M. Design, synthesis, and evaluation of novelly substituted benzimidazole compounds as angiotensin II receptor antagonists. 2005. *Bioorganic & Medicinal Chemistry Letters*, **15(17):** 3962-3965.

REFERENCES

1. ABRAHAM, E., CARMODY, A., SHENKAR, R. and ARCAROLI, J., 2000. Neutrophils as early immunologic effectors in hemorrhage- or endotoxemia-induced acute lung injury. *American Journal of Physiology - Lung Cellular and Molecular Physiology*, **279**(6 23-6), pp. L1137-L1145.

2. ADAM, J.F., BAYAT, S., PORRA, L., ELLEAUME, H., ESTVE, F. and SUORTTI, P., 2009. Quantitative functional imaging and kinetic studies with high-Z contrast agents using synchrotron radiation computed tomography. *Clinical and experimental pharmacology physiology*, **36**(1), pp. 95.

3. ALBINI, A., BRIGATI, C., VENTURA, A., LORUSSO, G., PINTER, M., MORINI, M., MANCINO, A., SICA, A. and NOONAN, D.M., 2009. Angiostatin anti-angiogenesis requires IL-12: the innate immune system as a key target. *Journal of translational medicine*, **7**, pp. 5.

4. ANDONEGUI, G., BONDER, C.S., GREEN, F., MULLALY, S.C., ZBYTNUIK, L., RAHARJO, E. and KUBES, P., 2003. Endothelium-derived toll-like receptor-4 is the key molecule in LPS-induced neutrophil sequestration into lungs. *Journal of Clinical Investigation*, **111**(7), pp. 1011-1020.

5. ANDONEGUI, G., KERFOOT, S.M., MCNAGNY, K., EBBERT, K.V.J., PATEL, K.D. and KUBES, P., 2005. Platelets express functional Toll-like receptor-4. *Blood*, **106**(7), pp. 2417-2423.

6. ANDONEGUI, G., TREVANI, A.S., LÓPEZ, D.H., RAIDEN, S., GIORDANO, M. and GEFFNER, J.R., 1997. Inhibition of Human Neutrophil Apoptosis by Platelets. *Journal of Immunology,* **158**(7), pp. 3372-3377.

7. ANDREW, N. and INSALL, R.H., 2007. Chemotaxis in shallow gradients is mediated independently of PtdIns 3-kinase by biased choices between random protrusions. *Nature cell biology,* **9**(2), pp. 193-200.

8. AOSHIBA, K., YASUI, S., HAYASHI, M., TAMAOKI, J. and NAGAI, A., 1999. Role of p38-mitogen-activated protein kinase in spontaneous apoptosis of human neutrophils. *Journal of Immunology,* **162**(3), pp. 1692-1700.

9. AUFFRAY, C., FOGG, D., GARFA, M., ELAIN, G., JOIN-LAMBERT, O., KAYAL, S., SARNACKI, S., CUMANO, A., LAUVAU, G. and GEISSMANN, F., 2007. Monitoring of blood vessels and tissues by a population of monocytes with patrolling behavior. *Science,* **317**(5838), pp. 666-670.

10. BAHRAMSOLTANI, M. and PLENDL, J., 2007. Different ways to antiangiogenesis by angiostatin and suramin, and quantitation of angiostatin-induced antiangiogenesis. *APMIS,* **115**(1), pp. 30-46.

11. BARREIRO, O., DE LA FUENTE, H., MITTELBRUNN, M. and SÁNCHEZ-MADRID, F., 2007. Functional insights on the polarized redistribution of leukocyte integrins and their ligands during leukocyte migration and immune interactions. *Immunological reviews,* **218**(1), pp. 147-164.

12. BARREIRO, O., YÁÑEZ-MÓ, M., SERRADOR, J.M., MONTOYA, M.C., VICENTE-MANZANARES, M., TEJEDOR, R., FURTHMAYR, H. and SÁNCHEZ-MADRID, F., 2002. Dynamic interaction of VCAM-1 and ICAM-1 with moesin and ezrin in a novel endothelial docking structure for adherent leukocytes. *Journal of Cell Biology*, **157**(7), pp. 1233-1245.

13. BENELLI, R., MORINI, M., CARROZZINO, F., FERRARI, N., MINGHELLI, S., SANTI, L., CASSATELLA, M., NOONAN, D.M. and ALBINI, A., 2002. Neutrophils as a key cellular target for angiostatin: implications for regulation of angiogenesis and inflammation 1. *The FASEB Journal*, **16**(2), pp. 267-269.

14. BENELLI, R., MORINI, M., BRIGATI, C., NOONAN, D.M. and ALBINI, A., 2003. Angiostatin inhibits extracellular HIV-Tat-induced inflammatory angiogenesis. *International journal of oncology*, **22**(1), pp. 87-91.

15. BESTEBROER, J., POPPELIER, M.J.J.G., ULFMAN, L.H., LENTING, P.J., DENIS, C.V., VAN KESSEL, K.P.M., VAN STRIJP, J.A.G. and DE HAAS, C.J.C., 2007. Staphylococcal superantigen-like 5 binds PSGL-1 and inhibits P-selectin-mediated neutrophil rolling. *Blood*, **109**(7), pp. 2936-2943.

16. BOURS, M.J.L., SWENNEN, E.L.R., DI VIRGILIO, F., CRONSTEIN, B.N. and DAGNELIE, P.C., 2006. *Adenosine 5'-triphosphate and adenosine as endogenous signaling molecules in immunity and inflammation.* Oxford: Pergamon.

17. BRATT, A., BIROT, O., SINHA, I., VEITONMÄKI, N., AASE, K., ERNKVIST, M. and HOLMGREN, L., 2005. Angiomotin regulates endothelial cell-cell junctions and cell motility. *Journal of Biological Chemistry*, **280**(41), pp. 34859-34869.

18. BRATT, A., WILSON, W.J., TROYANOVSKY, B., AASE, K., KESSLER, R., MEIR, E.G.V. and HOLMGREN, L., 2002. Angiomotin belongs to a novel protein family with conserved coiled-coil and PDZ binding domains. *Gene*, **298**(1), pp. 69-77.

19. BRATT, A., WILSON, W.J., TROYANOVSKY, B., AASE, K., KESSLER, R., VAN MEIR, E.G. and HOLMGREN, L., 2003. Erratum: Angiomotin belongs to a novel protein family with conserved coiled-coil and PDZ binding domains (Gene (2002) 298 (69-77)). *Gene*, **310**(1-2), pp. 221.

20. BRUNET, A., BONNI, A., ZIGMOND, M.J., LIN, M.Z., JUO, P., HU, L.S., ANDERSON, M.J., ARDEN, K.C., BLENIS, J. and GREENBERG, M.E., 1999. Akt promotes cell survival by phosphorylating and inhibiting a forkhead transcription factor. *Cell*, **96**(6), pp. 857-868.

21. CAMPELLONE, K.G. and WELCH, M.D., 2010. A nucleator arms race: Cellular control of actin assembly. *Nature Reviews Molecular Cell Biology*, **11**(4), pp. 237-251.

22. CARA, D.C. and KUBES, P., 2003. Intravital microscopy as a tool for studying recruitment and chemotaxis. *METHODS IN MOLECULAR BIOLOGY-CLIFTON THEN TOTOWA-*, **239**, pp. 123-132.

23. CARDONE, M.H., ROY, N., STENNICKE, H.R., SALVESEN, G.S., FRANKE, T.F., STANBRIDGE, E., FRISCH, S. and REED, J.C., 1998. Regulation of cell death protease caspase-9 by phosphorylation. *Science*, **282**(5392), pp. 1318-1321.

24. CARMAN, C.V. and SPRINGER, T.A., 2004. A transmigratory cup in leukocyte diapedesis both through individual vascular endothelial cells and between them. *Journal of Cell Biology,* **167**(2), pp. 377-388.

25. CASTEL, S., PAGAN, R., MITJANS, F., PIULATS, J., GOODMAN, S., JONCZYK, A., HUBER, F., VILARÓ, S. and REINA, M., 2001. RGD peptides and monoclonal antibodies, antagonist of α_v-integrin, enter the cells by independent endocytic pathways. *Laboratory Investigation,* **81**(12), pp. 1615-1626.

26. CHAPMAN, D., NESCH, I., HASNAH, M.O. and MORRISON, T.I., 2006. X-ray optics for emission line X-ray source diffraction enhanced systems. *Nuclear Instruments and Methods in Physics Research, Section A: Accelerators, Spectrometers, Detectors and Associated Equipment,* **562**(1), pp. 461-467.

27. CHAPMAN, D., PISANO, E., THOMLINSON, W., ZHONG, Z., JOHNSTON, R.E., WASHBURN, D., SAYERS, D. and MALINOWSKA, K., 1998. Medical applications of diffraction enhanced imaging. *Breast Disease,* **10**(3-4), pp. 197-207.

28. CHAPMAN, D., THOMLINSON, W., JOHNSTON, R.E., WASHBURN, D., PISANO, E., GMÜR, N., ZHONG, Z., MENK, R., ARFELLI, F. and SAYERS, D., 1997. Diffraction enhanced x-ray imaging. *Physics in Medicine and Biology,* **42**(11), pp. 2015-2025.

29. CHAVAKIS, T., ATHANASOPOULOS, A., RHEE, J.S., ORLOVA, V., SCHMIDT-WOLL, T., BIERHAUS, A., MAY, A.E., CELIK, I., NAWROTH, P.P. and PREISSNER, K.T., 2005. Angiostatin is a novel anti-inflammatory factor by inhibiting leukocyte recruitment. *Blood,* **105**(3), pp. 1036.

30. CHAVAKIS, T., HUSSAIN, M., KANSE, S.M., PETERS, G., BRETZEL, R.G., FLOCK, J.-., HERRMANN, M. and PREISSNER, K.T., 2002. Staphylococcus aureus extracellular adherence protein serves as anti-inflammatory factor by inhibiting the recruitment of host leukocytes. *Nature medicine,* **8**(7), pp. 687-693.

31. CHEN, Y., WU, H., LI, C., HUANG, Y., CHIANG, C., WU, M. and WU, L., 2006. *Anti-angiogenesis mediated by angiostatin K1-3, K1-4 and K1-4.5. Involvement of p53, FasL, AKT and mRNA deregulation.* Stuttgart,: F.K. Schattauer.

32. CHEN, Y., HUANG, Y., WU, H., WU, M., CHANG, W., KUO, Y., LU, K. and WU, L., 2008. *Angiostatin K1-3 induces E-selectin via AP1 and Ets1: a mediator for anti-angiogenic action of K1-3.* [Oxford]: Blackwell Pub., c2003-.

33. CHENG, D.S., HAN, W., CHEN, S.M., SHERRILL, T.P., CHONT, M., PARK, G.Y., SHELLER, J.R., POLOSUKHIN, V.V., CHRISTMAN, J.W., YULL, F.E. and BLACKWELL, T.S., 2007. Airway epithelium controls lung inflammation and injury through the NF-kappa B pathway. *Journal of immunology (Baltimore, Md.: 1950),* **178**(10), pp. 6504-6513.

34. CHI, S.L. and PIZZO, S.V., 2006. *Angiostatin is directly cytotoxic to tumor cells at low extracellular pH: a mechanism dependent on cell surface-associated ATP synthase.* Philadelphia: American Association for Cancer Research.

35. CHI, S.L., WAHL, M.L., MOWERY, Y.M., SHAN, S., MUKHOPADHYAY, S., HILDERBRAND, S.C., KENAN, D.J., LIPES, B.D., JOHNSON, C.E., MARUSICH, M.F., CAPALDI, R.A., DEWHIRST, M.W. and PIZZO, S.V., 2007. *Angiostatin-like*

activity of a monoclonal antibody to the catalytic subunit of F1F0 ATP synthase. Philadelphia: American Association for Cancer Research.

36. CINAMON, G., SHINDER, V., SHAMRI, R. and ALON, R., 2004. Chemoattractant signals and β2 integrin occupancy at apical endothelial contacts combine with shear stress signals to promote transendothelial neutrophil migration. *Journal of Immunology,* **173**(12), pp. 7282-7291.

37. CLARK, S.R., MA, A.C., TAVENER, S.A., MCDONALD, B., GOODARZI, Z., KELLY, M.M., PATEL, K.D., CHAKRABARTI, S., MCAVOY, E., SINCLAIR, G.D., KEYS, E.M., ALLEN-VERCOE, E., DEVINNEY, R., DOIG, C.J., GREEN, F.H.Y. and KUBES, P., 2007. Platelet TLR4 activates neutrophil extracellular traps to ensnare bacteria in septic blood. *Nature medicine,* **13**(4), pp. 463-469.

38. COFFER, P.J., JIN, J. and WOODGETT, J.R., 1998. Protein kinase B (c-Akt): A multifunctional mediator of phosphatidylinositol 3-kinase activation. *Biochemical Journal,* **335**(1), pp. 1-13.

39. CZERMAK, B.J., BRECKWOLDT, M., RAVAGE, Z.B., HUBER-LANG, M., SCHMAL, H., BLESS, N.M., FRIEDL, H.P. and WARD, P.A., 1999. Mechanisms of enhanced lung injury during sepsis. *American Journal of Pathology,* **154**(4), pp. 1057-1065.

40. CZERMAK, B.J., SARMA, V., PIERSON, C.L., WARNER, R.L., HUBER-LANG, M., BLESS, N.M., SCHMAL, H., FRIEDL, H.P. and WARD, P.A., 1999. Protective effects of C5a blockade in sepsis. *Nature medicine,* **5**(7), pp. 788-792.

41. DALLEGRI, F. and OTTONELLO, L., 1997. Tissue injury in neutrophilic inflammation. *Inflammation research : official journal of the European Histamine Research Society ...[et al.]*, **46**(10), pp. 382-391.

42. DATTA, S.R., DUDEK, H., XU, T., MASTERS, S., HAIAN, F., GOTOH, Y. and GREENBERG, M.E., 1997. Akt phosphorylation of BAD couples survival signals to the cell- intrinsic death machinery. *Cell*, **91**(2), pp. 231-241.

43. DE CASTRO JUNIOR, G., PUGLISI, F., DE AZAMBUJA, E., EL SAGHIR, N.S. and AWADA, A., 2006. Angiogenesis and cancer: a cross-talk between basic science and clinical trials (the "do ut des" paradigm). *Critical Reviews in Oncology and Hematology*, **59**(1), pp. 40-50.

44. DEL PESO, L., GONZÁLEZ-GARCÍA, M., PAGE, C., HERRERA, R. and NUÑEZ, G., 1997. Interleukin-3-induced phosphorylation of BAD through the protein kinase Akt. *Science*, **278**(5338), pp. 687-689.

45. DIMMELER, S., FLEMING, I., FISSLTHALER, B., HERMANN, C., BUSSE, R. and ZEIHER, A.M., 1999. Activation of nitric oxide synthase in endothelial cells by Akt-dependent phosphorylation. *Nature*, **399**(6736), pp. 601-605.

46. DIRKX, A.E.M., OUDE EGBRINK, M.G.A., CASTERMANS, K., VAN DER SCHAFT, D.W.J., THIJSSEN, V.L.J.L., DINGS, R.P.M., KWEE, L., MAYO, K.H., WAGSTAFF, J. and TER STEEGE, J.C.A.B., 2006. Anti-angiogenesis therapy can overcome endothelial cell anergy and promote leukocyte-endothelium interactions and infiltration in tumors. *The FASEB Journal*, **20**(6), pp. 621-630.

47. DOERSCHUK, C.M., ALLARD, M.F., MARTIN, B.A., MACKENZIE, A., AUTOR, A.P. and HOGG, J.C., 1987. Marginated pool of neutrophils in rabbit lungs. *Journal of applied physiology,* **63**(5), pp. 1806-1815.

48. DOERSCHUK, C.M., DOWNEY, G.P., DOHERTY, D.E., ENGLISH, D., GIE, R.P., OHGAMI, M., WORTHEN, G.S., HENSON, P.M. and HOGG, J.C., 1990. Leukocyte and platelet margination within microvasculature of rabbit lungs. *Journal of applied physiology,* **68**(5), pp. 1956-1961.

49. DOERSCHUK, C.M., QUINLAN, W.M., DOYLE, N.A., BULLARD, D.C., VESTWEBER, D., JONES, M.L., TAKEI, F., WARD, P.A. and BEAUDET, A.L., 1996. The Role of P-Selectin and ICAM-1 in Acute Lung Injury as Determined Using Blocking Antibodies and Mutant Mice. *Journal of Immunology,* **157**(10), pp. 4609-4614.

50. DUDANI, A.K., MEHIC, J. and MARTYRES, A., 2007. Plasminogen and angiostatin interact with heat shock proteins. *Molecular and cellular biochemistry,* **300**(1-2), pp. 197-205.

51. EDDY, R.J., PIERINI, L.M. and MAXFIELD, F.R., 2002. Microtubule asymmetry during neutrophil polarization and migration. *Molecular biology of the cell,* **13**(12), pp. 4470-4483.

52. EHRENGRUBER, M.U., DERANLEAU, D.A. and COATES, T.D., 1996. Shape oscillations of human neutrophil leukocytes: Characterization and relationship to cell motility. *Journal of Experimental Biology,* **199**(4), pp. 741-747.

53. ESPINOSA, A., LEIVA, A., PEÑA, M., MÜLLER, M., DEBANDI, A., HIDALGO, C., ANGÉLICA CARRASCO, M. and JAIMOVICH, E., 2006. Myotube depolarization generates reactive oxygen species through NAD(P)H oxidase; ROS-elicited Ca^{2+} stimulates ERK, CREB, early genes. *Journal of cellular physiology,* **209**(2), pp. 379-388.

54. FABBRI, M., DI MEGLIO, S., GAGLIANI, M.C., CONSONNI, E., MOLTENI, R., BENDER, J.R., TACCHETTI, C. and PARDI, R., 2005. Dynamic partitioning into lipid rafts controls the endo-exocytic cycle of the $\alpha L/\beta_2$ integrin, LFA-1, during leukocyte chemotaxis. *Molecular biology of the cell,* **16**(12), pp. 5793-5803.

55. FALCONE, D.J., KHAN, K.M.F., LAYNE, T. and FERNANDES, L., 1998. Macrophage Formation of Angiostatin during Inflammation A BYPRODUCT OF THE ACTIVATION OF PLASMINOGEN. *Journal of Biological Chemistry,* **273**(47), pp. 31480-31485.

56. FENG, D., NAGY, J.A., PYNE, K., DVORAK, H.F. and DVORAK, A.M., 1998. Neutrophils emigrate from venules by a transendothelial cell pathway in response to FMLP. *Journal of Experimental Medicine,* **187**(6), pp. 903-915.

57. FERGUSON, G.J., MILNE, L., KULKARNI, S., SASAKI, T., WALKER, S., ANDREWS, S., CRABBE, T., FINAN, P., JONES, G., JACKSON, S., CAMPS, M., ROMMEL, C., WYMANN, M., HIRSCH, E., HAWKINS, P. and STEPHENS, L., 2007. PI(3)Kγ has an important context-dependent role in neutrophil chemokinesis. *Nature cell biology,* **9**(1), pp. 86-91.

58. FOLKESSON, H.G., MATTHAY, M.A., HEBERT, C.A. and BROADDUS, V.C., 1995. Acid aspiration-induced lung injury in rabbits is mediated by interleukin- 8-dependent mechanisms. *Journal of Clinical Investigation,* **96**(1), pp. 107-116.

59. FOSSATI, G., MOULDING, D.A., SPILLER, D.G., MOOTS, R.J., WHITE, M.R.H. and EDWARDS, S.W., 2003. The mitochondrial network of human neutrophils: Role in chemotaxis, phagocytosis, respiratory burst activation, and commitment to apoptosis. *Journal of Immunology,* **170**(4), pp. 1964-1972.

60. FOXMAN, E.F., CAMPBELL, J.J. and BUTCHER, E.C., 1997. Multistep navigation and the combinatorial control of leukocyte chemotaxis. *Journal of Cell Biology,* **139**(5), pp. 1349-1360.

61. FRIEDL, P., BORGMANN, S. and BROCKER, E.B., 2001. Amoeboid leukocyte crawling through extracellular matrix: lessons from the Dictyostelium paradigm of cell movement. *Journal of leukocyte biology,* **70**(4), pp. 491-509.

62. GAGNE, V., MOREAU, J., PLOURDE, M., LAPOINTE, M., LORD, M., GAGNON, E. and FERNANDES, M.J., 2009. Human angiomotin-like 1 associates with an angiomotin protein complex through its coiled-coil domain and induces the remodeling of the actin cytoskeleton. *Cell motility and the cytoskeleton,* **66**(9), pp. 754-768.

63. GEISZT, M., DAGHER, M.C., HAVASI, A. and LIGETI, E., 1998. Characterization of Rac GTPase activating proteins in neutrophil granulocytes. *FASEB Journal,* **12**(5),.

64. GIAGULLI, C., OTTOBONI, L., CAVEGGION, E., ROSSI, B., LOWELL, C., CONSTANTIN, G., LAUDANNA, C. and BERTON, G., 2006. The Src family kinases

Hck and Fgr are dispensable for inside-out, chemoattractant-induced signaling regulating β2 integrin affinity and valency in neutrophils, but are required for β2 integrin-mediated outside-in signaling involved in sustained adhesion. *Journal of Immunology*, **177**(1), pp. 604-611.

65. GROMMES, J. and SOEHNLEIN, O., 2011. Contribution of neutrophils to acute lung injury. *Molecular Medicine*, **17**(3-4), pp. 293-307.

66. GUPTA, N., NODZENSKI, E., KHODAREV, N.N., YU, J., KHORASANI, L., BECKETT, M.A., KUFE, D.W. and WEICHSELBAUM, R.R., 2001. *Angiostatin effects on endothelial cells mediated by ceramide and RhoA.* Oxford, UK: Published for EMBO by Oxford University Press.

67. HALL, A., 1992. Ras-related GTPases and the cytoskeleton. *Molecular biology of the cell*, **3**(5), pp. 475-479.

68. HALL, A. and NOBES, C.D., 2000. Rho GTPases: Molecular switches that control the organization and dynamics of the actin cytoskeleton. *Philosophical Transactions of the Royal Society B: Biological Sciences*, **355**(1399), pp. 965-970.

69. HAMACHER, J., LUCAS, R., LIJNEN, H.R., BUSCHKE, S., DUNANT, Y., WENDEL, A., GRAU, G.E., SUTER, P.M. and RICOU, B., 2002. Tumor Necrosis Factor-{alpha} and Angiostatin Are Mediators of Endothelial Cytotoxicity in Bronchoalveolar Lavages of Patients with Acute Respiratory Distress Syndrome. *American Journal of Respiratory and Critical Care Medicine*, **166**(5), pp. 651.

70. HARI, D., BECKETT, M.A., SUKHATME, V.P., DHANABAL, M., NODZENSKI, E., LU, H., MAUCERI, H.J., KUFE, D.W. and WEICHSELBAUM, R.R., 2000. *Angiostatin induces mitotic cell death of proliferating endothelial cells.* San Diego, CA: Academic Press.

71. HASLETT, C., 1999. Granulocyte Apoptosis and Its Role in the Resolution and Control of Lung Inflammation. *American Journal of Respiratory and Critical Care Medicine,* **160**(5), pp. 5.

72. HASLETT, C., SAVILL, J.S. and MEAGHER, L., 1989. The neutrophil. *Current opinion in immunology,* **2**(1), pp. 10-18.

73. HASNAH, M.O. and CHAPMAN, D., 2008. Alternative method of diffraction-enhanced imaging. *Nuclear Instruments and Methods in Physics Research, Section A: Accelerators, Spectrometers, Detectors and Associated Equipment,* **584**(2-3), pp. 424-427.

74. HEIT, B., ROBBINS, S.M., DOWNEY, C.M., GUAN, Z., COLARUSSO, P., MILLER, J.B., JIRIK, F.R. and KUBES, P., 2008. PTEN functions to 'prioritize' chemotactic cues and prevent 'distraction' in migrating neutrophils. *Nature immunology,* **9**(7), pp. 743-752.

75. HEIT, B., TAVENER, S., RAHARJO, E. and KUBES, P., 2002. An intracellular signaling hierarchy determines direction of migration in opposing chemotactic gradients. *Journal of Cell Biology,* **159**(1), pp. 91-102.

76. HENDEY, B., LAWSON, M., MARCANTONIO, E.E. and MAXFIELD, F.R., 1996. Intracellular calcium and calcineurin regulate neutrophil motility on vitronectin through a receptor identified by antibodies to integrins αv and β3. *Blood,* **87**(5), pp. 2038-2048.

77. HICKEY, M.J. and KUBES, P., 2009. Intravascular immunity: The host-pathogen encounter in blood vessels. *Nature Reviews Immunology,* **9**(5), pp. 364-375.

78. HICKEY, M.J., KWAN, R.Y.Q., AWAD, M.M., KENNEDY, C.L., YOUNG, L.F., HALL, P., CORDNER, L.M., LYRAS, D., EMMINS, J.J. and ROOD, J.I., 2008. Molecular and cellular basis of microvascular perfusion deficits induced by Clostridium perfringens and Clostridium septicum. *PLoS Pathogens,* **4**(4),.

79. HINO, M. and HOSOYA, H., 2003. Small heat shock protein Hsp27 directly binds to alpha/beta tubulin heterodimer and inhibits DMSO-induced tubulin polymerization. *Biomedical Research,* **24**(1), pp. 27-30.

80. HINO, M., KUROGI, K., OKUBO, M.-., MURATA-HORI, M. and HOSOYA, H., 2000. Small heat shock protein 27 (HSP27) associates with tubulin/microtubules in HeLa cells. *Biochemical and biophysical research communications,* **271**(1), pp. 164-169.

81. HOFFMAN, R., STARKEY, S. and COAD, J., 1998. Wound Fluid from Venous Leg Ulcers Degrades Plasminogen and Reduces Plasmin Generation by Keratinocytes. *Journal of Investigative Dermatology,* **111**, pp. 1140-1144.

82. HOGG, J.C., DOERSCHUK, C.M., WIGGS, B. and MINSHALL, D., 1992. Neutrophil retention during a single transit through the pulmonary circulation. *Journal of applied physiology,* **73**(4), pp. 1683-1685.

83. HUANG, J., ROTH, R., HEUSER, J.E. and SADLER, J.E., 2009a. Integrin {alpha} v {beta} 3 on human endothelial cells binds von Willebrand factor strings under fluid shear stress. *Blood,* **113**(7), pp. 1589.

84. HUANG, J., ROTH, R., HEUSER, J.E. and SADLER, J.E., 2009b. Integrin {alpha}v{beta}3 on human endothelial cells binds von Willebrand factor strings under fluid shear stress. *Blood,* **113**(7), pp. 1589-1597.

85. HUBER-LANG, M., SARMA, J.V., ZETOUNE, F.S., RITTIRSCH, D., NEFF, T.A., MCGUIRE, S.R., LAMBRIS, J.D., WARNER, R.L., FLIERL, M.A., HOESEL, L.M., GEBHARD, F., YOUNGER, J.G., DROUIN, S.M., WETSEL, R.A. and WARD, P.A., 2006. Generation of C5a in the absence of C3: A new complement activation pathway. *Nature medicine,* **12**(6), pp. 682-687.

86. IBBOTSON, G.C., DOIG, C., KAUR, J., GILL, V., OSTROVSKY, L., FAIRHEAD, T. and KUBES, P., 2001. Functional α4-integrin: A newly identified pathway of neutrophil recruitment in critically ill septic patients. *Nature medicine,* **7**(4), pp. 465-470.

87. IDZKO, M., HAMMAD, H., VAN NIMWEGEN, M., KOOL, M., WILLART, M.A.M., MUSKENS, F., HOOGSTEDEN, H.C., LUTTMANN, W., FERRARI, D., DI VIRGILIO, F., VIRCHOW, J.C. and LAMBRECHT, B.N., 2007. *Extracellular ATP triggers and maintains asthmatic airway inflammation by activating dendritic cells.* New York, NY: Nature Pub. Co.

88. INSALL, R.H., 2010. Understanding eukaryotic chemotaxis: A pseudopod-centred view. *Nature Reviews Molecular Cell Biology,* **11**(6), pp. 453-458.

89. INSALL, R.H. and MACHESKY, L.M., 2009. Actin Dynamics at the Leading Edge: From Simple Machinery to Complex Networks. *Developmental Cell,* **17**(3), pp. 310-322.

90. JAIN, S. and BELLINGAN, G., 2007. Basic science of acute lung injury. *Surgery (Oxford),* **25**(3), pp. 112-116.

91. JANARDHAN, K.S., APPLEYARD, G.D. and SINGH, B., 2004. Expression of integrin subunits alphav and beta3 in acute lung inflammation. *Histochemistry and cell biology,* **121**(5), pp. 383-390.

92. JOG, N.R., JALA, V.R., WARD, R.A., RANE, M.J., HARIBABU, B. and MCLEISH, K.R., 2007. Heat shock protein 27 regulates neutrophil chemotaxis and exocytosis through two independent mechanisms. *Journal of Immunology,* **178**(4), pp. 2421-2428.

93. JURASZ, P., SANTOS-MARTINEZ, M., RADOMSKA, A. and RADOMSKI, M., 2006. Generation of platelet angiostatin mediated by urokinase plasminogen activator: effects on angiogenesis. *Journal of Thrombosis and Haemostasis,* **4**(5), pp. 1095-1106.

94. KAMEI, M. and CARMAN, C.V., 2010. New observations on the trafficking and diapedesis of monocytes. *Current opinion in hematology,* **17**(1), pp. 43-52.

95. KENAN, D.J. and WAHL, M.L., 2005. *Ectopic localization of mitochondrial ATP synthase: a target for anti-angiogenesis intervention?* New York,: Plenum Press.

96. KHAN, A.I., HEIT, B., ANDONEGUI, G., COLARUSSO, P. and KUBES, P., 2005. Lipopolysaccharide: A p38 MAPK-dependent disrupter of neutrophil chemotaxis. *Microcirculation,* **12**(5), pp. 421-432.

97. KNALL, C., WORTHEN, G.S. and JOHNSON, G.L., 1997. Interleukin 8-stimulated phosphatidylinositol-3-kinase activity regulates the migration of human neutrophils independent of extracellular signal-regulated kinase and p38 mitogen-activated protein

kinases. *Proceedings of the National Academy of Sciences of the United States of America,* **94**(7), pp. 3052-3057.

98. KOHN, A.D., SUMMERS, S.A., BIRNBAUM, M.J. and ROTH, R.A., 1996. Expression of a constitutively active Akt Ser/Thr kinase in 3T3-L1 adipocytes stimulates glucose uptake and glucose transporter 4 translocation. *Journal of Biological Chemistry,* **271**(49), pp. 31372-31378.

99. KOSTENKO, S. and MOENS, U., 2009. Heat shock protein 27 phosphorylation: kinases, phosphatases, functions and pathology. *Cellular and molecular life sciences : CMLS,* **66**(20), pp. 3289-3307.

100. KREISEL, D., NAVA, R.G., LI, W., ZINSELMEYER, B.H., WANG, B., LAI, J., PLESS, R., GELMAN, A.E., KRUPNICK, A.S. and MILLER, M.J., 2010. In vivo two-photon imaging reveals monocyte-dependent neutrophil extravasation during pulmonary inflammation. *Proceedings of the National Academy of Sciences of the United States of America,* **107**(42), pp. 18073-18078.

101. KRETSCHMER, D., GLESKE, A.-., RAUTENBERG, M., WANG, R., KÖBERLE, M., BOHN, E., SCHÖNEBERG, T., RABIET, M.-., BOULAY, F., KLEBANOFF, S.J., VAN KESSEL, K.A., VAN STRIJP, J.A., OTTO, M. and PESCHEL, A., 2010. Human formyl peptide receptor 2 senses highly pathogenic Staphylococcus aureus. *Cell Host and Microbe,* **7**(6), pp. 463-473.

102. KUBES, P. and KANWAR, S., 1994. Histamine induces leukocyte rolling in post-capillary venules: A P- selectin-mediated event. *Journal of Immunology,* **152**(7), pp. 3570-3577.

103. KUKULSKI, F., BEN YEBDRI, F., LEFEBVRE, J., WARNY, M., TESSIER, P.A. and SÉVIGNY, J., 2007. *Extracellular nucleotides mediate LPS-induced neutrophil migration in vitro and in vivo.* Bethesda, Md.: Society for Leukocyte Biology.

104. KUNISAKI, Y., NISHIKIMI, A., TANAKA, Y., TAKII, R., NODA, M., INAYOSHI, A., WATANABE, K.-., SANEMATSU, F., SASAZUKI, T., SASAKI, T. and FUKUI, Y., 2006. DOCK2 is a Rac activator that regulates motility and polarity during neutrophil chemotaxis. *Journal of Cell Biology*, **174**(5), pp. 647-652.

105. KUTSUNA, H., SUZUKI, K., KAMATA, N., KATO, T., HATO, F., MIZUNO, K., KOBAYASHI, H., ISHII, M. and KITAGAWA, S., 2004. Actin reorganization and morphological changes in human neutrophils stimulated by TNF, GM-CSF, and G-CSF: The role of MAP kinases. *American Journal of Physiology - Cell Physiology*, **286**(1 55-1),.

106. LAD, P.M., OLSON, C.V. and SMILEY, P.A., 1985. Association of the N-formyl-Met-Leu-Phe receptor in human neutrophils with a GTP-binding protein sensitive to pertussis toxin. *Proceedings of the National Academy of Sciences of the United States of America*, **82**(3), pp. 869-873.

107. LAMMERMANN, T., BADER, B.L., MONKLEY, S.J., WORBS, T., WEDLICH-SOLDNER, R., HIRSCH, K., KELLER, M., FORSTER, R., CRITCHLEY, D.R., FASSLER, R. and SIXT, M., 2008. Rapid leukocyte migration by integrin-independent flowing and squeezing. *Nature*, **453**(7191), pp. 51-55.

108. LAUFE, M.D., SIMON, R.H., FLINT, A. and KELLER, J.B., 1986. Adult respiratory distress syndrome in neutropenic patients. *The American Journal of Medicine,* **80**(6), pp. 1022-1026.

109. LAWSON, M.A. and MAXFIELD, F.R., 1995. Ca^{2+}- and calcineurin-dependent recycling of an integrin to the front of migrating neutrophils. *Nature*, **377**(6544), pp. 75-79.

110. LAY, A.J., JIANG, X.M., KISKER, O., FLYNN, E., UNDERWOOD, A., CONDRON, R. and HOGG, P.J., 2000. Phosphoglycerate kinase acts in tumour angiogenesis as a disulphide reductase. *Nature,* **408**(6814), pp. 869-873.

111. LEE, T.-., MUSCHAL, S., PRAVDA, E.A., FOLKMAN, J., ABDOLLAHI, A. and JAVAHERIAN, K., 2009a. Angiostatin regulates the expression of antiangiogenic and proapoptotic pathways via targeted inhibition of mitochondrial proteins. *Blood,* **114**(9), pp. 1987-1998.

112. LEE, T.-., MUSCHAL, S., PRAVDA, E.A., FOLKMAN, J., ABDOLLAHI, A. and JAVAHERIAN, K., 2009b. Angiostatin regulates the expression of antiangiogenic and proapoptotic pathways via targeted inhibition of mitochondrial proteins. *Blood,* **114**(9), pp. 1987-1998.

113. LEWIS, R.A., 2004. Medical phase contrast x-ray imaging: Current status and future prospects. *Physics in Medicine and Biology,* **49**(16), pp. 3573-3583.

114. LEWIS, R.A., YAGI, N., KITCHEN, M.J., MORGAN, M.J., PAGANIN, D., SIU, K.K.W., PAVLOV, K., WILLIAMS, I., UESUGI, K., WALLACE, M.J., HALL,

C.J., WHITLEY, J. and HOOPER, S.B., 2005. Dynamic imaging of the lungs using x-ray phase contrast. *Physics in Medicine and Biology*, **50**(21), pp. 5031-5040.

115. LEY, K., LAUDANNA, C., CYBULSKY, M.I. and NOURSHARGH, S., 2007. Getting to the site of inflammation: the leukocyte adhesion cascade updated. *Nature reviews.Immunology*, **7**(9), pp. 678-689.

116. LI, Z., DONG, X., WANG, Z., LIU, W., DENG, N., DING, Y., TANG, L., HLA, T., ZENG, R., LI, L. and WU, D., 2005. Regulation of PTEN by Rho small GTPases. *Nature cell biology*, **7**(4), pp. 399-404.

117. LIAO, Z., SEYE, C.I., WEISMAN, G.A. and ERB, L., 2007. *The P2Y2 nucleotide receptor requires interaction with alpha v integrins to access and activate G12*. Cambridge, U.K.: Co. of Biologists.

118. LIU, L. and KUBES, P., 2003. Molecular mechanisms of leukocyte recruitment: Organ-specific mechanisms of action. *Thrombosis and haemostasis*, **89**(2), pp. 213-220.

119. LIU, L., PURI, K.D., PENNINGER, J.M. and KUBES, P., 2007. Leukocyte PI3Kγ and PI3Kδ have temporally distinct roles for leukocyte recruitment in vivo. *Blood*, **110**(4), pp. 1191-1198.

120. LIU, S., KIOSSES, W.B., ROSE, D.M., SLEPAK, M., SALGIA, R., GRIFFIN, J.D., TURNER, C.E., SCHWARTZ, M.A. and GINSBERG, M.H., 2002. A fragment of paxillin binds the α4 integrin cytoplasmic domain (tail) and selectively inhibits α4-mediated cell migration. *Journal of Biological Chemistry*, **277**(23), pp. 20887-20894.

121. LOKUTA, M.A. and HUTTENLOCHER, A., 2005. TNF-α promotes a stop signal that inhibits neutrophil polarization and migration via a p38 MAPK pathway. *Journal of leukocyte biology,* **78**(1), pp. 210-219.

122. LU, H., DHANABAL, M., VOLK, R., WATERMAN, M.J.F., RAMCHANDRAN, R., KNEBELMANN, B., SEGAL, M. and SUKHATME, V.P., 1999. Kringle 5 Causes Cell Cycle Arrest and Apoptosis of Endothelial Cells. *Biochemical and biophysical research communications,* **258**(3), pp. 668-673.

123. LUCAS, R., LIJNEN, H.R., SUFFREDINI, A.F., PEPPER, M.S., STEINBERG, K.P., MARTIN, T.R. and PUGIN, J., 2002. Increased angiostatin levels in bronchoalveolar lavage fluids from ARDS patients and from human volunteers after lung instillation of endotoxin. *Thrombosis and haemostasis,* **87**(6), pp. 966-971.

124. LUO, J., LIN, J., PARANYA, G. and BISCHOFF, J., 1998. Angiostatin Upregulates E-Selectin in Proliferating Endothelial Cells. *Biochemical and biophysical research communications,* **245**(3), pp. 906-911.

125. MARKVICHEVA, K.N., GOROKHOVATSKII, A.Y., MISHINA, N.M., MUDRIK, N.N., VINOKUROV, L.M., LUK'YANOV, S.A. and BELOUSOV, V.V., 2010. Signaling function of phagocytic NADPH oxidase: Activation of MAP kinase cascades in phagocytosis. *Russian Journal of Bioorganic Chemistry*, **36**(1), pp. 124-129.

126. MARTIN, T.R., PISTORESE, B.P., CHI, E.Y., GOODMAN, R.B. and MATTHAY, M.A., 1989. Effects of leukotriene B4 in the human lung. Recruitment of neutrophils into the alveolar spaces without a change in protein permeability. *Journal of Clinical Investigation,* **84**(5), pp. 1609-1619.

127. MARTINEZ GAKIDIS, M.A., CULLERE, X., OLSON, T., WILSBACHER, J.L., ZHANG, B., MOORES, S.L., LEY, K., SWAT, W., MAYADAS, T. and BRUGGE, J.S., 2004. Vav GEFs are required for β2 integrin-dependent functions of neutrophils. *Journal of Cell Biology,* **166**(2), pp. 273-282.

128. MATSUMOTO, T., MOLSKI, T.F.P. and KANAHO, Y., 1987. G-protein dissociation, GTP-GDP exchange and GTPase activity in control and PMA treated neutrophils stimulated by fMet-Leu-Phe. *Biochemical and biophysical research communications,* **143**(2), pp. 489-498.

129. MATTER, M.L. and RUOSLAHTI, E., 2001. A Signaling Pathway from the α5β1 and αvβ3 Integrins that Elevates bcl-2 Transcription. *Journal of Biological Chemistry,* **276**(30), pp. 27757-27763.

130. MATTHAY, M.A., ESCHENBACHER, W.L. and GOETZL, E.J., 1984. Elevated concentrations of leukotriene D4 in pulmonary edema fluid of patients with the adult respiratory distress syndrome. *Journal of clinical immunology,* **4**(6), pp. 479-483.

131. MATUTE-BELLO, G. and MARTIN, T.R., 2008. Science review: Apoptosis in acute lung injury. *feedback,* .

132. MAUS, U., VON GROTE, K., KUZIEL, W.A., MACK, M., MILLER, E.J., CIHAK, J., STANGASSINGER, M., MAUS, R., SCHLÖNDORFF, D., SEEGER, W. and LOHMEYER, J., 2002. The role of CC chemokine receptor 2 in alveolar monocyte and neutrophil immigration in intact mice. *American Journal of Respiratory and Critical Care Medicine,* **166**(3), pp. 268-273.

133. MAVROMMATIS, A.C., THEODORIDIS, T., ORFANIDOU, A., ROUSSOS, C., CHRISTOPOULOU-KOKKINOU, V. and ZAKYNTHINOS, S., 2000. Coagulation system and platelets are fully activated in uncomplicated sepsis. *Critical care medicine,* **28**(2), pp. 451-457.

134. MIRZA, A.M., KOHN, A.D., ROTH, R.A. and MCMAHON, M., 2000. Oncogenic transformation of cells by a conditionally active form of the protein kinase Akt/PKB. *Cell Growth and Differentiation,* **11**(6), pp. 279-292.

135. MIZGERD, J.P., 2008. Acute lower respiratory tract infection. *The New England journal of medicine,* **358**(7), pp. 716-727.

136. MIZGERD, J.P., MEEK, B.B., KUTKOSKI, G.J., BULLARD, D.C., BEAUDET, A.L. and DOERSCHUK, C.M., 1996. Selectins and neutrophil traffic: Margination and Streptococcus pneumoniae-induced emigration in murine lungs. *Journal of Experimental Medicine,* **184**(2), pp. 639-645.

137. MOREAU, J., LORD, M., BOUCHER, M., BELLEAU, P. and FERNANDES, M.J., 2005. Protein diversity is generated within the motin family of proteins by alternative pre-mRNA splicing. *Gene,* **350**(2), pp. 137-148.

138. MOSER, T.L., KENAN, D.J., ASHLEY, T.A., ROY, J.A., GOODMAN, M.D., MISRA, U.K., CHEEK, D.J. and PIZZO, S.V., 2001. *Endothelial cell surface F1-F0 ATP synthase is active in ATP synthesis and is inhibited by angiostatin.* National Academy of Sciences.

139. MOULTON, K.S., VAKILI, K., ZURAKOWSKI, D., SOLIMAN, M., BUTTERFIELD, C., SYLVIN, E., LO, K.M., GILLIES, S., JAVAHERIAN, K. and FOLKMAN, J., 2003. Inhibition of plaque neovascularization reduces macrophage accumulation and progression of advanced atherosclerosis. *Proceedings of the National Academy of Sciences*, **100**(8), pp. 4736-4741.

140. MU, W., LONG, D.A., OUYANG, X., AGARWAL, A., CRUZ, P.E., RONCAL, C.A., NAKAGAWA, T., YU, X., HAUSWIRTH, W.W. and JOHNSON, R.J., 2009. Angiostatin overexpression is associated with an improvement in chronic kidney injury by an anti-inflammatory mechanism. *American journal of physiology.Renal physiology*, **296**(1), pp. F145-52.

141. MULLER, W., 2009. Mechanisms of transendothelial migration of leukocytes. *Circulation research*, **105**(3), pp. 223.

142. NAKAGAMI, H., MORISHITA, R., YAMAMOTO, K., TANIYAMA, Y., AOKI, M., MATSUMOTO, K., NAKAMURA, T., KANEDA, Y., HORIUCHI, M. and OGIHARA, T., 2001. Mitogenic and antiapoptotic actions of hepatocyte growth factor through ERK, STAT3, and Akt in endothelial cells. *Hypertension*, **37**(2 II), pp. 581-586.

143. NIGGLI, V., 2003. Signaling to migration in neutrophils: Importance of localized pathways. *International Journal of Biochemistry and Cell Biology*, **35**(12), pp. 1619-1638.

144. NISHIKIMI, A., FUKUHARA, H., SU, W., HONGU, T., TAKASUGA, S., MIHARA, H., CAO, Q., SANEMATSU, F., KANAI, M., HASEGAWA, H., TANAKA, Y., SHIBASAKI, M., KANAHO, Y., SASAKI, T., FROHMAN, M.A. and FUKUI, Y.,

2009. Sequential regulation of DOCK2 dynamics by two phospholipids during neutrophil chemotaxis. *Science,* **324**(5925), pp. 384-387.

145. NISHIOKA, T., FROHMAN, M.A., MATSUDA, M. and KIYOKAWA, E., 2010. Heterogeneity of phosphatidic acid levels and distribution at the plasma membrane in living cells as visualized by a Förster Resonance Energy Transfer (FRET) biosensor. *Journal of Biological Chemistry,* **285**(46), pp. 35979-35987.

146. NOBES, C. and HALL, A., 1994. Regulation and function of the Rho subfamily of small GTPases. *Current Opinion in Genetics and Development,* **4**(1), pp. 77-81.

147. NOZAWA, H., CHIU, C. and HANAHAN, D., 2006. Infiltrating neutrophils mediate the initial angiogenic switch in a mouse model of multistage carcinogenesis. *Proceedings of the National Academy of Sciences,* **103**(33), pp. 12493.

148. NUZZI, P.A., LOKUTA, M.A. and HUTTENLOCHER, A., 2007. Analysis of neutrophil chemotaxis. *Methods in molecular biology (Clifton, N.J.),* **370**, pp. 23-36.

149. OGNIBENE, F.P., MARTIN, S.E. and PARKER, M.M., 1986. Adult respiratory distress syndrome in patients with severe neutropenia. *New England Journal of Medicine,* **315**(9), pp. 547-551.

150. O'REILLY, M.S., HOLMGREN, L., SHING, Y., CHEN, C., ROSENTHAL, R.A., MOSES, M., LANE, W.S., CAO, Y., SAGE, E.H. and FOLKMAN, J., 1994. Angiostatin: a novel angiogenesis inhibitor that mediates the suppression of metastases by a Lewis lung carcinoma. *Cell,* **79**(2), pp. 315-328.

151. PARSONS, P.E., FOWLER, A.A., HYERS, T.M. and HENSON, P.M., 1985. Chemotactic activity in bronchoalveolar lavage fluid from patients with adult respiratory distress syndrome. *American Review of Respiratory Disease,* **132**(3), pp. 490-493.

152. PEARSON, G., ROBINSON, F., GIBSON, T.B., XU, B.-., KARANDIKAR, M., BERMAN, K. and COBB, M.H., 2001. Mitogen-activated protein (MAP) kinase pathways: Regulation and physiological functions. *Endocrine reviews,* **22**(2), pp. 153-183.

153. PERL, M., LOMAS-NEIRA, J., CHUNG, C. and AYALA, A., 2008. *Epithelial cell apoptosis and neutrophil recruitment in acute lung injury-a unifying hypothesis? What we have learned from small interfering RNAs.* Cambridge, Mass.: Blackwell Scientific Publications.

154. PERRI, S.R., ANNABI, B. and GALIPEAU, J., 2007. Angiostatin inhibits monocyte/macrophage migration via disruption of actin cytoskeleton. *The FASEB Journal,* **21**(14), pp. 3928.

155. PETRI, B., KAUR, J., LONG, E.M., LI, H., PARSONS, S.A., BUTZ, S., PHILLIPSON, M., VESTWEBER, D., PATEL, K.D., ROBBINS, S.M. and KUBES, P., 2011. Endothelial LSP1 is involved in endothelial dome formation, minimizing vascular permeability changes during neutrophil transmigration in vivo. *Blood,* **117**(3), pp. 942-952.

156. PHILLIPSON, M., HEIT, B., COLARUSSO, P., LIU, L., BALLANTYNE, C.M. and KUBES, P., 2006. Intraluminal crawling of neutrophils to emigration sites: A

molecularly distinct process from adhesion in the recruitment cascade. *Journal of Experimental Medicine,* **203**(12), pp. 2569-2575.

157. PLUSKOTA, E., SOLOVIEV, D.A., SZPAK, D., WEBER, C. and PLOW, E.F., 2008. *Neutrophil apoptosis: selective regulation by different ligands of integrin alphaMbeta2.* Bethesda, Md.: American Association of Immunologists.

158. PLYTYCZ, B. and SELJELID, R., 2003. From inflammation to sickness: Historical perspective. *Archivum Immunologiae et Therapiae Experimentalis,* **51**(2), pp. 105-109.

159. POSTMA, B., POPPELIER, M.J., VAN GALEN, J.C., PROSSNITZ, E.R., VAN STRIJP, J.A.G., DE HAAS, C.J.C. and VAN KESSEL, K.P.M., 2004. Chemotaxis inhibitory protein of Staphylococcus aureus binds specifically to the C5a and formylated peptide receptor. *Journal of Immunology,* **172**(11), pp. 6994-7001.

160. PRAT, C., HAAS, P.-., BESTEBROER, J., DE HAAS, C.J.C., VAN STRIJP, J.A.G. and VAN KESSEL, K.P.M., 2009. A homolog of formyl peptide receptor-like 1 (FPRL1) inhibitor from Staphylococcus aureus (FPRL1 inhibitory protein) that inhibits FPRL1 and FPR. *Journal of Immunology,* **183**(10), pp. 6569-6578.

161. PURI, K.D., DOGGETT, T.A., DOUANGPANYA, J., HOU, Y., TINO, W.T., WILSON, T., GRAF, T., CLAYTON, E., TURNER, M., HAYFLICK, J.S. and DIACOVO, T.G., 2004. Mechanisms and implications of phosphoinositide 3-kinase δ in promoting neutrophil trafficking into inflamed tissue. *Blood,* **103**(9), pp. 3448-3456.

162. PURI, K.D., DOGGETT, T.A., HUANG, C.-., DOUANGPANYA, J., HAYFLICK, J.S., TURNER, M., PENNINGER, J. and DIACOVO, T.G., 2005. The role of endothelial PI3Kγ activity in neutrophil trafficking. *Blood*, **106**(1), pp. 150-157.

163. RIETHMULLER, C., NASDALA, I. and VESTWEBER, D., 2008. Nano-surgery at the leukocyte-endothelial docking site. *Pflugers Archiv European Journal of Physiology*, **456**(1), pp. 71-81.

164. RITTIRSCH, D., FLIERL, M.A., NADEAU, B.A., DAY, D.E., HUBER-LANG, M., MACKAY, C.R., ZETOUNE, F.S., GERARD, N.P., CIANFLONE, K., KÖHL, J., GERARD, C., SARMA, J.V. and WARD, P.A., 2008. Functional roles for C5a receptors in sepsis. *Nature medicine*, **14**(5), pp. 551-557.

165. ROOIJAKKERS, S.H.M., RUYKEN, M., ROOS, A., DAHA, M.R., PRESANIS, J.S., SIM, R.B., VAN WAMEL, W.J.B., VAN KESSEL, K.P.M. and VAN STRIJP, J.A.G., 2005. Immune evasion by a staphylococcal complement inhibitor that acts on C3 convertases. *Nature immunology*, **6**(9), pp. 920-927.

166. ROOIJAKKERS, S.H.M., RUYKEN, M., VAN ROON, J., VAN KESSEL, K.P.M., VAN STRIJP, J.A.G. and VAN WAMEL, W.J.B., 2006. Early expression of SCIN and CHIPS drives instant immune evasion by Staphylococcus aureus. *Cellular microbiology*, **8**(8), pp. 1282-1293.

167. SABROE, I., DOWER, S.K. and WHYTE, M.K.B., 2005. The role of Toll-like receptors in the regulation of neutrophil migration, activation, and apoptosis. *Clinical Infectious Diseases*, **41**(SUPPL. 7),.

168. SCAPINI, P., NESI, L., MORINI, M., TANGHETTI, E., BELLERI, M., NOONAN, D., PRESTA, M., ALBINI, A. and CASSATELLA, M.A., 2002. Generation of Biologically Active Angiostatin Kringle 1-3 by Activated Human Neutrophils 1. *The Journal of Immunology,* **168**(11), pp. 5798-5804.

169. SCHENKEL, A.R., MAMDOUH, Z. and MULLER, W.A., 2004. Locomotion of monocytes on endothelium is a critical step during extravasation. *Nature immunology,* **5**(4), pp. 393-400.

170. SCHIERWAGEN, C., BYLUND-FELLENIUS, A.C. and LUNDBERG, C., 1990. Improved method for quantification of tissue PMN accumulation measured by myeloperoxidase activity. *Journal of pharmacological methods,* **23**(3), pp. 179-186.

171. SELBY, C. and MACNEE, W., 1993. Factors affecting neutrophil transit during acute pulmonary inflammation: Minireview. *Experimental lung research,* **19**(4), pp. 407-428.

172. SHARMA, M.R., ROTHMAN, V., TUSZYNSKI, G.P. and SHARMA, M.C., 2006. Antibody-directed targeting of angiostatin's receptor annexin II inhibits Lewis Lung Carcinoma tumor growth via blocking of plasminogen activation: Possible biochemical mechanism of angiostatin's action. *Experimental and molecular pathology,* **81**(2), pp. 136-145.

173. SHARMA, M.C. and SHARMA, M., 2007. The role of annexin II in angiogenesis and tumor progression: A potential therapeutic target. *Current pharmaceutical design,* **13**(35), pp. 3568-3575.

174. SHARMA, M.R., TUSZYNSKI, G.P. and SHARMA, M.C., 2004. *Angiostatin-induced inhibition of endothelial cell proliferation/apoptosis is associated with the down-regulation of cell cycle regulatory protein cdk5.* New York: A.R. Liss.

175. SHARMA, P., VEERANNA, V., SHARMA, M., AMIN, N.D., SIHAG, R.K., GRANT, P., AHN, N., KULKARNI, A.B. and PANT, H.C., 2002. Phosphorylation of MEK1 by cdk5/p35 down-regulates the mitogen-activated protein kinase pathway. *Journal of Biological Chemistry,* **277**(1), pp. 528-534.

176. SHETTY, S. and IDELL, S., 2004. *Regulation of urokinase receptor expression by phosphoglycerate kinase,* .

177. SINGH, B., FU, C. and BHATTACHARYA, J., 2000. Vascular expression of the αvβ3-integrin in lung and other organs. *American Journal of Physiology- Lung Cellular and Molecular Physiology,* **278**(1), pp. 217-226.

178. SINGH, B., JANARDHAN, K.S. and KANTHAN, R., 2005. Expression of angiostatin, integrin αvβ3, and vitronectin in human lungs in sepsis. *Experimental lung research,* **31**(8), pp. 771-782.

179. SINGH, R.D., MARKS, D.L., HOLICKY, E.L., WHEATLEY, C.L., KAPTZAN, T., SATO, S.B., KOBAYASHI, T., LING, K. and PAGANO, R.E., 2010. Gangliosides and β1-integrin are required for caveolae and membrane domains. *Traffic,* **11**(3), pp. 348-360.

180. SIVAN, Y., MOR, C., AL-JUNDI, S. and NEWTH, C.J., 1990. Adult respiratory distress syndrome in severely neutropenic children. *Pediatric pulmonology,* **8**(2), pp. 104-108.

181. SMITH, E. and HOFFMAN, R., 2005. Multiple fragments related to angiostatin and endostatin in fluid from venous leg ulcers. *Wound Repair and Regeneration,* **13**(2), pp. 148-157.

182. SMITH, D.F., DEEM, T.L., BRUCE, A.C., REUTERSHAN, J., WU, D. and LEY, K., 2006. Leukocyte phosphoinositide-3 kinase γ is required for chemokine-induced, sustained adhesion under flow in vivo. *Journal of leukocyte biology,* **80**(6), pp. 1491-1499.

183. SNIGIREV, A., SNIGIREVA, I., KOHN, V., KUZNETSOV, S. and SCHELOKOV, I., 1995. On the possibilities of x-ray phase contrast microimaging by coherent high-energy synchrotron radiation. *Review of Scientific Instruments,* **66**(12), pp. 5486-5492.

184. SPISANI, S., FALZARANO, S., TRANIELLO, S., NALLI, M. and SELVATICI, R., 2005. A 'pure' chemoattractant formylpeptide analogue triggers a specific signalling pathway in human neutrophil chemotaxis. *FEBS Journal,* **272**(4), pp. 883-891.

185. STEPHENS, L., ELLSON, C. and HAWKINS, P., 2002. Roles of PI3Ks in leukocyte chemotaxis and phagocytosis. *Current opinion in cell biology,* **14**(2), pp. 203-213.

186. STOHLAWETZ, P., FOLMAN, C.C., VON DEM BORNE, A.E.K., PERNERSTORFER, T., EICHLER, H.-., PANZER, S. and JILMA, B., 1999. Effects of endotoxemia on thrombopoiesis in men. *Thrombosis and haemostasis,* **81**(4), pp. 613-617.

187. SUGIHARA-MIZUNO, Y., ADACHI, M., KOBAYASHI, Y., HAMAZAKI, Y., NISHIMURA, M., IMAI, T., FURUSE, M. and TSUKITA, S., 2007. Molecular characterization of angiomotin/JEAP family proteins: Interaction with MUPP1/Patj and their endogenous properties. *Genes to Cells,* **12**(4), pp. 473-486.

188. SUZUKI, Y., YAGI, N. and UESUGI, K., 2002. X-ray refraction-enhanced imaging and a method for phase retrieval for a simple object. *Journal of Synchrotron Radiation,* **9**(3), pp. 160-165.

189. SYED, S.P., MARTIN, A.M., HAUPT, H.M., ARENAS-ELLIOT, C.P. and BROOKS, J.J., 2007. Angiostatin receptor annexin II in vascular tumors including angiosarcoma. *Human pathology,* **38**(3), pp. 508-513.

190. SZARKA, R.J., WANG, N., GORDON, L., NATION, P. and SMITH, R.H., 1997. A murine model of pulmonary damage induced by lipopolysaccharide via intranasal instillation. *Journal of immunological methods,* **202**(1), pp. 49-57.

191. SZCZUR, K., ZHENG, Y. and FILIPPI, M.-., 2009. The small Rho GTPase Cdc42 regulates neutrophil polarity via CD11b integrin signaling. *Blood,* **114**(20), pp. 4527-4537.

192. TABRUYN, S.P. and GRIFFIOEN, A.W., 2007. Molecular pathways of angiogenesis inhibition. *Biochemical and biophysical research communications,* **355**(1), pp. 1-5.

193. TARUI, T., MILES, L.A. and TAKADA, Y., 2001. Specific Interaction of Angiostatin with Integrin αvβ3 in Endothelial Cells. *Journal of Biological Chemistry,* **276**(43), pp. 39562-39568.

194. TARUI, T., MAJUMDAR, M., MILES, L.A., RUF, W. and TAKADA, Y., 2002. Plasmin-induced migration of endothelial cells: A potential target for the anti-angiogenic action of angiostatin. *Journal of Biological Chemistry*, **277**(37), pp. 33564-33570.

195. TE VELDE, E.A., KUSTERS, B., MAASS, C., DE WAAL, R. and RINKES, I.H.M.B., 2003. Histological analysis of defective colonic healing as a result of angiostatin treatment. *Experimental and molecular pathology*, **75**(2), pp. 119-123.

196. TROYANOVSKY, B., LEVCHENKO, T., MANSSON, G., MATVIJENKO, O. and HOLMGREN, L., 2001a. Angiomotin An Angiostatin Binding Protein That Regulates Endothelial Cell Migration and Tube Formation. *The Journal of cell biology,* **152**(6), pp. 1247-1254.

197. TROYANOVSKY, B., LEVCHENKO, T., MÅNSSON, G., MATVIJENKO, O. and HOLMGREN, L., 2001b. Angiomotin: An angiostatin binding protein that regulates endothelial cell migration and tube formation. *Journal of Cell Biology*, **152**(6), pp. 1247-1254.

198. TUSZYNSKI, G.P., SHARMA, M.R., ROTHMAN, V.L. and SHARMA, M.C., 2002. Angiostatin binds to tyrosine kinase substrate annexin II through the lysine-binding domain in endothelial cells. *Microvascular research,* **64**(3), pp. 448-462.

199. VEITONMÄKI, N., CAO, R., WU, L., MOSER, T.L., LI, B., PIZZO, S.V., ZHIVOTOVSKY, B. and CAO, Y., 2004. *Endothelial cell surface ATP synthase-triggered caspase-apoptotic pathway is essential for k1-5-induced antiangiogenesis.* Philadelphia: American Association for Cancer Research.

200. VESTWEBER, D., 2007. Adhesion and signaling molecules controlling the transmigration of leukocytes through endothelium. *Immunological reviews,* **218**(1), pp. 178-196.

201. WAGNER, J.G. and ROTH, R.A., 2000. Neutrophil migration mechanisms, with an emphasis on the pulmonary vasculature. *Pharmacological reviews,* **52**(3), pp. 349-374.

202. WAHL, M.L., KENAN, D.J., GONZALEZ-GRONOW, M. and PIZZO, S.V., 2005. Angiostatin's Molecular Mechanism: Aspects of Specificity and Regulation Elucidated. *Journal of cellular biochemistry,* **96**(2), pp. 242.

203. WAJIH, N. and SANE, D.C., 2003. Angiostatin selectively inhibits signaling by hepatocyte growth factor in endothelial and smooth muscle cells. *Blood,* **101**(5), pp. 1857-1863.

204. WANG, R., BRAUGHTON, K.R., KRETSCHMER, D., BACH, T.-.L., QUECK, S.Y., LI, M., KENNEDY, A.D., DORWARD, D.W., KLEBANOFF, S.J., PESCHEL, A.,

DELEO, F.R. and OTTO, M., 2007. Identification of novel cytolytic peptides as key virulence determinants for community-associated MRSA. *Nature medicine,* **13**(12), pp. 1510-1514.

205. WELLS, C.D., FAWCETT, J.P., TRAWEGER, A., YAMANAKA, Y., GOUDREAULT, M., ELDER, K., KULKARNI, S., GISH, G., VIRAG, C., LIM, C., COLWILL, K., STAROSTINE, A., METALNIKOV, P. and PAWSON, T., 2006. A Rich1/Amot Complex Regulates the Cdc42 GTPase and Apical-Polarity Proteins in Epithelial Cells. *Cell,* **125**(3), pp. 535-548.

206. WENINGER, W., ULFMAN, L.H., CHENG, G., SOUCHKOVA, N., QUACKENBUSH, E.J., LOWE, J.B. and VON ANDRIAN, U.H., 2000. Specialized contributions by α(1,3)-fucosyltransferase-IV and FucT-VII during leukocyte rolling in dermal microvessels. *Immunity,* **12**(6), pp. 665-676.

207. WILKINS, S.W., GUREYEV, T.E., GAO, D., POGANY, A. and STEVENSON, A.W., 1996. Phase-contrast imaging using polychromatic hard X-rays. *Nature,* **384**(6607), pp. 335-338.

208. WITKO-SARSAT, V., 2010. Apoptosis, cell death and inflammation. *Journal of Innate Immunity,* **2**(3), pp. 201-203.

209. WITKO-SARSAT, V., RIEU, P., DESCAMPS-LATSCHA, B., LESAVRE, P. and HALBWACHS-MECARELLI, L., 2000. Neutrophils: Molecules, functions and pathophysiological aspects. *Laboratory Investigation,* **80**(5), pp. 617-654.

210. WONG, C.H.Y., HEIT, B. and KUBES, P., 2010. Molecular regulators of leucocyte chemotaxis during inflammation. *Cardiovascular research,* **86**(2), pp. 183-191.

211. YAGI, N., SUZUKI, Y., UMETANI, K., KOHMURA, Y. and YAMASAKI, K., 1999. Refraction-enhanced x-ray imaging of mouse lung using synchrotron radiation source. *Medical physics,* **26**(10), pp. 2190-2193.

212. YAN, S.R. and NOVAK, M.J., 1999. Diverse effects of neutrophil integrin occupation on respiratory burst activation. *Cellular immunology,* **195**(2), pp. 119-126.

213. YIPP, B.G., ANDONEGUI, G., HOWLETT, C.J., ROBBINS, S.M., HARTUNG, T., HO, M. and KUBES, P., 2002. Profound differences in leukocyte-endothelial cell responses to lipopolysaccharide versus lipoteichoic acid. *Journal of Immunology,* **168**(9), pp. 4650-4658.

214. ZHONG, B., JIANG, K., GILVARY, D.L., EPLING-BURNETTE, P.K., RITCHEY, C., LIU, J., JACKSON, R.J., HONG-GELLER, E. and WEI, S., 2003. Human neutrophils utilize a Rac/Cdc42-dependent MAPK pathway to direct intracellular granule mobilization toward ingested microbial pathogens. *Blood,* **101**(8), pp. 3240-3248.